LA-UR- 93-1790

CONCEPTUAL DESIGN
of a
7 MeV RFQ LINAC
for the
ACCELERATOR PRODUCTION OF TRITIUM

D. Schrage, L. Young, J. Browman, J. Merson, & A. Naranjo
Los Alamos National Laboratory
Accelerator Technology Division

J. Rathke & B. Abel
Grumman Aerospace Corporation
Energy Systems Division

May 1993

Los Alamos

AT-1

GRUMMAN

DO NOT CIRCULATE

I. INTRODUCTION

The Radio Frequency Quadrupole (RFQ) linac proposed for the Accelerator Production of Tritium (APT) Project is a 100 percent duty factor (CW, continuous wave) linac which will produce a 100 milliampere beam of protons with energy of 7 MeV. This document addresses the physics and engineering design plus the fabrication of the APT RFQ. The information presented herein is considered to be demonstration of feasibility of this design concept; it is not intended to be representative of the details of the final design. Thus far, there has been little optimization of the design. Such activities will clearly be necessary prior to finalizing the design.

The current RFQ concept is shown on Figure I-1 with the specifications given on Table I-1. For the APT project, there will be two such RFQ's followed by drift tube linac's (DTL's) and then a funnel. A bridge-coupled DTL (BCDTL) and coupled cavity linac (CCL) follow the funnel to bring the energy of the combined 200 mA beam up to one GeV. An overview of the APT linac is shown on Figure I-2.

The choice of the 7 MeV output energy for the RFQ is the result of a desire to extend the output energy of the RFQ to the highest practical level in order to minimize the number of low energy DTL tanks. Such DTL tanks would incorporate the smallest magnets and would have high design and manufacturing costs. Furthermore, pushing the transition from the RFQ to the DTL to the highest energy level allows the use of radiation-hard electromagnetic quadrupole magnets in both the DTL and in the matching section.

At the present time, the state of the art with respect to output energy for four-vane RFQ linacs in this frequency range (250 - 450 MHz) is 2.5 MeV for the Superconducting Super Collider (SSC) Laboratory[1]. The proposed APT RFQ will have an output energy of 7.0 MeV. This energy level poses no significant challenges except as it relates to the physical length of the structure. The design utilizes beam dynamics codes developed for the RFQ for the SSC Laboratory[2]. These codes include multi-pole effects and have been benchmarked against existing linacs. The APT RFQ system design incorporates a "beam current independent match" to the RFQ/DTL matching section.

It has been the practice in the design of previous RFQ's to utilize longitudinal variation of the ratio of the vane tip transverse radius of curvature (ρ) to the vane tip displacement (r_o) to maintain a longitudinally-uniform local resonant frequency while the aperture varies. For the APT RFQ, the value of ρ/r_o is held constant at 0.85 which is a compromise between minimum peak surface fields ($\rho/r_o = 0.75$) and minimum multi-pole effects $\rho/r_o \sim 1.00$). The resonant frequency is held constant while ro changes by varying the cavity cross-section (inductance) by adjusting the width of the vane base. This also maintains a low capacitance which reduces the structure power. The beam dynamics design is described in Section II.

The proposed APT RFQ will have an electrical length of 9.5 wavelengths. The Continuous Wave Deuterium Demonstrator (CWDD) RFQ[3] at 4.6 wavelengths is currently the longest. Use of a coupled-cavity structure[4] for the APT RFQ is described in Section III.

RADIO FREQUENCY QUADRUPOLE LINAC
for the
ACCELERATOR PRODUCTION of TRITIUM

Table I-1

BEAM SPECIFICATIONS:

Input Energy	75	keV
Output Energy	7.0	MeV
Output Current	105	mA
Transmission	~95	%
Emittance (rms, normatlized) input	0.020π	cm−mrad
output	0.022π	cm−mrad
Duty Factor	100	%

ACCELERATOR SPECIFICATIONS:

Resonant Frequency	350	MHz
Peak Surface Field	1.8	E_k
Structure Power	1.2	MW
Total Power	1.9	MW
Length	8.1	Meters

Special Features	Four 2 Meter Segments Resonantly Coupled
	Dipole Mode Suppression
	Variable Radius Poletips
	Loop Coupled
	Minimized Multipole Content
Construction	Integral Vacuum/rf/structural Envelope
	OFHC Copper Structure Joined by Electroforming

Los Alamos National Laboratory
Accelerator Technology Division
Group AT−1

Los Alamos

AT-1

GRUMMAN

PRELIMINARY CONCEPT
of a
7 MeV 350 MHz RFQ LINAC
for the
ACCELERATOR PRODUCTION of TRITIUM

April 1993

SEGMENT
D

8.1 Meters

SECTION
D2

SEGMENT
C

SECTION
D1

SECTION
C2

SEGMENT
B

SECTION
C1

SECTION
B2

2.03 Meters
ea/SEGMENT

SECTION
B1

SEGMENT
A

SEE DETAIL A

SECTION
A2

HIGH
ENERGY
END

rf DRIVE LOOPS (12)

1.015 Meters
ea/SECTION

ELECTROFORMED JOINT
(4 per SECTION)

SECTION
A1

SPARE rf DRIVE PORTS (4)

COUPLING
PLATE

.28 cm GAP
BETWEEN VANE TIPS
AT SEGMENT INTERFACE

COOLANT FITTINGS
(40 per SECTION)

STABILIZER
ROD

FIXTURING/MOUNTING PADS
(8 per SECTION)

FIXED SLUG TUNERS
(24 per SEGMENT, 96 TOTAL)

LOW
ENERGY
END

VACUUM PUMP PORTS
(4 per SEGMENT)

PICKUP LOOPS
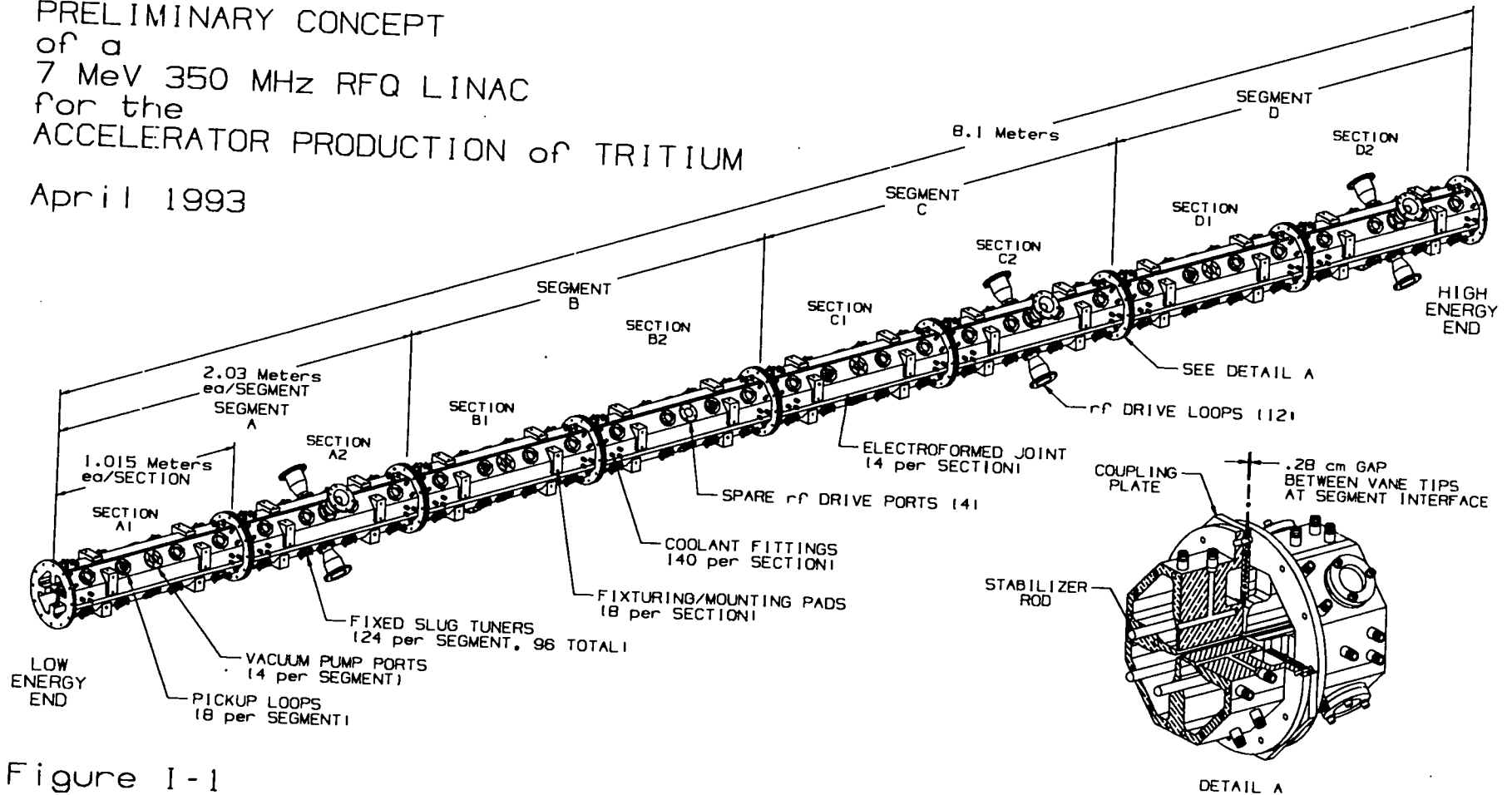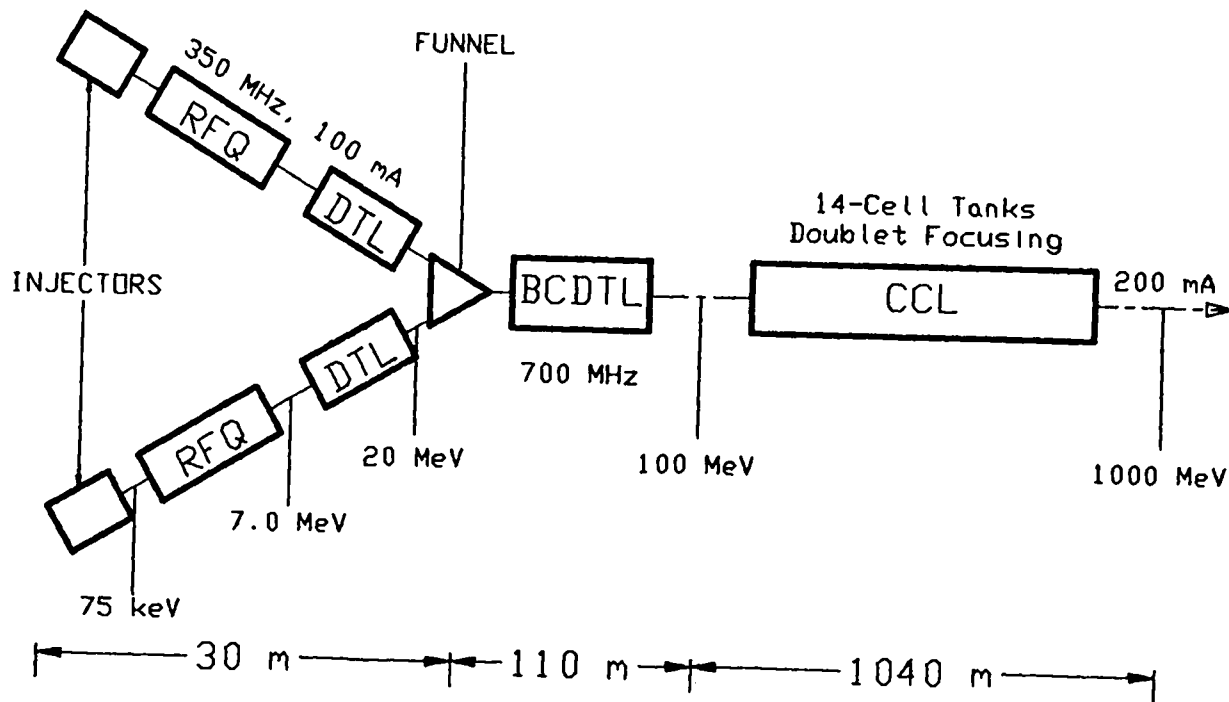(8 per SEGMENT)

DETAIL A

Figure I-1

Los Alamos National Laboratory
Accelerator Technology Division

Figure I-2:
APT Accelerator General Arrangement

There is limited experience in the operation of CW RFQ's, the majority of it residing at the Chalk River Nuclear Laboratory (CRNL)[5] and at LANL[6]. Thus far, CW RFQ's have only been operated up the 2.00 MeV[6]. Most of the problems associated with CW operation result from the rf thermal loads on the cavity. The 7 MeV RFQ poses new challenges. It will be the longest RFQ ever built, both physically and electrically. The solution to this has been found in the resonant coupling of shorter segments. Secondly, the cooling system will be a challenge because the power dissipated in the structure will not be longitudinally uniform. The thermal analysis of the APT RFQ is described in Section V.

The mechanical design of the APT RFQ is an extension of the mechanical design concept developed for the RFQ for the Beam Experiment Aboard a Rocket (BEAR) Project[7]. This concept incorporates four individual vane-cavity quadrants which are joined by electroforming to produce monolithic one-meter long sections. The concept design is described in Section IV with the fabrication plan described in Section VI.

The long electrical length produces concerns with regard to longitudinal stability which are to a large extent mitigated by the coupled-cavity concept. There is also the matter of rf tuning of the structure. The eight meter long structure will contain 128 fixed slug tuners. It is planned that the rf tuning of the APT RFQ be carried out by the method described in Reference 8. This scheme was utilized for the SSC and CWDD RFQ's. The tuning of the APT RFQ is described in Section VII.

The longest physical length of a 4-vane RFQ is currently the 7-meter long 100-MHz heavy ion RFQ "TALL" for the TARN II synchrotron[9]. At 100 MHz, the cavity cross-section diameter is 58 centimeters giving a length-to-diameter ratio of 12 which corresponds to a moderately stiff structure. The APT RFQ has a length-to-diameter ratio of 35. The bending stiffness of such a structure varies roughly as the inverse fourth power of the length to diameter ratio. Mechanical support of the long slender APT RFQ structure is thus a matter of concern. A concept design for this support is described in section VIII.

While the basic operational vacuum requirements of the APT RFQ are no different than for similar devices, the necessity of handling a full dump of the ion beam without exceeding 5×10^{-5} Torr is a unique requirement. The vacuum pumping system is described in Section IX.

II. BEAM DYNAMICS

DESIGN OF RFQ FOR APT

The APT system requires 100 mA of proton beam from each of the two 350 MHz RFQ's. The energy needs to be as high as possible for injection into the drift tube linac. Therefore, this RFQ design is 8 m long with an output energy of 7 MeV. A recent experiment with the CWDD RFQ[10] cold model shows that resonant coupling 2 m long segments together to form an 8 m long RFQ is feasible. The APT RFQ will consist of four resonantly coupled two meter sections

Using CURLI[11] and RFQUICK[12] for the first pass at this design gives a reasonable start. The rest of the design process is iterative. Make a change in the input file then run PARI and PARMULT[2]to check on the results then change the input file again.

Table II-1 shows the print out from CURLI for the basic design of the RFQ. The line that is underlined is the selected data for RFQUICK. CURLI generates a self consistent list of parameters that describe focusing, vane voltage and accelerating efficiency.

TABLE II-1

CURLI output screen showing the selected parameters of the APT RFQ.

```
Curli RFQ     1.00728   1ñ   -50ø   110mA   350.000MHz   0.075MeV   0.300MeV   67.0kV
BETA = 0.02529      WAVEL =   85.65      BETA*LAMBDA =   2.166    BZ =   0.301
```

m	A	chi	Field MV/m	dW/dz MeV/m	B	del	ani/ n,t,cm.mrad	/0	f	Ct amps	Cl amps
1.300	0.224	0.750	35.6	0.700	7.431	0.095	44.6 0.256	0.779	0.22	0.2355	0.1297
1.310	0.230	0.744	35.5	0.719	7.365	0.097	44.0 0.252	0.774	0.22	0.2305	0.1334
1.320	0.236	0.737	35.3	0.737	7.299	0.100	43.4 0.248	0.768	0.22	0.2256	0.1371
1.330	0.242	0.730	35.2	0.756	7.233	0.102	42.9 0.243	0.763	0.22	0.2208	0.1408
1.340	0.248	0.724	35.1	0.774	7.169	0.105	42.3 0.239	0.757	0.22	0.2160	0.1444
1.350	0.254	0.717	34.9	0.792	7.106	0.107	41.8 0.235	0.750	0.22	0.2114	0.1480
1.360	0.259	0.711	34.8	0.810	7.043	0.109	41.3 0.231	0.744	0.22	0.2067	0.1516
1.370	0.265	0.705	34.7	0.827	6.981	0.112	40.7 0.226	0.737	0.22	0.2021	0.1551
1.380	0.270	0.699	34.5	0.844	6.920	0.114	40.2 0.222	0.730	0.22	0.1976	0.1586
1.390	0.276	0.693	34.4	0.861	6.860	0.116	39.7 0.217	0.722	0.22	0.1932	0.1621
1.400	0.281	0.687	34.3	0.878	6.801	0.119	39.2 0.213	0.715	0.22	0.1888	0.1655
1.410	0.286	0.681	34.1	0.895	6.742	0.121	38.6 0.208	0.706	0.23	0.1845	0.1689
1.420	0.292	0.675	34.0	0.911	6.684	0.123	38.1 0.204	0.698	0.23	0.1802	0.1722
1.430	0.297	0.669	33.9	0.927	6.627	0.125	37.6 0.199	0.689	0.23	0.1760	0.1756
1.440	0.302	0.663	33.7	0.943	6.571	0.127	37.1 0.194	0.680	0.23	0.1719	0.1789
1.450	0.307	0.658	33.6	0.959	6.515	0.130	36.6 0.189	0.670	0.23	0.1678	0.1821
1.460	0.312	0.652	33.5	0.974	6.460	0.132	36.1 0.185	0.660	0.23	0.1637	0.1853
1.470	0.317	0.647	33.4	0.990	6.406	0.134	35.6 0.180	0.649	0.23	0.1597	0.1885
1.480	0.322	0.641	33.3	1.005	6.353	0.136	35.1 0.174	0.638	0.23	0.1558	0.1917
1.490	0.327	0.636	33.1	1.020	6.300	0.138	34.6 0.169	0.626	0.23	0.1520	0.1948

By running RFQUICK with data from CURLI, RFQUICK generates the following table and an input file for PARI. Table II-2 is a prescription for generating a·RFQ.

TABLE II-2

Summary of parameters generated by RFQUICK for this design.

```
Program RFQUICK  07/09/92  13:34:38
Parameters used in PARMULT input file RFQ.IN

The following design summary includes approximate lengths of the RFQ sections
and rf power estimates.

q   = 1              F   = 350.000 MHz      I   = 110.0 mA
M   = 1.00728 amu    B   = 6.981            in  =   0.020 Å cm rad (RMS)
Wi  = 0.075 MeV      A   = 0.265            V   =  67.0 kV
Wgb = 0.297 MeV      igb = -50.0 degrees    Nrm =   4 cells
Wf  = 1.000 MeV      if  = -40.0 degrees    Zp  =   0.150Zs
Ws  = 0.085 MeV      isr = -83.6 degrees

        Radial matching section length =      2.2 cm
                         Shaper length =     53.2 cm
                 Gentle buncher length =     74.7 cm
            Accelerator section length =    104.3 cm
                          Total length =    234.4 cm

                          Copper power =    156.6 kW
                            Beam power =    101.8 kW
                           Total power =    258.3 kW
```

z	B	phi	m	V	W	A	a	psi
-2.166	0.349	-90.000	1.000	0.067	0.075	0.000	1.225	360.000
0.000	6.981	-90.000	1.000	0.067	0.075	0.000	0.274	360.000
7.980	6.981	-90.000	1.015	0.067	0.075	0.009	0.272	360.000
19.285	6.981	-88.390	1.037	0.067	0.075	0.021	0.269	325.529
30.590	6.981	-86.780	1.060	0.067	0.077	0.034	0.266	310.714
41.895	6.981	-85.170	1.081	0.067	0.080	0.046	0.263	299.022
53.200	6.981	-83.560	1.101	0.067	0.085	0.058	0.261	288.911
71.801	6.981	-79.296	1.113	0.067	0.100	0.070	0.260	266.172
83.183	6.981	-75.360	1.126	0.067	0.115	0.081	0.258	248.075
91.285	6.981	-71.833	1.140	0.067	0.130	0.094	0.256	233.230
97.547	6.981	-68.694	1.156	0.067	0.146	0.107	0.254	220.766
102.640	6.981	-65.896	1.172	0.067	0.161	0.120	0.252	210.108
106.929	6.981	-63.392	1.190	0.067	0.176	0.134	0.250	200.858
110.630	6.981	-61.139	1.208	0.067	0.191	0.149	0.248	192.731
113.884	6.981	-59.100	1.228	0.067	0.206	0.164	0.246	185.517
116.789	6.981	-57.246	1.249	0.067	0.221	0.180	0.243	179.057
119.410	6.981	-55.552	1.271	0.067	0.236	0.196	0.241	173.228
121.799	6.981	-53.996	1.294	0.067	0.252	0.212	0.238	167.934
123.993	6.981	-52.561	1.318	0.067	0.267	0.229	0.236	163.097
126.022	6.981	-51.234	1.344	0.067	0.282	0.247	0.233	158.655
127.908	6.981	-50.000	1.371	0.067	0.297	0.265	0.230	154.557
232.234	6.981	-40.000	1.371	0.067	1.000	0.293	0.229	122.175

The discussion that follows assumes the reader is familiar with the input file to PARI and the use of CURLI and RFQUICK. RFQUICK gives an input file that is a good starting point, but it only generates a good design up to the end of the gentle buncher. The accelerator section is just a continuation of the same modulation, focusing strength, and voltage as at the end of the gentle buncher. Therefore, for this part of the design a final voltage of 1 MV was chosen. The design of the accelerator section from the end of the gentle buncher (0.3 MeV) up to 7 MeV is all done by hand. CURLI calculates the current limits at specified energies; by running CURLI with energies between 0.3 MeV and 7 MeV, appropriate values of the modulation, the focusing parameter "B" and the vane voltage can be selected based on the current limits. These values can then be used in the "zdata" part of the input file to PARI that describes the accelerator section. By running PARI multiple times the "z" position of each "zdata" entry in the accelerator section can be determined. The maximum vane voltage is determined by the maximum surface heating by the rf and by the peak electric field that could cause sparking. The peak electric field in this design was limited to 1.8 times the Kilpatrick criterion.

The formulas that CURLI uses to calculate transverse current limit and longitudinal current limit were added to the program PARI to calculate these limits at each cell in the RFQ. Figure II-1 shows a plot of these current limits versus position throughout the RFQ. These formulas do not take into account the higher order multipole fields. Therefore they can only be used as a guide.

Figure II-1

Longitudinal and transverse current limits in the APT RFQ.
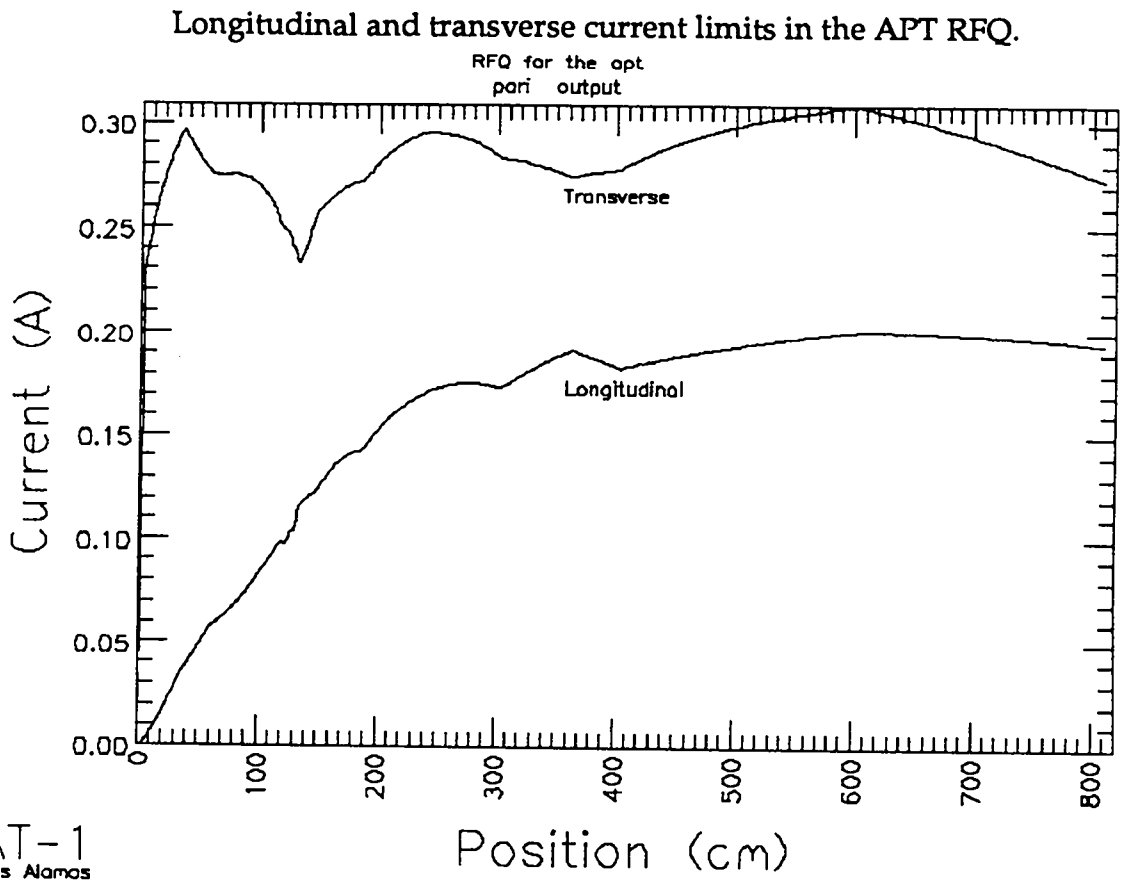
For this RFQ the requirement on the transverse current limit was established to be twice the required current, i.e., 200 mA. The rule of thumb for the longitudinal current limit is: at the 1 MeV point in the RFQ, the current limit should be at least 1.5 to 1.8 times the required current. The old rule of thumb for the longitudinal current limit of 2 times the required current was too restrictive. Requiring too large a longitudinal current limit reduces the transverse current limit.

Note that the longitudinal current limit is calculated for a single bunch. Therefore, when the modulation parameter "m" is 1.00, (i.e., no modulation) there is no longitudinal field that would keep the beam from spreading to infinite length. Thus the longitudinal current limit starts out as zero at the beginning of the RFQ. The current limit formulas show that as the modulation increases, the longitudinal current limit increases. At the beginning of the RFQ the beam is unbunched and therefore does not require any fields to keep the bunch from unbunching. The need for stronger longitudinal electric fields, to maintain the bunch, increases as the beam becomes more bunched. The longitudinal current limit is *a measure*

of the strength of the longitudinal fields. Therefore the longitudinal current limit should increase as the beam progresses along the RFQ.

RFQ designs with a small aperture at the entrance require the beam to be focused very strongly at the entrance aperture for proper matching to the RFQ. To relax the focusing required to match the beam to the RFQ requires a larger aperture and weaker focusing at the beginning of the RFQ. At the entrance to the RFQ, where m = 1, the focusing can be weaker and still have a large transverse current limit. CURLI and RFQUICK were used to design a radial matching section with a large aperture and weak focusing that would be easy to match the beam into. The "zdata" for the matching section in the design for the APT RFQ was replaced with this weak focusing matching section. Then the focusing parameter "B" in the "zdata" was replaced with interpolated values to smoothly increase the value of "B" to the original value at z = 32 cm. The beam diameter in this RFQ is smoothly reduced as it moves from the entrance to z = 32 cm where the focusing is at full strength.

Figure II-2 and Figure II-3 show various parameters that define the design of the APT RFQ. Both figures show the same parameters described below. Figure II-2 shows them versus cell number while Figure II-3 shows them versus position. The curve labeled "-phi/10 deg" shows the synchronous phase divided by 10°. The curve labeled "B" shows the unitless quantity that is a measure of the focusing strength. The curves labeled "r_0(mm)" and "a(mm)" show the average radius and radius of clear aperture respectively. The curve labeled "m" shows the modulation parameter defined by the following; let "a" be the distance of closest approach of a pair of opposing vane tips to the axis then "m×a" is the distance the adjacent vane-tips are from the axis at the same point.

Figure II-2
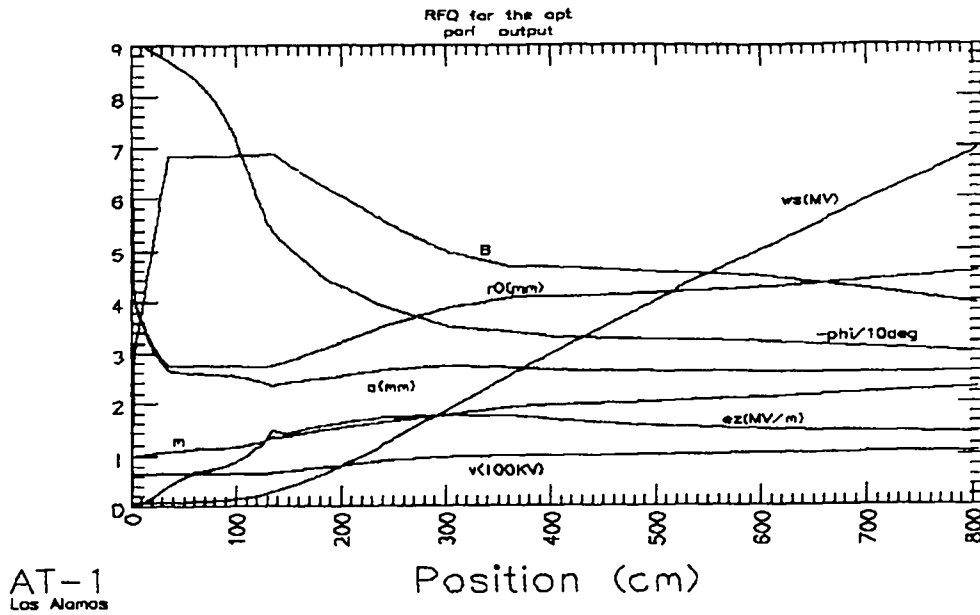Various parameters defining the RFQ design versus cell number.

RFQ for the apt
pari output
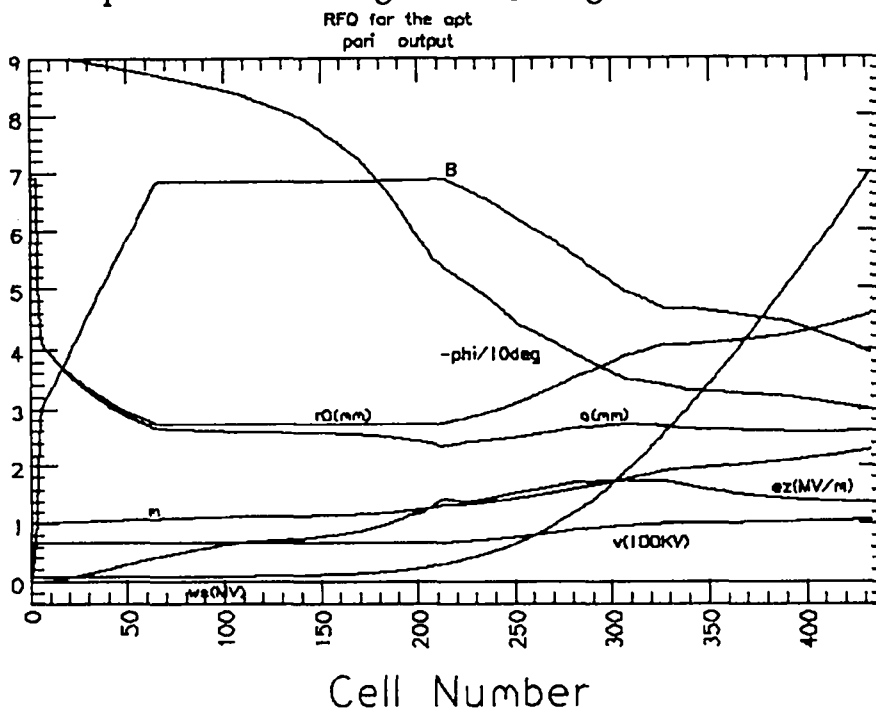
AT-1
Los Alamos

Cell Number

Figure II-3
Various parameters defining the RFQ design versus position.

AT-1
Los Alamos

Position (cm)

The curve labeled "v (100 kV)" shows the voltage difference between adjacent vane-tips in units of 100 kV. The curve labled "ws (MV)" shows the design energy of the beam along the RFQ.

Figure II-4 shows the peak electric field on the vane tips throughout the RFQ. The peak surface field chosen for this RFQ design was 1.8 times Kilpatrick's criterion.[13] This value of the peak surface field is the same as the peak surface field in the Chalk River RFQ1-1250 proton accelerator.[5] The rf conditioning to the design fields went smoothly in this CW RFQ.[14] Peak fields of 2.1 times Kilpatrick's criterion were reached in RFQ1-1250.

Figure II-4

Peak surface field in the APT RFQ design.

AT-1
Los Alamos

Position (cm)
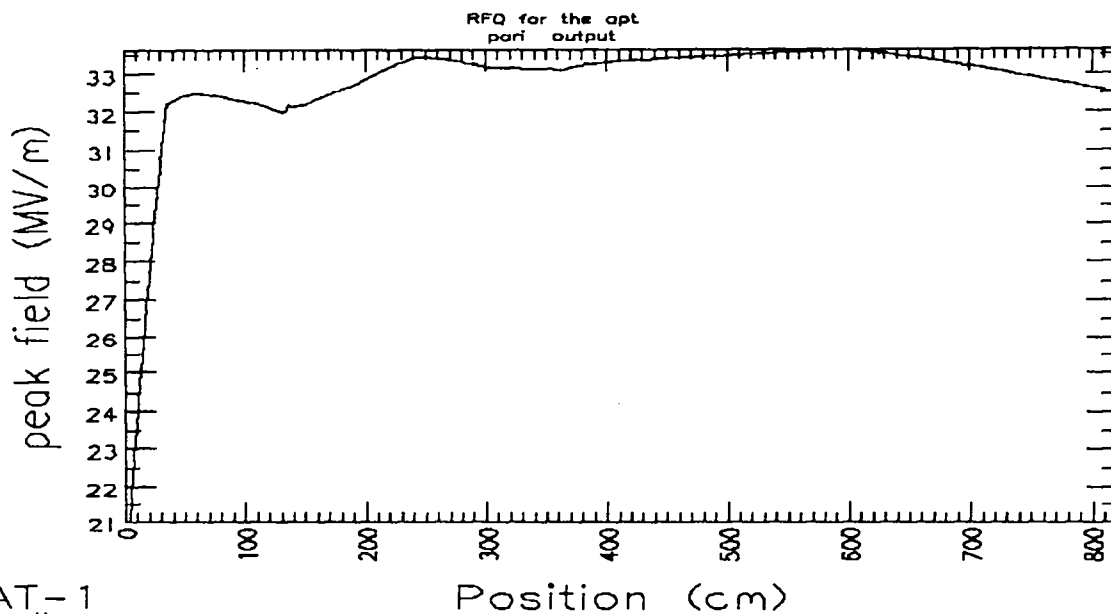
The APT RFQ was originally designed as a 3 MeV accelerator. An error study of this 3 MeV RFQ was performed and written up as Technical Note AT-1-92-281.[15] Figure II-5 through Figure. II-10 show the results of this error study with data points for the 7 MeV RFQ shown on the same figures. The transmission for the 7 MeV RFQ is almost the same as for the 3 MeV RFQ for the errors shown in these figures because most of the losses caused by the errors occur in the front end of the accelerator. Only a small fraction of the beam loss occurs between 3 MeV and 7 MeV. These simulations were carried out using PARMULT with 2D space charge calculations, with higher order multipoles and with image charges. The higher order multipoles are used to provide a more accurate calculation of the rf electric fields that focus and accelerate the beam. The image charge calculation uses a multipole expansion to approximate the effect of the image charge on the vane tips on the beam. PARMULT gives basically identical results to another version of PARMTEQ[16] called PGAVF[17] with 3D space charge and 3D image charge calculations on the 3 MeV RFQ. PGAVF does not include the effects of the rf multipoles. PGAVF calculation yielded 94.1% transmission with image charge calculation turned on and 93.2% transmission with the image charge calculation turned off. PARMULT with the higher order multipoles turned off and image charge calculation turned on gave a transmission of 95.7%. With the multipoles turned on and images turned off PARMULT gave a transmission of 94.2%.

Figure II-5
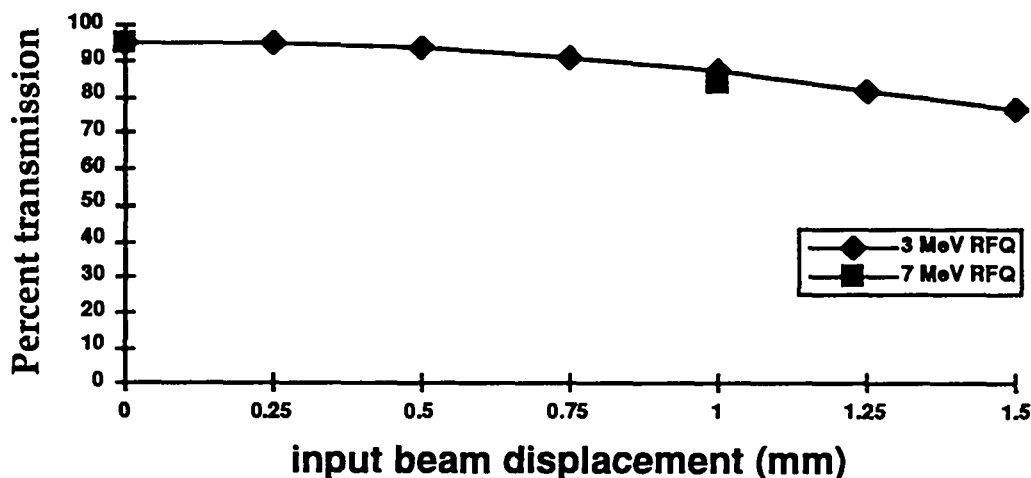## Beam transmission versus input beam displacement

Figure II-5 shows the transmission versus the displacement of the input beam. This shows the sensitivity to errors in alignment of the input beam. Figure II-6 shows the transmission versus beam steering errors into the RFQ. There is essentially no difference between the 3 MeV design and the 7 MeV design for these errors.

Figure II-6
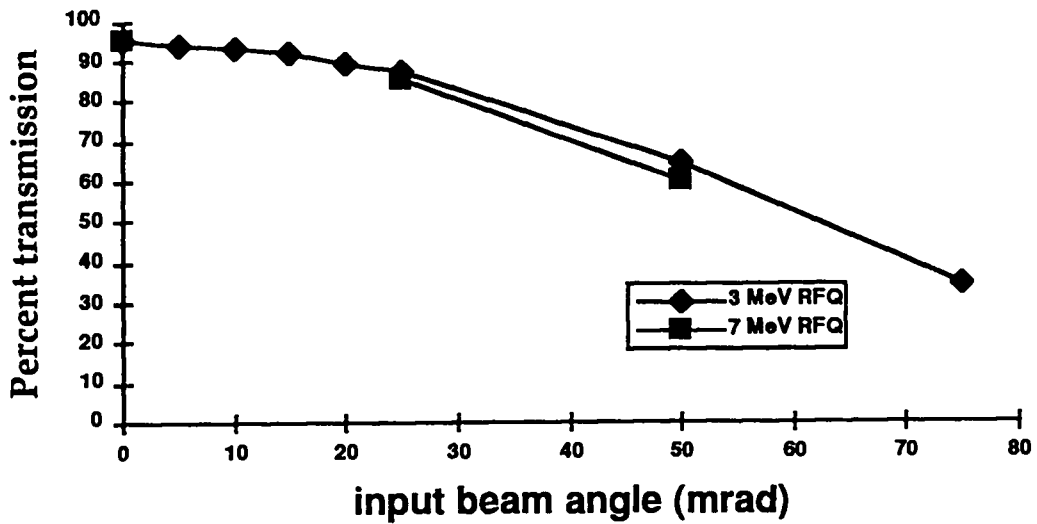## Beam transmission versus input beam angle

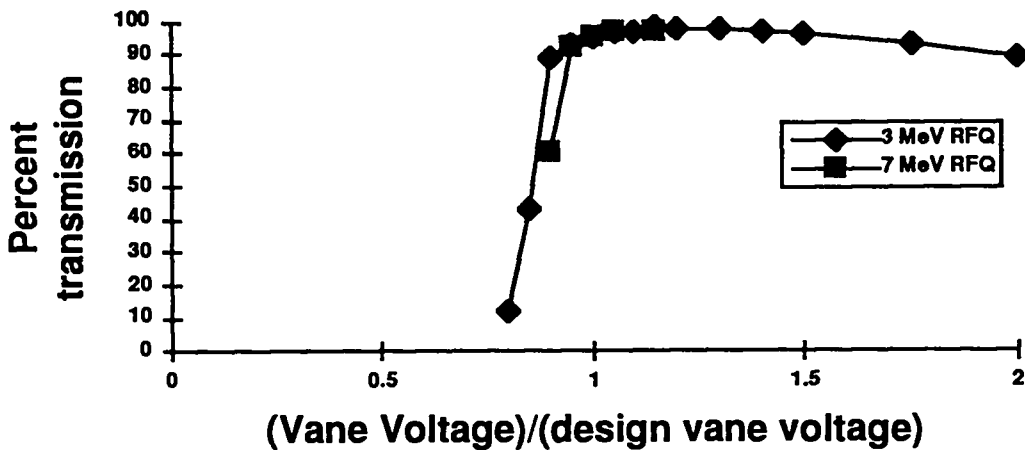Figure II-6: Beam transmission versus input beam angle (Percent transmission vs input beam angle (mrad)), with curves for 3 MeV RFQ and 7 MeV RFQ.

Figure II-7
Transmission versus vane voltage factor

Figure II-7: Transmission versus vane voltage factor (Percent transmission vs (Vane Voltage)/(design vane voltage)), with curves for 3 MeV RFQ and 7 MeV RFQ.

Figure II-7 shows a small problem with the current design of the 7 MeV RFQ. If the vane voltage is reduced 0.9 of nominal the transmission drops to 60% compared to 90% for the 3 MeV RFQ. This drop in transmission is caused by some of the beam falling out of longitudinal bucket. Because the accelerating gradient is lower than nominal, the bunch drops behind the synchronous particle and a large fraction of the beam simply falls behind and leaks out of the longitudinal accelerating bucket. This may or may not be a problem but it certainly establishes a tolerance on the tuning of fields in this RFQ. The fields in the high energy end of the RFQ must not be lower than about 95% of nominal.

The 7 MeV APT RFQ design limits the average power loading on the outer walls of the RFQ to about 12 watts per cm². The optimization procedure that minimized the power dissipation in the high energy region of the RFQ results in increased beam loss sensitivity with lower than nominal fields in this RFQ.

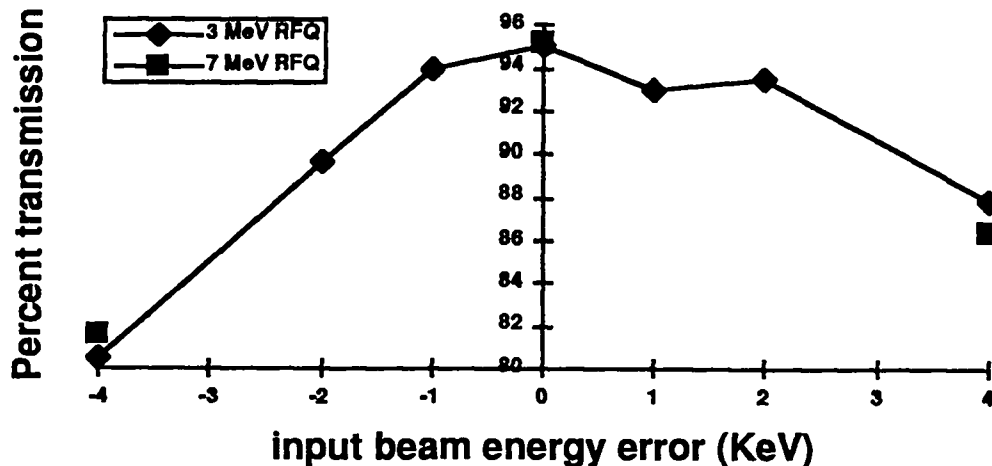**Figure II-8**
Effect of input beam energy shift from 75 KeV

Figure II-8 shows the effect on transmission if the input beam is not at the correct voltage. However, the input beam energy can be controlled within ±0.1 KeV of the desired value.

Figure II-9
Transmission versus input Emittance
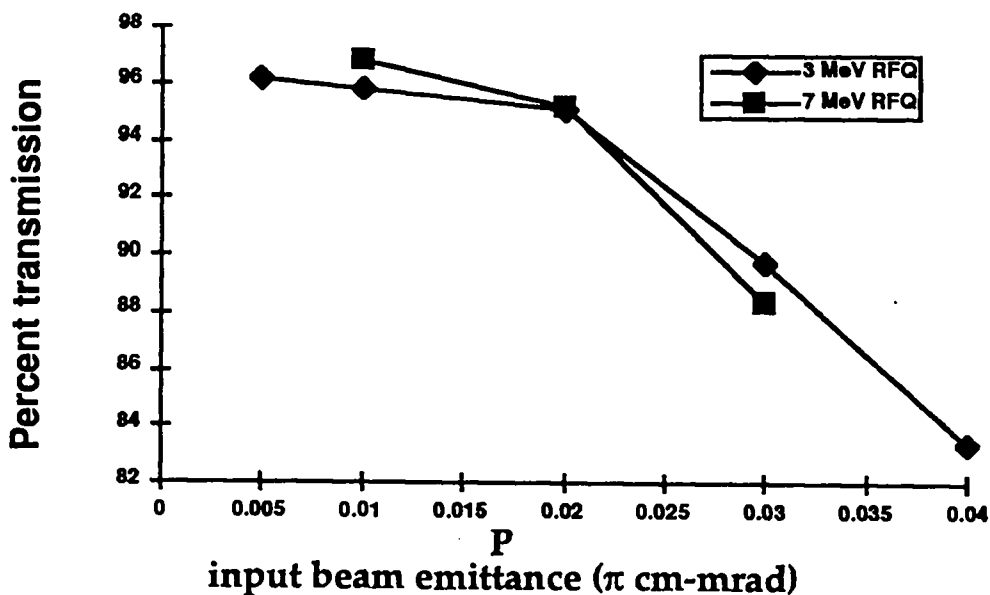
Figure II-9 and II-10 show a slightly greater transmission for some of the data points in the 7 MeV RFQ than in the 3 MeV RFQ. The reason for this is an improved method for calculating the input match used in the 7 MeV RFQ simulations. These RFQ designs are identical for the first 3 MeV. The low energy end of this RFQ has a tapered focusing section that makes matching the beam from the ion source into the RFQ easier than earlier RFQ's. The new matching procedure matches the beam at the end of the tapered focusing section, where the focusing is constant. The program TR2D then transports the beam backwards to the entrance of the RFQ to calculate the twiss parameters of the matched beam.

Figure II-10
Transmission versus input Current
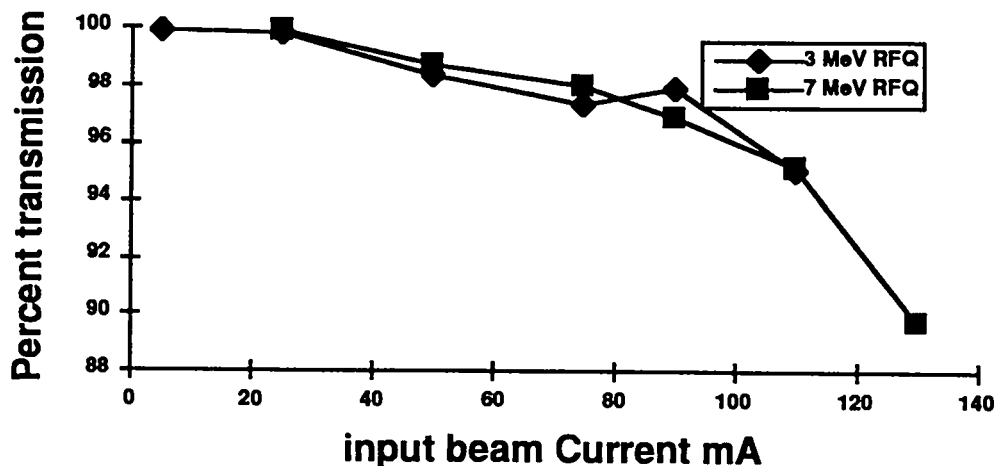
The comparison of the sensitivity to field tilts, shown in Figure II-11, in the 3 MeV and 7 MeV RFQ's is not as straightforward as the preceding error calculations. The tilt sensitivity for the 3 MeV RFQ has the tilt defined from one end to the other. A 10% tilt is defined as having fields equal to 90% of nominal at the low energy end and fields equal to 110% at the high energy end. The fields increase linearly from one end to the other. In this case the fields increase 20% in 4 meters or 5%/m. The 7 MeV RFQ has 2 m segments that are resonantly coupled. Perturbations that can cause field tilt in this accelerator will cause the field to have a saw tooth pattern. An equivalent perturbation in the 7 MeV RFQ to one in the 3 MeV RFQ might cause the same slope in a segment of 5%/m. However in this case the fields would have a saw-tooth pattern with fields varying ± 5%. A 5% field tilt is defined as a field that linearly increases from 95% at one end to 105% of nominal at the other end of a segment. The field would then jump down to 95% at the segment gap. The field would then increase from 95% at the start of this segment to 105% at the next segment gap and so forth. To compare the sensitivity of the 3 MeV RFQ to the 7 MeV RFQ the transmission will be plotted with respect to percentage tilt per meter.

Figure II-11
Transmission versus tilt factor
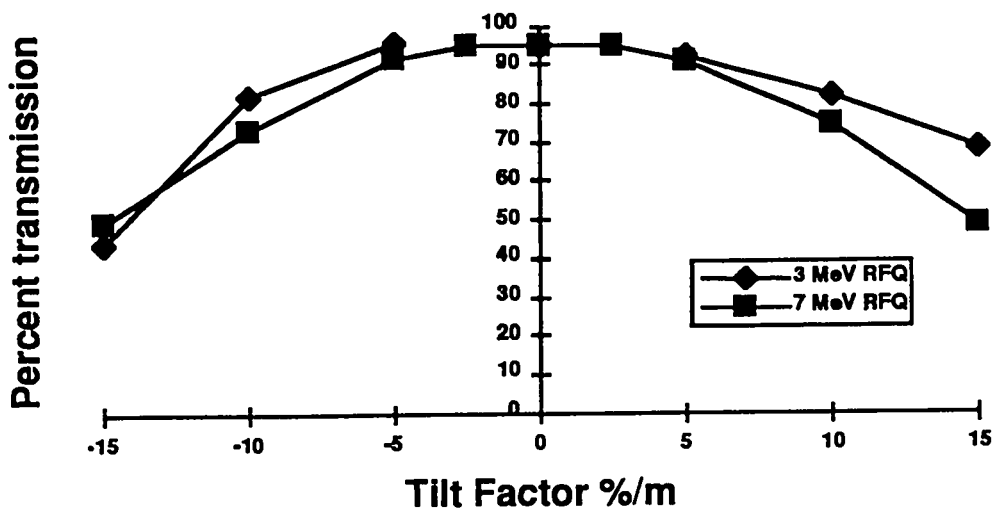
On the basis of these simulations a tolerance of about ±2.5% per m tilt with respect to the nominal field is required for good performance of the RFQ. Figure II-12 and Figure II-13 show that the performance of the RFQ with a 2.5% per m tilt is nearly as good as the performance (not shown) with ideal fields.

Figure II-12

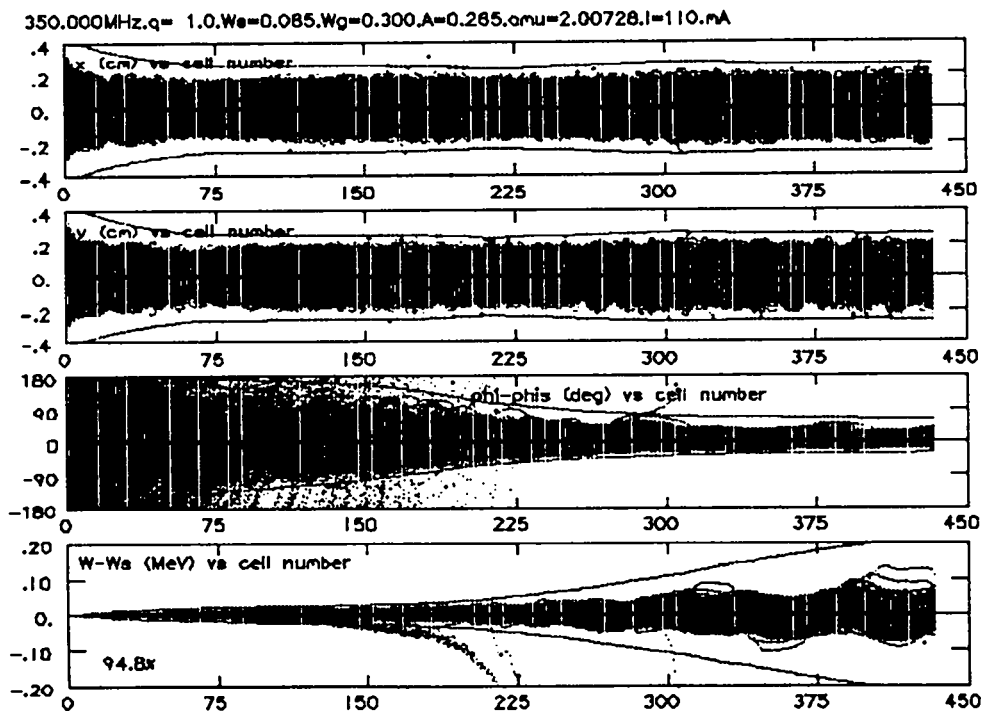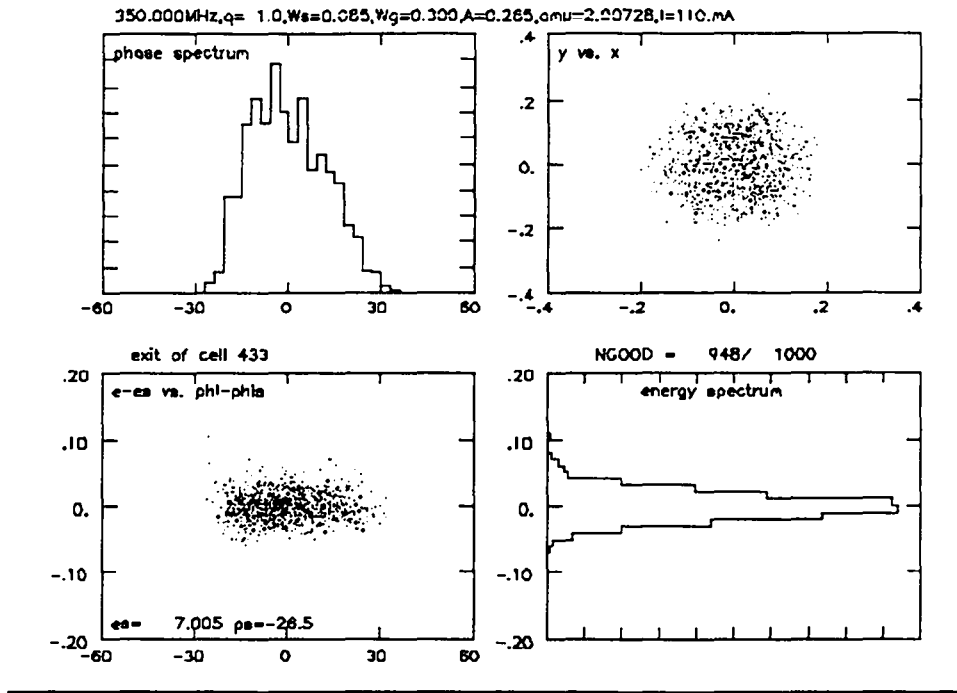PARMULT simulation of the APT RFQ with a 2.5%/m field tilt in each segment

Figure II-13

PARMULT simulation shows beam at end of the RFQ with 2.5%/m field tilt.

MULTIPOLES

The mathematical description of the electric potential used in the RFQ design codes has eight terms. The first four terms of the radial electric field (E_r) correspond to quadrupole, duodecapole, rf defocusing and the octupole field components respectively.

$$E_r = \frac{-V}{r_0}\left[A_{01}\left(\frac{r}{r_0}\right)\cos2\Theta + A_{03}\left(\frac{r}{r_0}\right)^5 \cos6\Theta + \left\{A_{10}\left(\frac{kr_0}{2}\right)I_0'(kr) + A_{12}\left(\frac{kr_0}{2}\right)I_4'(kr)\cos4\Theta\right\}\cos kz \right]$$

where $k = \frac{2\pi}{\beta\lambda}$

Alternate focusing and defocusing is not provided by the rf defocusing and octupole terms. The voltage varies at the rf frequency ($\cos\omega t$), while the beam moves along the z coordinate such that the factor ($\cos kz$) and the rf factors ($\cos\omega t$) both change sign with the same periodicity. Therefore, the defocusing fields can be very important even though these fields are an order of magnitude weaker than the primary quadrupole focusing fields. Figure II-14 show the relative contribution of the different radial electric components along the length of the RFQ. The quadrupole term is −1 and only the difference between 1 and the quadrupole is shown. The duodecapole, rf defocusing, and the octupole terms in the APT RFQ are significantly smaller than the same terms in the GTA RFQ.[18] They are also smaller than these terms in the SSC RFQ[2] that was designed for reduced multipole effects.

Figure II-14

Relative contribution of the first four terms of the multipole expansion
of the radial electric fields.

7 MeV RFQ for APT
parmult output

AT-1
Los Alamos
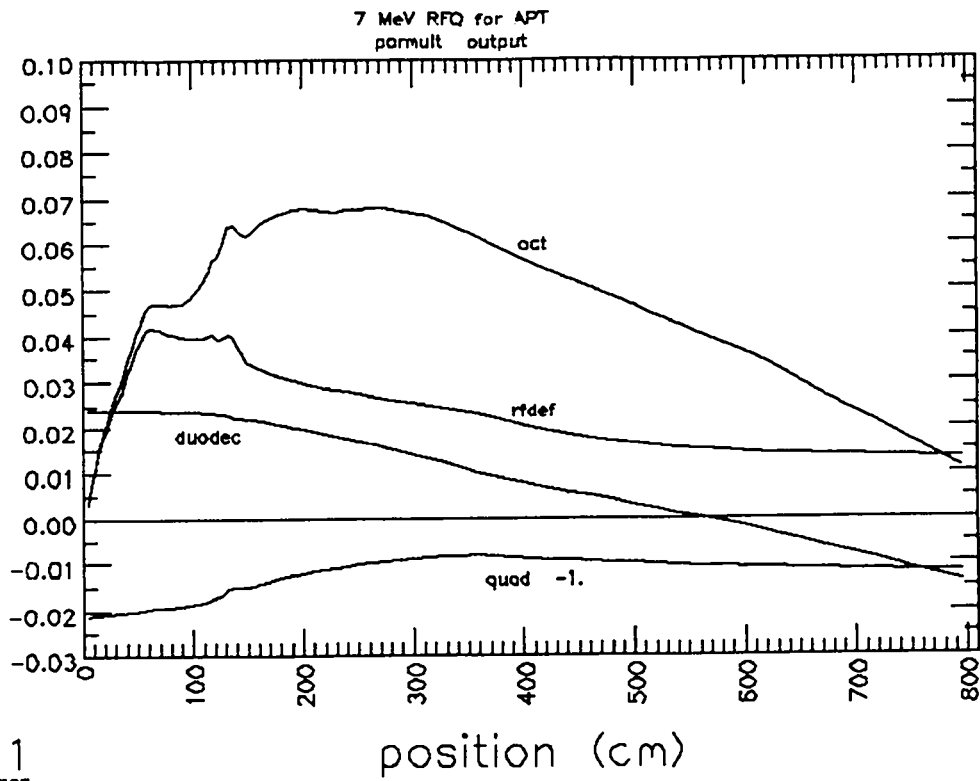
III. CAVITY DESIGN

The APT RFQ is 8.1 m long. The length is determined by the final energy which is 7 MeV. The DTL requires this energy because it uses electromagnetic quadrupoles for focusing the beam. The 7 MeV beam energy also allows a current independent match of the beam from the RFQ into the DTL. If the DTL used permanent magnet quadrupoles a lower energy RFQ could be used. However, permanent magnet quadrupoles may not tolerate the radiation conditions and the matching section could not be made current independent. The 7 MeV matching section from the RFQ to the DTL is much easier to build than a 3 MeV matching section.

The development of a method of resonant coupling shorter RFQ segments together made the 7 MeV RFQ feasible.[19] The resonant coupling provides longitudinal field stabilization. This method also provides a stop band in the dipole mode dispersion curve around the frequency of the RFQ. This stop band improves the transverse stability of the RFQ by eliminating dipole modes close to the frequency of the operating mode. Figure III-1 shows the quadrupole and dipole modes in the cold model for the CWDD RFQ. This figure shows the modes in the continuous RFQ without segments. It also shows the estimated frequencies of the additional modes in an unsegmented 8 m long RFQ.

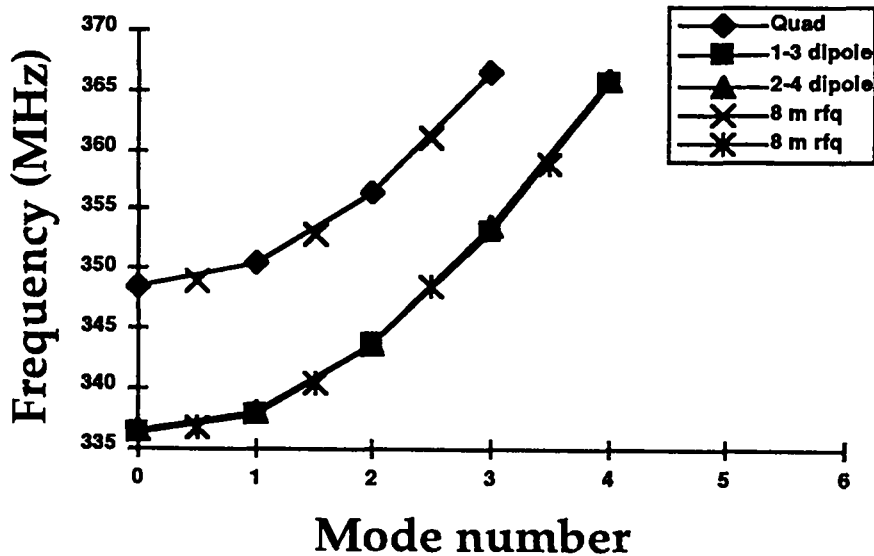## Figure III-1
Modes in CWDD RFQ cold model

Figure III-2
Dispersion curve of the modes in resonant coupled CWDD RFQ cold model
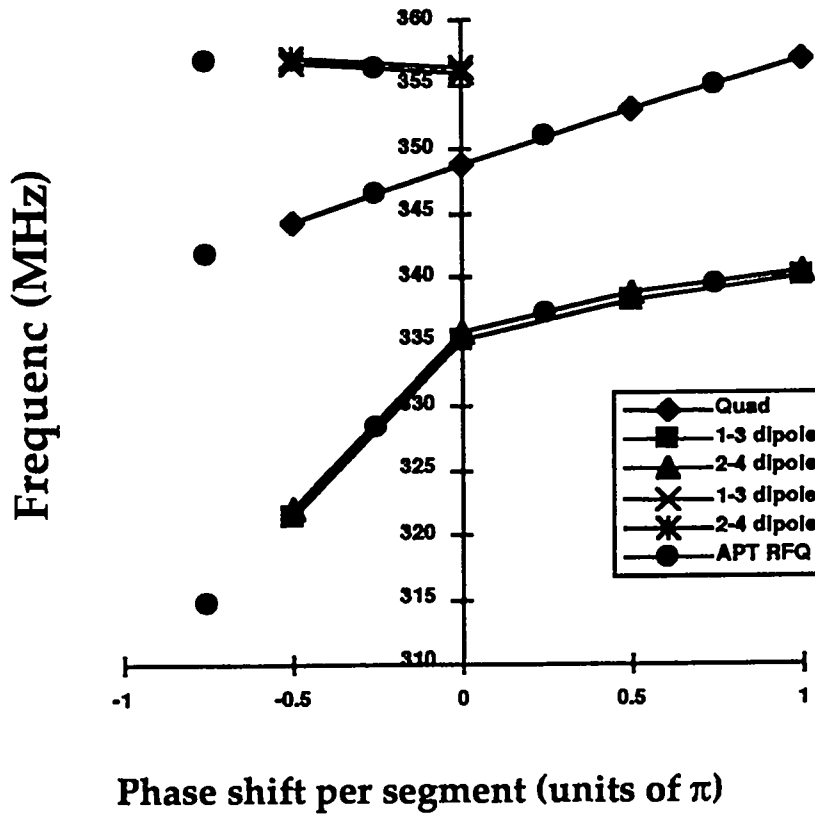

Phase shift per segment (units of π)

Figure III-2 shows the dispersion curve of this same cold model after it was modified with resonant coupling. These figures also show the estimated frequencies of additional modes (labeled APT RFQ) that occur in the 8m long RFQ. The operating mode is the quadrupole mode near 348 MHz in these figures. In Figure III-1 the operating mode is the quadrupole mode number 0. In Figure III-2 the operating mode is the quadrupole mode with 0 phase shift per segment. Note that the mode nearest the operating mode in both cases is a quadrupole mode. In the CWDD cold model the nearest mode is mode number 1 that is 2.1 MHz higher. Doubling this RFQ in length would make the nearest quadrupole mode only 0.5 MHz higher than the accelerating mode. That would probably make it untunable. The dipole could be moved away from the quadrupole mode in this RFQ but not more than about 2 MHz. In the segmented CWDD RFQ cold model with resonant coupling the nearest modes are at ± 4.45 MHz. In The APT RFQ the nearest modes will be at ± 2.2 MHz. Therefore perturbations will tend to mix these two modes equally and opposite with the operating mode. These nearest modes will have similar characteristics. Therefore, the effect of mixing one of these modes with the quadrupole accelerating mode is canceled by the other mode. This is one way of describing the stabilization of the fields in a compensated resonant coupled system.

However, in this RFQ with 2 m long segments the modes differ enough that the cancellation is not complete. In fact in some places there is no cancellation. The nearest dipole is about 8 MHz from the operating mode. This is better by a factor of two over the CWDD RFQ. It is also better than the 2.2 m long SSC RFQ that has dipole modes at ± 6.4 MHz from the operating mode.

Using the program RFQTUNE[9] an estimate of the tolerance to tuning errors of frequency shifts caused by rf heating can be made. A frequency error in one 2 meter segment of 160 KHz will cause the fields to deviate approximately 2.5% from the nominal. Figure II-8 shows that if the fields do not deviate by more than 2.5% there will be no discernible effect on the beam transmission. Therefore the resonant frequency of each 2 m segment in the 8 m long RFQ should be maintained within ± 80 KHz of nominal. The RFQ cooling system must control the frequency of each segment within this frequency range. Pickup probes will be placed at the end of each segment to sample the amplitude of the rf at that location. The amplitude of the rf sampled by these probes will depend on the frequency of the respective segment relative to the average frequency of the other segments. A dedicated water-system-control-computer will use the information from these probes and the phase difference between the rf input power and the cavity fields. This computer will control the water temperatures in each segment of the RFQ. In section V of this report, for example the coolant temperature in the base of the vane and in the wall was 41° F above the coolant temperature in the tip passage for zero frequency shift. This temperature difference will be different in each segment of the RFQ because the rf field strength is not constant. The power dissipated at the low energy end is about half the power dissipated at the high energy end. Figure III-3 shows the SUPERFISH[20] power estimates of the APT RFQ.

Figure III-3

Estimated rf power dissipated by the APT RFQ versus position.

RFQ for the opt
860KW (SF) 1.15MW (est. Cu)
File: POWER.QKP

AT-1
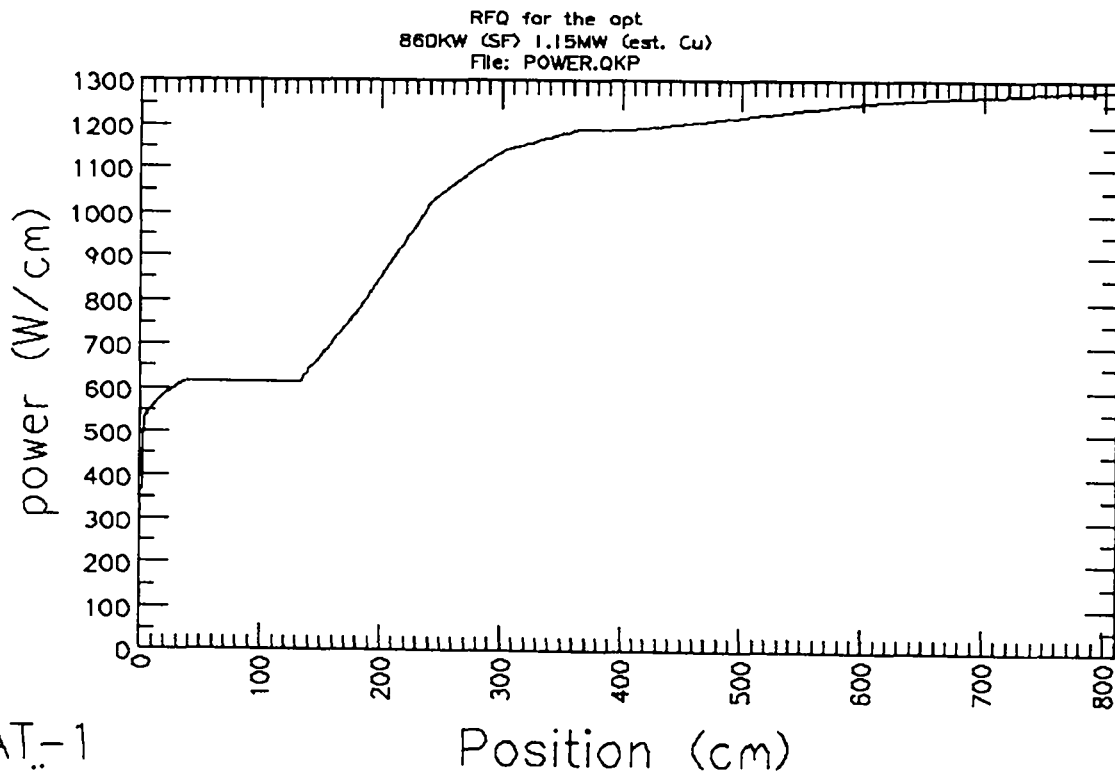
IV. DESIGN CONCEPT

The mechanical design concept of the APT RFQ structure is described in this section. The preliminary concept for the APT RFQ is shown on Figure I-1. The cavity dimensions at the high energy end are shown on Figure IV-1.The selected structural concept is an extension of that which was flown on the BEAR Project in 1988[7,21]. A second BEAR RFQ was fabricated for use in the Grumman industrial research laboratory. The same concept was also utilized for the CWDD Project[3] and for the SSC RFQ[1].

RFQ STRUCTURE:

The APT RFQ will consist of four resonantly-coupled two-meter long segments. Each segment is made up of two one-meter long sections. Each section is fabricated as four vane-cavity quadrants which are joined longitudinally by an electroformed high-strength copper joint. A cross-section of the cavity and the electroformed joint are shown on Figure IV-2. The main advantages of this concept are as follows:

- Integral Vacuum Vessel: The cavity walls form the vacuum vessel, thus minimizing the number of vacuum seals and allowing easy access to tuners, rf probes, drive loops, and coolant fittings. This eliminates any requirement for vacuum feedthroughs for utilities.

- No RF Joints: There are no longitudinal mechanical rf joints. This minimizes concerns regarding cavity Q degradation due to corrosion of rf seals and surfaces. In other CW RFQ applications, high power dissipation which resulted in high temperatures at such joints has been a problem. The electroformed joint concept produces a thick rf joint which is thermally continuous and has high thermal conductivity.

- RF Tuning Stability: The vanes are an integral parts of a monolithic structure. There is no stored mechanical energy to be released due to thermal cycling (or other causes) to produce changes in the mechanical alignment and rf tuning.

- High Structural Efficiency: The completed monolithic structure, with the exception of the tuners, drive loops, and pickup loops, is entirely load-carrying. This serves to mitigate the cost and complexity of the mechanical support system.

The electroformed joint concept produces a structure which is monolithic and in which the vanes are permanently aligned. One major advantage is that the rf field distributions within each section can be measured prior to the electroforming process. Details of the fabrication process are described in Section VI.

There are other concepts which have been used for four-vane RFQ's. One is the "bolted" structure where the independent vane-cavity elements are bolted together and longitudinal rf joints (e.g., C-seals) are used at the base of the vanes. This structure is then mounted inside a separate vacuum chamber. This arrangement was proposed for a CW RFQ for CULHAM Laboratories[22].

Los Alamos National Laboratory
Accelerator Technology Division
Group AT-1

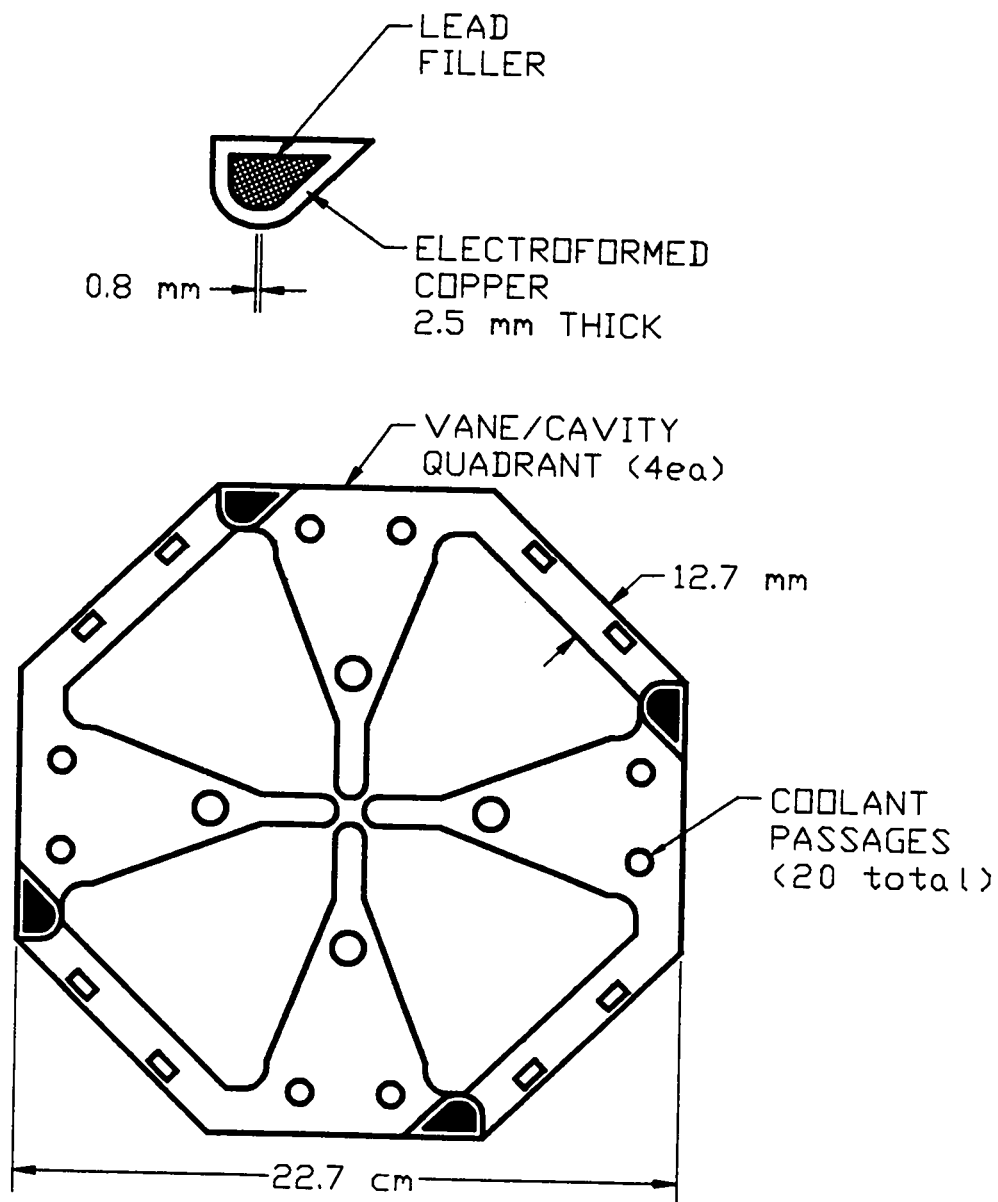## 350 MHz RFQ Linac for the Accelerator Production of Tritium

Figure IV-1:
Cavity Dimensions
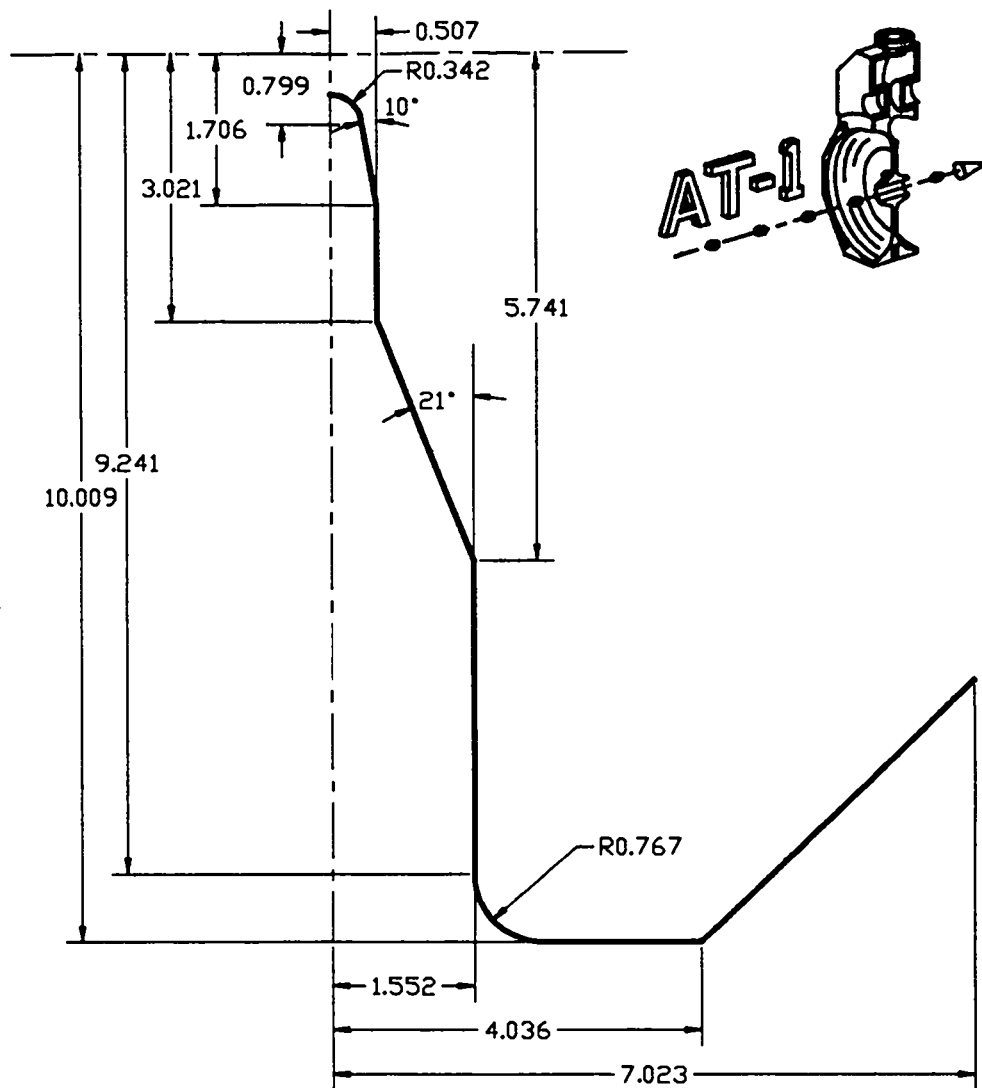
APT RFQ, HIGH ENERGY CROSSECTION
Revised: December 1992
Dimensions in Centimeters

Los Alamos National Laboratory
Accelerator Technology Division
Group AT-1
350 MHz RFQ Linac for the
Accelerator Production of Tritium

Figure IV-2:
Cavity Cross-Section

LEAD FILLER

0.8 mm

ELECTROFORMED COPPER 2.5 mm THICK

VANE/CAVITY QUADRANT (4ea)

12.7 mm

COOLANT PASSAGES (20 total)

22.7 cm

Another concept incorporates separate vanes which are mounted in a cylindrical cavity which forms the vacuum vessel. This arrangement also utilizes longitudinal rf seals at the base of the vanes. This concept has been utilized in CW RFQ's[5,6]. In both cases, problems were experienced with the longitudinal rf seals at the base of the vanes.

Both of these alternative concepts do have the advantage that the vanes are replaceable. In fact, the Chalk River CW RFQ is now operating with its second set of vanes; the replacements produce a higher energy beam.

While the electroformed joint technology is well-established and represents little risk in terms of cost, schedule, performance, or reliability, it is an expensive and time-consuming process. It would be desirable to substitute a joining process, such as welding, that would produce an equally monolithic, stable structure. Other RFQ concepts will be investigated at the time of final design. One concern is that under operating conditions the temperature of the structure in the vicinity of the electroformed joint will approach a value of about 80° F above the operating temperature. This could lead to local yielding in the electroformed joint area because of the difference between the thermal expansion coefficients of the copper substrate and the lead filler. One option under consideration would be to substitute plasma-sprayed copper for the lead filler. This would require a technical demonstration.

COOLING & RESONANCE CONTROL:

A comparison of CW RFQ designs is given on Table IV-1. Relative to CW RFQ's which have actually been fabricated, i. e., not including the LANL design proposed for the Culham Laboratories project which was cancelled, the item of major significance for the APT RFQ is the high surface heat flux. The APT RFQ has an average surface heat flux of 114 kilowatts per square meter, a factor of four greater than that of the CRNL1 RFQ. This results from the higher average power per unit length (150 kW/meter verses 65 kW/meter) along with the smaller cavity cross-section of the higher frequency APT RFQ.

The thermal and structural analysis of the APT RFQ is described in Section V. As a result of that analysis, it was determined that twenty coolant passages would be required. This is shown on Figure IV-2. By controlling the inlet temperatures of the coolant in the vane base and wall coolant passages at a temperature above the coolant in the tip passage, it is possible to minimize the frequency shift between power-off and power-on conditions.

Each section will have two sets of coolant passages running one-half the length of the structure. They will terminate on the sides of the rf port or vacuum port located at approximately the mid-length point of the section. Thus there will be total of 640 inlet or outlet coolant fittings on each of the APT RFQ's.

Resonance control will be by control of coolant temperatures. No active electro-mechanical tuner is planned at this time. There will be a number of thermal sensors, probably thermocouples, in each RFQ section.

TABLE IV-1

Comparison of CW RFQ's

Parameter		FMIT	CRNL	CRNL1	CULHAM	CWDD*	APT
Particle		H_2+	H+	H+	H-	D-	H+
Frequency	MHz	80.	267.	267.	352.	352.	350.
Injection Energy	MeV	0.070	0.050	0.050	0.100	0.200	0.075
Final Energy	MeV	2.000	0.600	1.270	2.000	2.000	7.000
Input Current	mA	105.	90.	86.	110.	92.	110.
Output Current	mA	100.	75.	75.	101.	80.	105.
Calculated Transmission	%	95.	83.	87.	91.	87.	95.
Current Limit	mA				200.	140.	215.
Length	Meters	4.00	1.47	1.47	2.52	3.97	8.10
Average Gradient	MeV/m	0.48	0.37	0.83	0.75	0.45	0.87
Wavelengths		1.00	1.31	1.31	3.00	4.66	9.48
Intervane Volt	KV				77.	92.	102.
Peak Surf Field	MV/m				33.5	33.7	33.6
Peak Surf Field	Kp	1.00	1.50	1.75	1.80	1.80	1.80
Total Power	KW	600.	133.	200.	410.	304	1923.
Beam Power	KW	193.	50.	105.	200.	144	963
Copper Power	KW	407.	83.	95.	210.	160.	1200.
Power/Length	KW/m	100.	56.	65.	84.	40.	150.
Power/Area	KW/m^2	4.	24.	28.	63.	30.	114.
Max Surf Power	W/cm^2		8.67	10.00	9.88	2.70	12.00
Max SF End Pwr	W/cm^2			60.00			65.00
Power Input		1LOOP	1LOOP	1LOOP	2LOOP	4LOOP	12LOOP

*Note: The CWDD RFQ operates at 35° K. The stated copper power includes the effect of high surface conduitivity.

MATERIALS:

For the purpose of the preliminary conceptual design, the material chosen for the APT RFQ is oxygen-free electronic copper (OFE, C10100). This issue should be revisited at the time of final design. A comparison of materials for RFQ's is given on Table IV-2. The requirement to dissipate the rf thermal load eliminates materials with lower thermal conductivity such as aluminum and steel from consideration even if the rf surfaces are copper-plated. The SSC and CWDD RFQ's were fabricated from tellurium-copper (C14500), a free machining copper generally produced by the addition of a very small amount of tellurium (~0.5%) to OFE copper. The machinability of tellurium-copper is 80 percent on the brass scale compared to the 20 percent of annealed OFE copper. However, tellurium-copper cannot be forged and electron-beam welding of it is a very unreliable process. It is planned that electron-beam welding be utilized to plug the ends of the coolant passages (Section VI). The trade-off of higher reliability coolant passage seals against higher machining costs seems worthwhile at this time.

The replacement vanes in the Chalk River RFQ[5] were fabricated from a GLIDCOP™ alloy, Al-15, an alumina dispersion-strengthened copper. This material has roughly 90 per-cent of the electrical and thermal conductivity of OFE copper while having a yield strength of up to 30000 #/in^2. Furthermore, the high yield strength is maintained through the hydrogen furnace brazing process. The suitability of GLIDCOP for various welding processes is not known at this time. Because of its high yield strength, GLIDCOP is potentially a desirable material for the APT RFQ and its use will be revisited at the time of final design.

Another high-strength, high-purity copper is zirconium-copper (C15000). Unfortunately tests have shown it to be incompatible with the electroforming process so it is removed from further consideration for the APT RFQ.

VACUUM SEALS:

It is currently planned that non-metallic vacuum seals be used on the RFQ because radiation-hard materials are not required at the relatively low (7 MeV) energy level. Ethylene-propylene rubber (Nordel™, Royalene™, or Epcar™) is more radiation resistant than fluorocarbon rubber (Viton™)[23]. In the event that metallic seals are required, the first choice would be indium. In the worst case, use of tellurium copper, OFE copper, or GLIDCOP would permit CONFLAT™ flanges to be brazed on for most vacuum seal locations; this would however not be possible at the section-to-section flanges. An alternative would be to utilize HELICOFLEX™ vacuum seals. The issue of vacuum seals will be revisited at the time of final design.

TABLE IV-2

Comparison of RFQ Materials

PROPERTY	OFE C10100	Te-Cu C14500	Zr-Cu C15000	GLIDCOP C15715	Al 6061-T6	Steel C1018
$\#/in^3$	0.323	0.323	0.323	0.322	0.098	0.283
E $\#/in^2$	1.7E+07	1.7E+07	1.7E+07	1.9E+07	1.1E+07	3.0E+07
E/ρ in	5.3E+07	5.3E+07	5.3E+07	5.9E+07	1.0E+08	1.0E+08
σ_y $\#/in^2$	9000	9000	58000	30000	30000	36000
σ_y/ρ in	2.8E+04	2.8E+04	1.8E+05	9.3E+04	3.1E+05	1.3E+05
Poissons	0.36	0.36	0.36	0.36	0.33	0.29
K Btu/hr-ft-F	226.	205.	210.	211.	104.	27.
C_p Btu/#-F	0.092	0.092	0.092	0.092	0.214	0.110
β ft^2/hr	4.40	4.00	4.20	4.20	2.90	0.50
α 1/F	9.6E-06	9.6E-06	9.6E-06	9.2E-06	13.1e-06	6.5E-06
β/α ft^2-° F/hr	4.7E+05	4.3E+05	4.5E+05	4.6E+05	2.2E+05	0.8E+05
IACS	101	93	93	90	43	13
R*K	2.3E+04	1.9E+04	2.0E+04	1.9E+04	4.5E+03	3.5E+02
R-plated*K	2.3E+04	2.1E+04	2.1E+04	2.1E+05	1.1E+04	2.7E+03
Cu-Plate	Not-Req'd	Not-Req'd	Not-Req'd	Maybe	Req'd	Req'd
Electroform	Yes	Yes	No	Yes	Yes	Yes
Machinability	20%	80%	20%	>20%	100	40
H^2 Furn Braze	Yes	Yes	?	Yes	No	Yes
E-BeamWeld	Yes	No	?	?	Yes	Yes
TigWeld	Yes	Yes	?	?	Yes	Yes
PREVIOUS RFQ'S	MANY	CWDD SSC	?	CRNL1	BEAR GAC/BEAR	CRNL FMIT

V. THERMAL/STRUCTURAL ANALYSIS

The thermal behavior of the RFQ during CW operation is a major concern. As shown on Table IV-1, the average thermal load resulting from the rf power for the APT RFQ, 114 kilowatts per square meter, is a factor of four greater than what has thus far been achieved during room temperature operation of a CW RFQ (CRNL @ 28 kw/m^2). The main consequence of a conclusion that the thermal loading is unacceptably large would be that the accelerating gradient would have to be reduced. This would result in a longer structure, possibly a fifth segment, with reduced transverse focusing strength - resulting in lower beam current. Thus, considerable attention was paid to this aspect of the design.

CAVITY THERMAL & STRUCTURAL ANALYSIS:

Finite element thermal and structural analyses (FEA) were carried out on the two-dimensional crossection of the cavity. The purpose of the two-dimensional analyses of the cavity was to determine the trade-offs between the use of twelve, twenty, and twenty-eight longitudinal coolant passages in each section. From the point of view of manufacturing costs, the least number of coolant passages would be more desirable. These options are shown on Figure V-1. The coolant passage locations were selected somewhat arbitrarily; there was no attempt to optimize their locations with respect to thermal and displacement distributions.

The sizes and locations of the coolant passages in the vane were selected such that each could be reached independently by radially-drilled holes at the same axial station. Thus, as the number of coolant passages is increased, their bore diameter must be reduced. The choice of wall thickness between the coolant passage and interior of the cavity is conservative. The coolant passages in the cavity wall are shown as rectangular. These would be milled and then the external covers would be applied either by electroforming (ala CWDD) or by electron-beam welding. Alternatively, these could be circular coolant passages which are deep-hole drilled in the same fashion as the passages in the vane area.

The FEA, SUPERFISH, and MAFIA models assumed symmetry at the mid-plane of the vane whereas in fact the presence of the electroformed joint is asymmetric with respect to the mid-plane. This asymmetry would only affect the FEA models and this will need to be considered at the time of final design.

The thermal loads from the SUPERFISH analysis are shown on Figure V-2. Past experience has shown that RFQ's typically achieve cavity Q's in the range of 70 to 80 percent of the SUPERFISH value with those having longer electrical lengths having values near the higher end of the range. Most of the losses relative to the SUPERFISH predictions occur in the vicinity of penetrations and in the end regions. For the sake of these two-dimensional scoping analyses, a ten per-cent enhancement of the SUPERFISH heat loads shown on Figure V-2 was utilized. The material properties utilized for the analyses are given on Table V-1.

Los Alamos National Laboratory
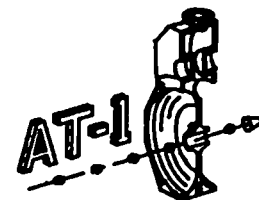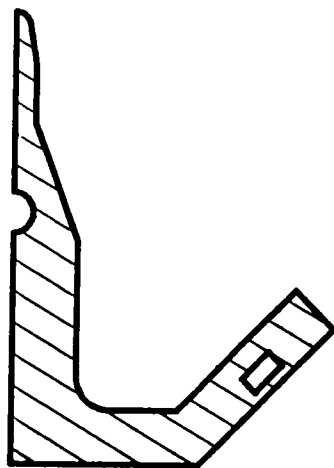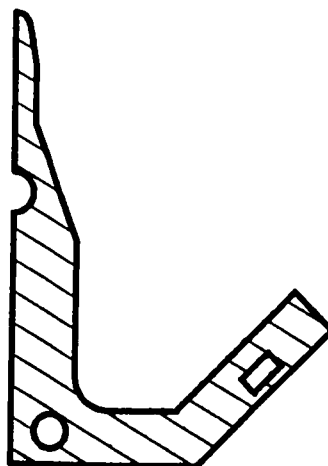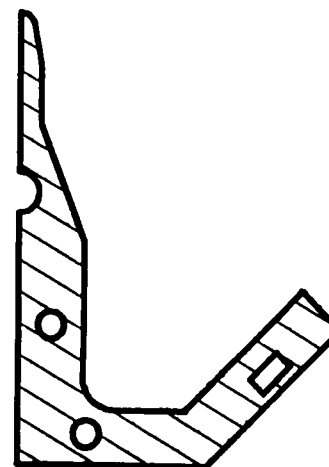Accelerator Technology Division
Group AT-1

Figure V-1:
Coolant Passage Options for the
350 MHz RFQ Linac for the
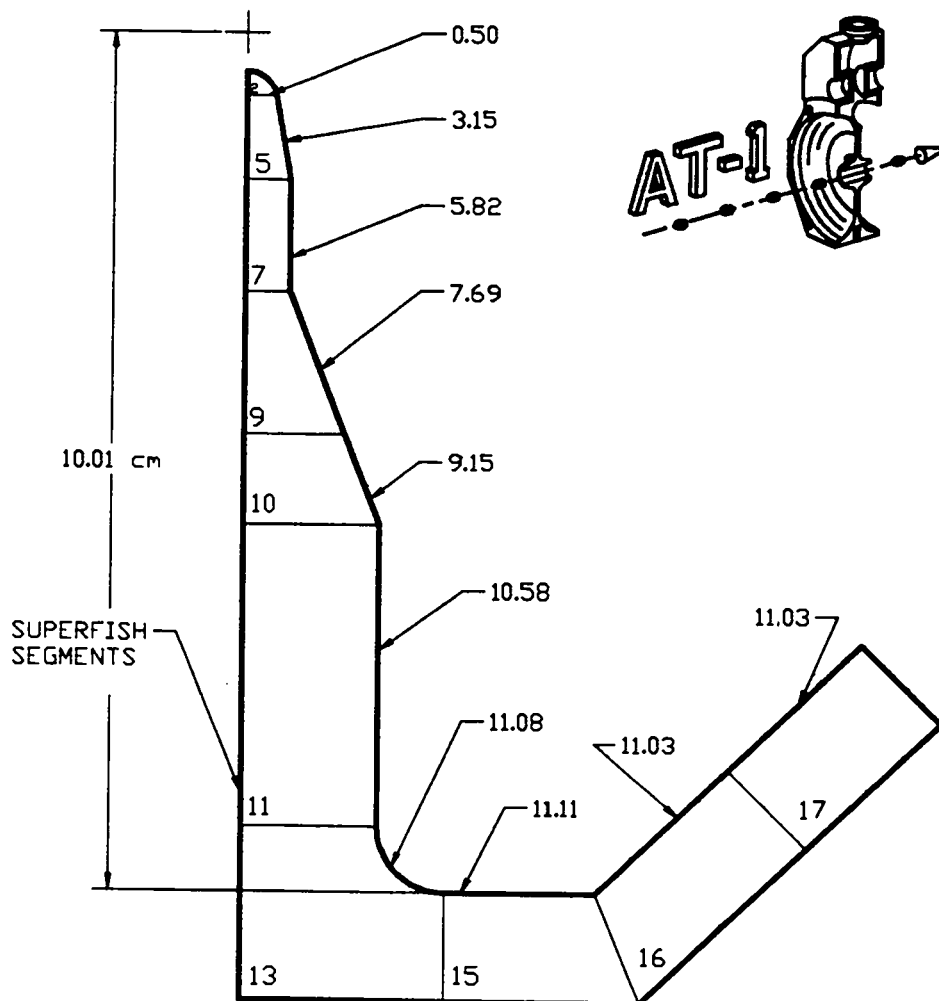Accelerator Production of Tritium

OPTION A
12 COOLANT PASSAGES

OPTION B
20 COOLANT PASSAGES

OPTION C
28 COOLANT PASSAGES

Los Alamos National Laboratory
Accelerator Technology Division
Group AT-1
350 MHz RFQ Linac for the Accelerator Production of Tritium

Figure V-21
CW Heat Loads for OFE Copper
Watts/Cm^2
Total = 1205 Watts/cm-length

APT RFQ, HIGH ENERGY CROSSECTION
Revised December 1992

TABLE V-1

Thermal & Structural Properties For FEA

k thermal conductivity	18.8	Btu/hr-in-° F
C_p specific heat	0.092	Btu/#-° F
ρ density	0.323	#/in^3
E modulus of elasticity	1.7×10^7	#/in^2
ν Poisson's ratio	0.36	
α thermal expansion coefficient	9.6×10^{-6}	1/° F

Steady state, constant property analyses were performed. For the preliminary analyses, the coolant passages were "clamped" at the ambient temperature. This effects the assumptions that both the film coefficients and the fluid thermal capacity are infinite. The results are thus the absolute minimum value for the temperature rise in the cavity. For these analyses, the ambient temperature is taken as 0° Fahrenheit. Thus the resulting temperatures are in fact "increases above ambient." The results of the deflection analyses were convolved with the SUPERFISH segment frequency shift values to determine the thermally-induced frequency shift. The results are given on Table V-2 and shown on Figures V-3 (Option A), V-4 (Option B) and V-5 (Option C).

TABLE V-2

Thermal/Structural/Frequency Calculations For Three Coolant Path Options Case 1, Coolant Passage Temperatures Clamped @ 0° F

OPTION	# of PASSAGES	MAX δT °F	δ_{tip} inch	δ_{base} inch	σ_{max} #/in^2	δFreq MHz
A	12	41	0.000126	-.000883	1511	-1.99
B	20	29	0.000273	-.000260	1006	-2.52
C	28	28	0.000159	-.000201	629	-1.55

It is interesting to note that the tip deflection and frequency shift for Option A are less than the values for Option B. The reason for this is clear from the temperature plots, Figures V-3 and V-4. For Option A, there is no coolant passage at the base of the vane. Thus, the maximum temperature is in this region. The mean temperature rise of the cross-section is greater for Option A than for Option B, thus the entire cavity expands outward, mitigating the inward expansion of the vane tip. Therefore, the frequency shift is less than in the case of Option B.

One deficiency in Option A is related to the presence of the electroformed joints (see Figure IV-1). Figure V-3 shows a high temperature gradient in this area. Furthermore, depending upon the joint filler selected, the effective thermal conductivity in the joint area might be significantly reduced. For this reason, Option A was rejected.
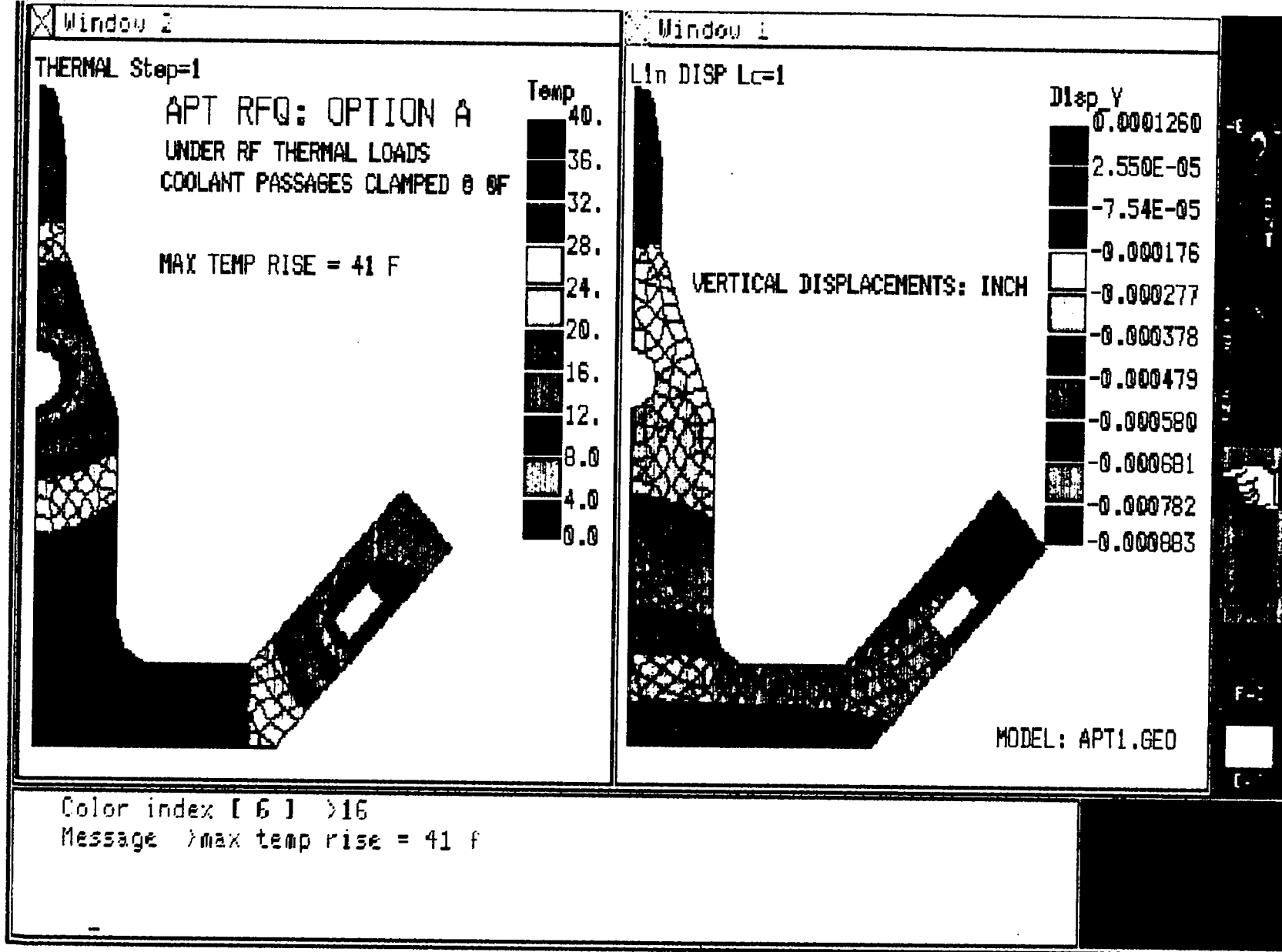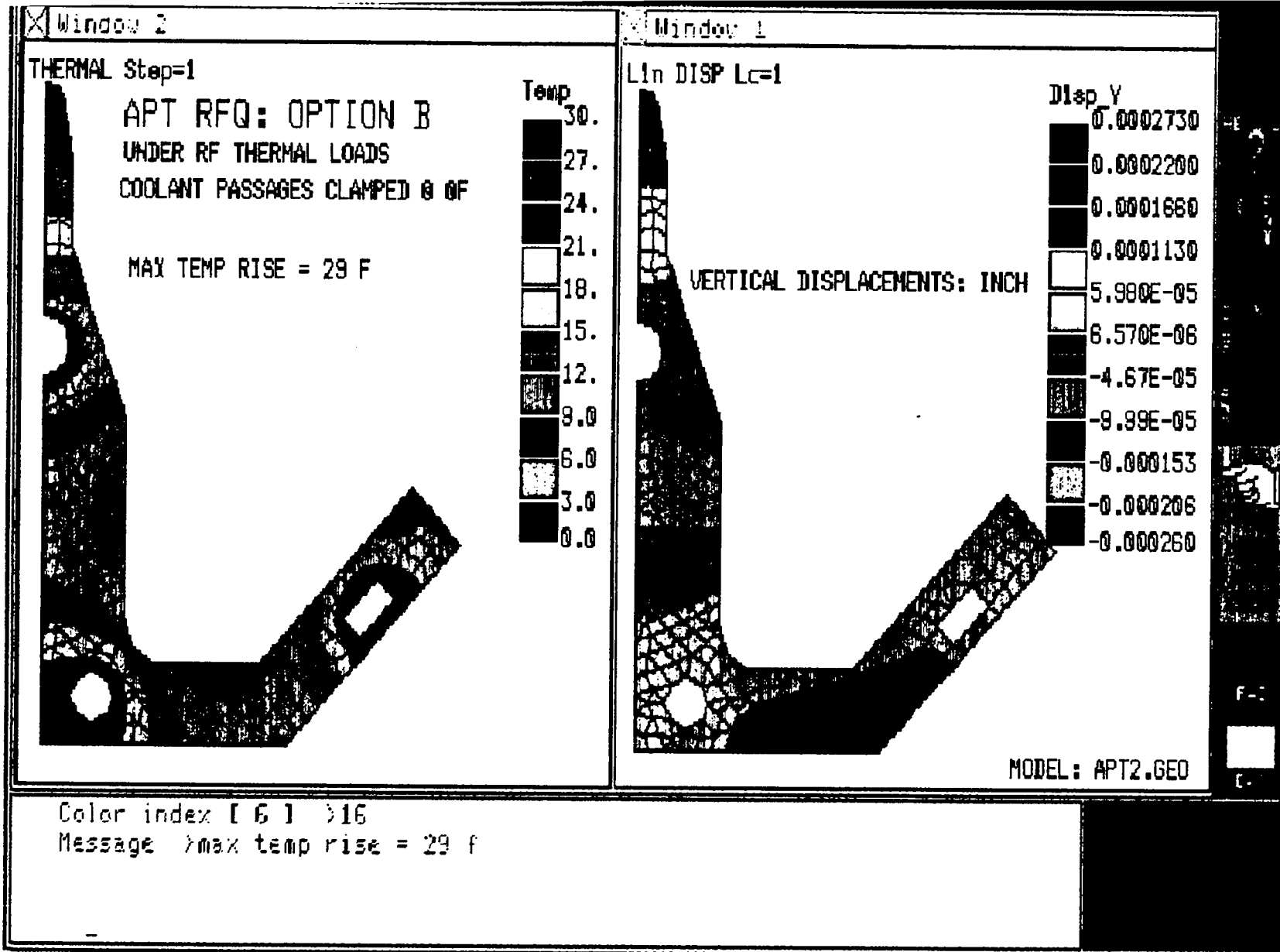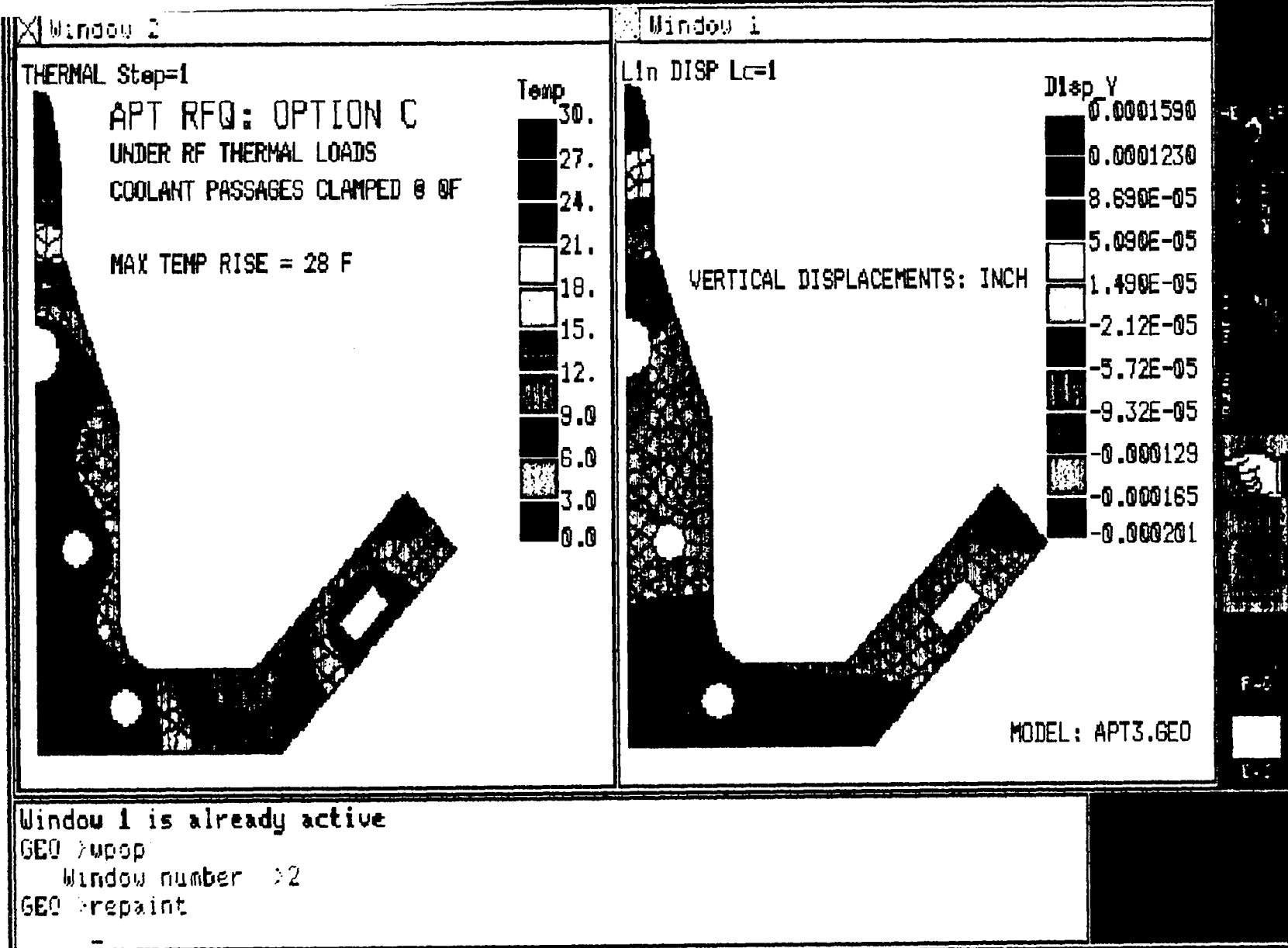
FIGURE V-3

FIGURE V-4

Window 2

THERMAL Step=1

APT RFQ: OPTION C

UNDER RF THERMAL LOADS

COOLANT PASSAGES CLAMPED @ 0F

MAX TEMP RISE = 28 F

Temp
30.
27.
24.
21.
18.
15.
12.
9.0
6.0
3.0
0.0

Window 1

Lin DISP Lc=1

VERTICAL DISPLACEMENTS: INCH

MODEL: APT3.GEO

Disp_Y
0.0001590
0.0001230
8.690E-05
5.090E-05
1.490E-05
-2.12E-05
-5.72E-05
-9.32E-05
-0.000129
-0.000165
-0.000201

Window 1 is already active
GEO >wpop
    Window number >2
GEO >repaint

FIGURE V-5

For the sake of preventing long term erosion of the coolant passages, the maximum allowable bulk velocity of the coolant has been established as 15 feet per second. The analysis was also run with this bulk velocity and with actual film coefficients for fully developed flow of water. The results are given on Table V-3. The differences between Options B and C are not significant, in part because the coolant passages in the vane base for Option C are reduced in cross-section to allow radial feed holes to be drilled. Given the limitation of 15 feet per second maximum bulk velocity, Option C does allow for more coolant to be pumped than in the case of Option B. However, the difference, 77 GPM for Option C verses 69 GPM for Option B, is not significant. For this reason, Option B, with a total of 20 coolant passages in the full cross- section, was selected.

TABLE V-3

Thermal/Structural/Frequency Calculations For Three Coolant Path Options
Case 2, Coolant Passage Bulk Velocity 15 ft/sec @ 0° F

OPTION	# of PASSAGES	MAX δT oF	δ_{tip} inch	δ_{base} inch	σ_{max} #/in²	δFreq MHz
A	12	71	0.000366	-0.001927	1710	-4.94
B	20	52	0.000456	-0.000746	1169	-4.59
C	28	47	0.000203	-0.000709	880	-2.46

For Option B, a separate FORTRAN program was written to enclose the FEA program within an interation loop which varied the temperatures of the base and wall coolant to achieve a zero frequency shift of the cavity between power-off and power-on conditions. It would also be possible to vary the coolant flow rates but it is clearly desirable to utilize the maximum coolant flow rates in all three passages in order to minimize the longitundial variations of temperature and local frequency. The result was that the temperatures of the base and wall coolant should be 41° F above the coolant in the tip passage.

END REGION DESIGN:

Each of the four segments is individually resonant. There is an undercut of the vanes at each end of each segment. This is necessary in order to correct the droop in the fields at the end of each segment which results from the segment's finite length. The volume of the undercut was determined empirically from resonant frequency and rf field distribution measurements performed on the four-meter long, two segment low power "Cold Model" RFQ[24]. Two types of undercut regions were considered: tapered, Figures V-6 and V-7 and rectangular, Figures V-8 and V-9. The advantage of the rectangular undercut is that sealing the end of the coolant passage is greatly facilitated. Furthermore, any trimming of the undercut depth for final tuning is much more straight-forward with the rectangular undercut.
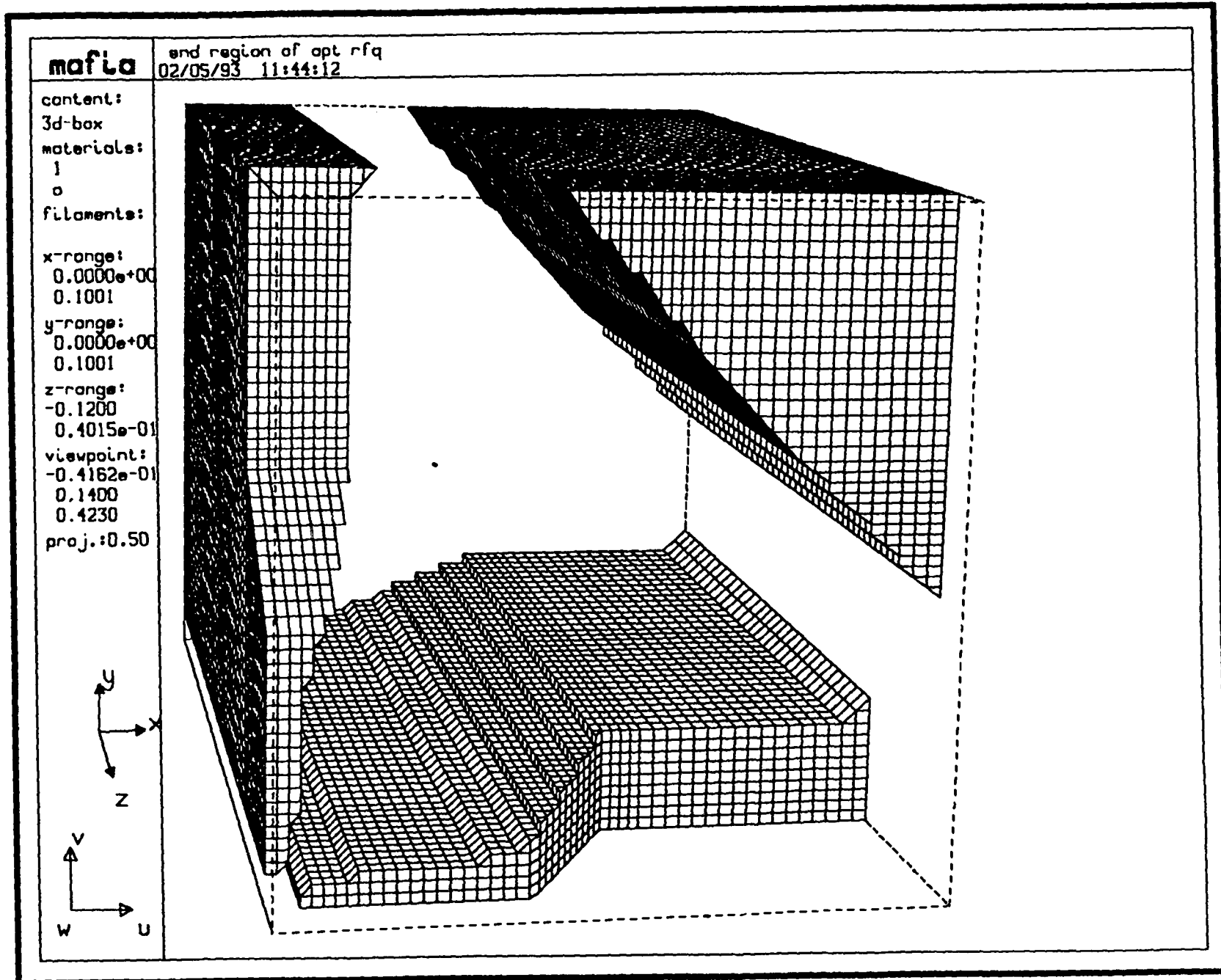
mafia
end region of opt rfq
02/05/93 11:44:12

content:
3d-box
materials:
1
o
filaments:

x-range:
0.0000e+00
0.1001

y-range:
0.0000e+00
0.1001

z-range:
-0.1200
0.4015e-01

viewpoint:
-0.4162e-01
0.1400
0.4230

proj.:0.50

FIGURE V-6: Tapered Undercut

Los Alamos National Laboratory
Accelerator Technology Division
Group AT-1

Figure V-71
Tapered End Undercut for the
350 MHz RFQ Linac for the
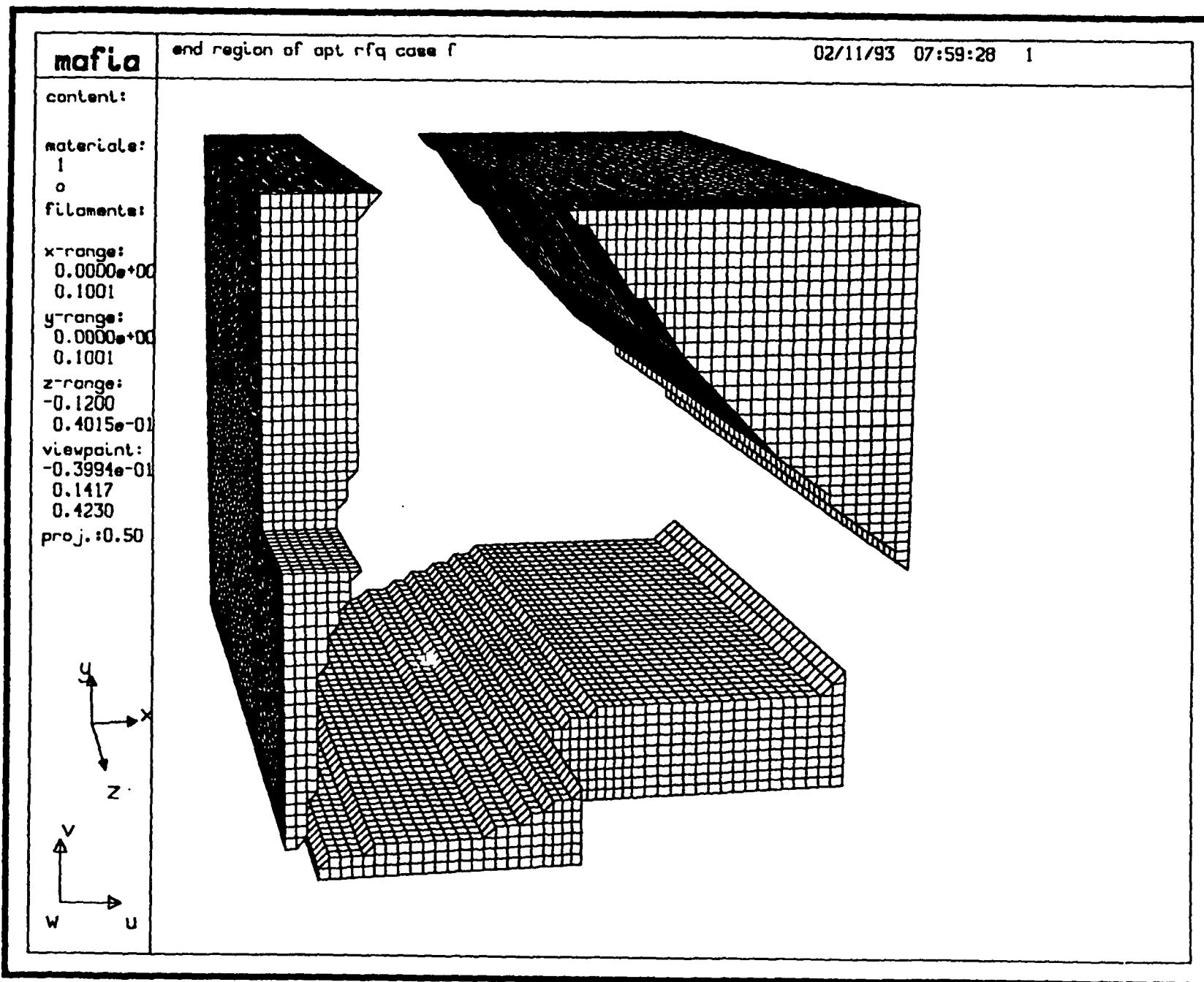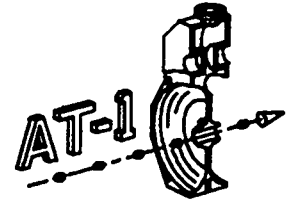Accelerator Production of Tritium
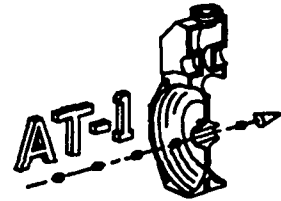
Revised: December 1992 Dimensions in Centimeters
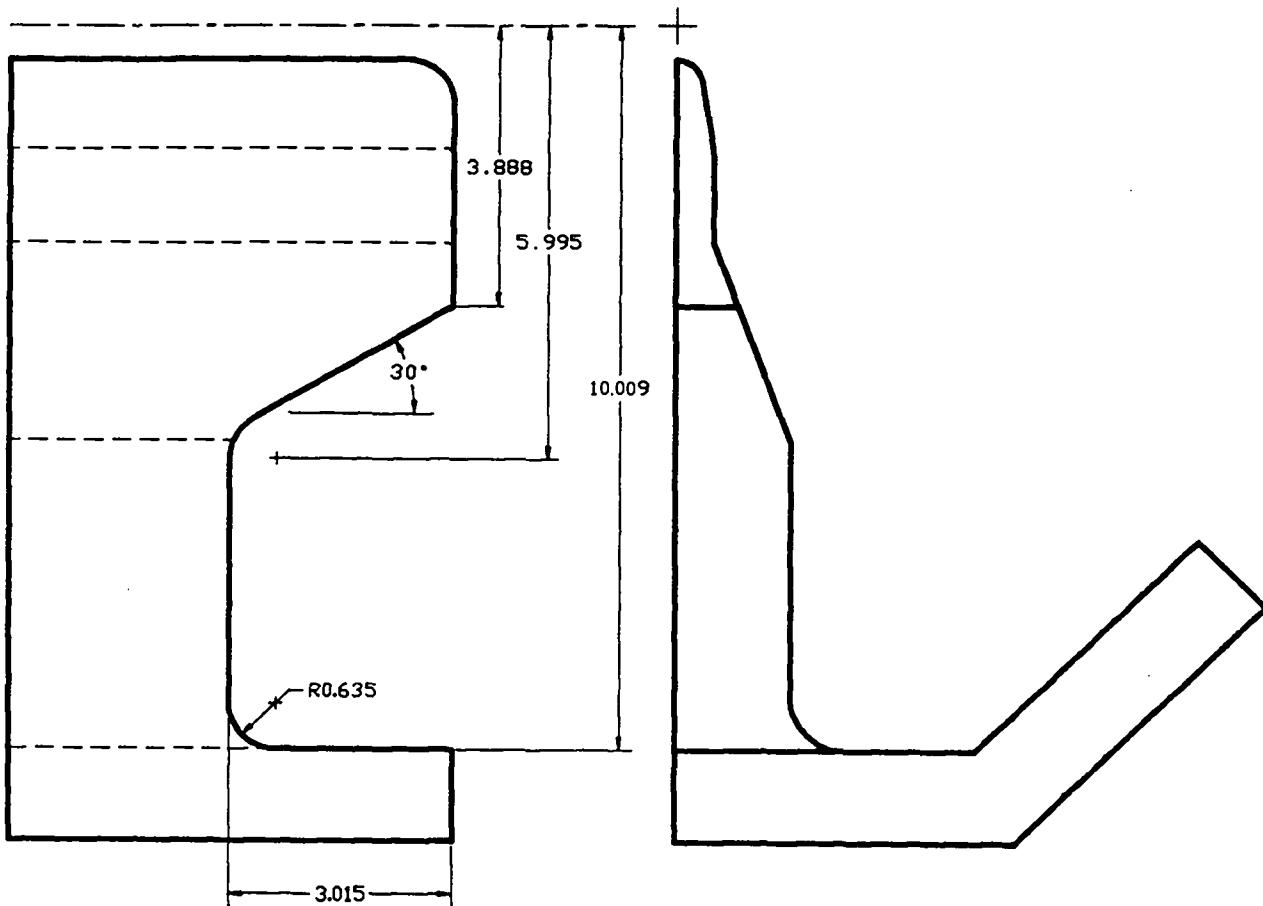
FIGURE V-8: Rectangular Undercut

Los Alamos National Laboratory
Accelerator Technology Division
Group AT-1

Figure V-9:
Rectangular End Undercut for the
350 MHz RFQ Linac for the
Accelerator Production of Tritium

Revised: February 1993   Dimensions in Centimeters

4.942

Ø0.877

10.009

R0.635

3.015
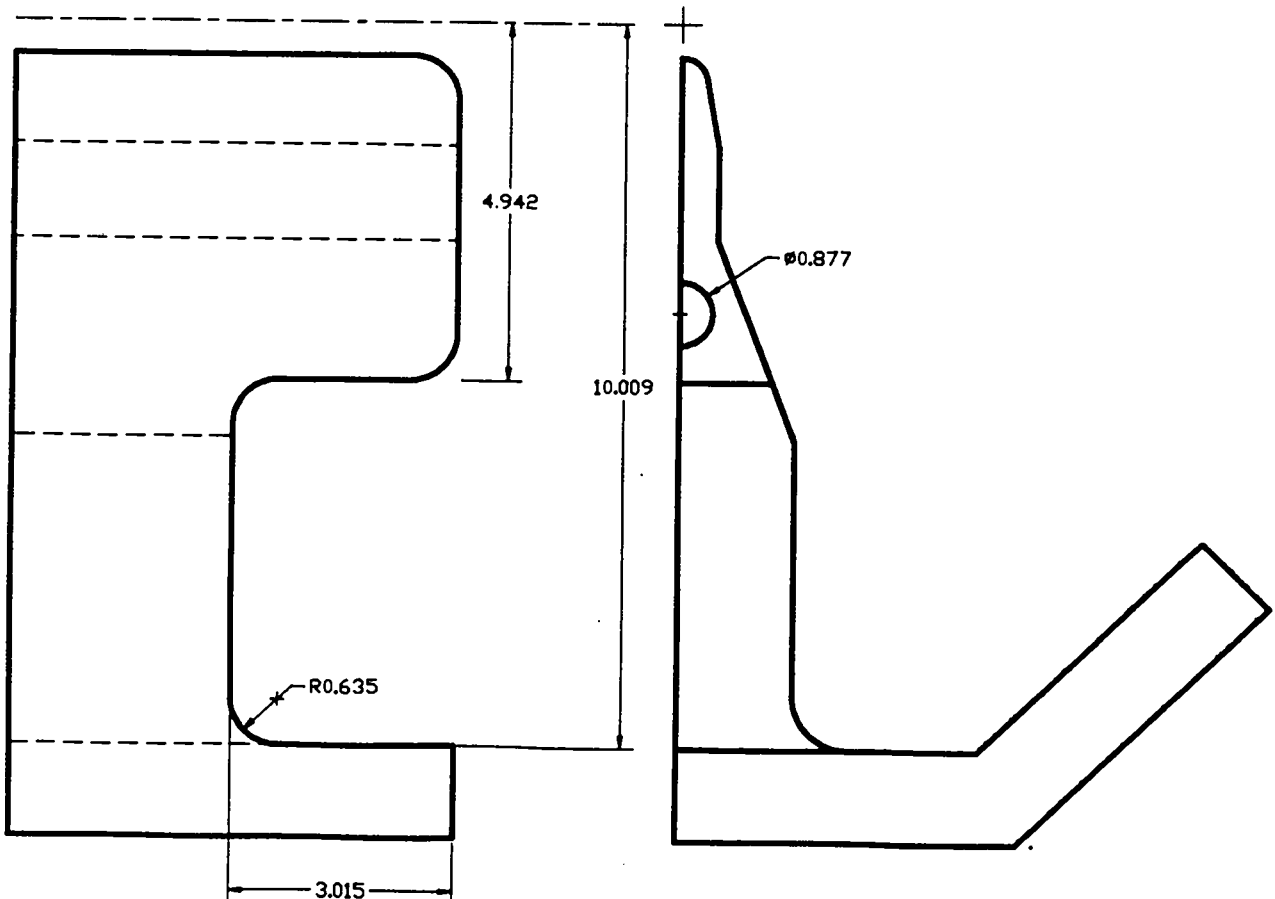
There was a concern that the rectangular undercut would have greater field enhancement and resulting greater rf thermal loads (proportional to the square of the fields). MAFIA runs[25] were carried out for both shapes in order to determine whether there was a significant difference in the peak surface heat flux. To assure consistency, the fields a distance inward from the end region were made equal to values calculated from SUPERFISH.

The conclusion from the MAFIA analysis was that maximum fields in both undercut forms were comparable and therefore the rectangular-shaped undercut region was selected. In both cases, the magnification of power density was a factor of eight (~90 w/cm^2) in the highest areas, typically sharp corners formed by the intersection of three surfaces. Rounding off such corners would drop the power density magnification to about a factor of five and this is applicable to both undercut forms.

A three-dimensional finite element model of a short length (1/8th of a segment) of the RFQ was created. The end region coolant path arrangement is shown on Figure V-10. The coolant enters the tip coolant passage via a radially drilled hole. This hole would be located as near as possible to the front surface of the undercut. For the sake of this preliminary analysis, the location with respect to the front surface of the undercut provides a rather conservative wall thickness. At the intersection of the tip coolant passage the coolant is directed toward the end of the vane, then reversed. This arrangement was utilized on the CWDD RFQ[3].

The thermal loads from the MAFIA analysis were applied to the surfaces of the model. The full 15 feet per second bulk velocity was applied to all three coolant passages. The temperatures of the base and tip coolant at the back plane were set at 41° F above the tip coolant passage as per the two- dimensional analysis. The coolant flow in all three passages is from the undercut region to the back plane. The temperature of the coolant at each element within the coolant passages was varied as heat was absorbed by the coolant. The analyses were carried out using constant properties as listed in Table V-1.

The results of the thermal analysis are shown on Figure V-11. The maximum structure temperature rise is 101° F above the coolant temperature. If the coolant were supplied at 90° F, then the structure would reach 191° F. The maximum structure temperature occurs, as expected, in the undercut region. Less conservative placement of the radial hole to the tip coolant passage would serve to reduce the maximum structure temperature. Except at the very end of the tip, the longitudinal temperature gradient of the vane tip is small. Figure V-12 shows a comparison of the temperature distribution at sections taken at the face of the undercut and at the back plane.

The deformations resulting from the temperature distribution are shown on Figure V-13. As in the case of the temperature, the longitudinal variation of the vertical displacements is small. Figure V-14 shows a comparison of the vertical displacements at sections taken at the face of the undercut and at the back plane.

Los Alamos National Laboratory
Accelerator Technology Division
Group AT-1

Figure V-10
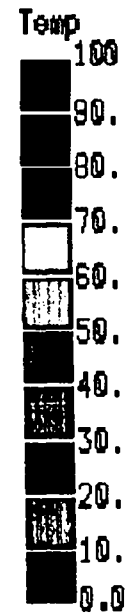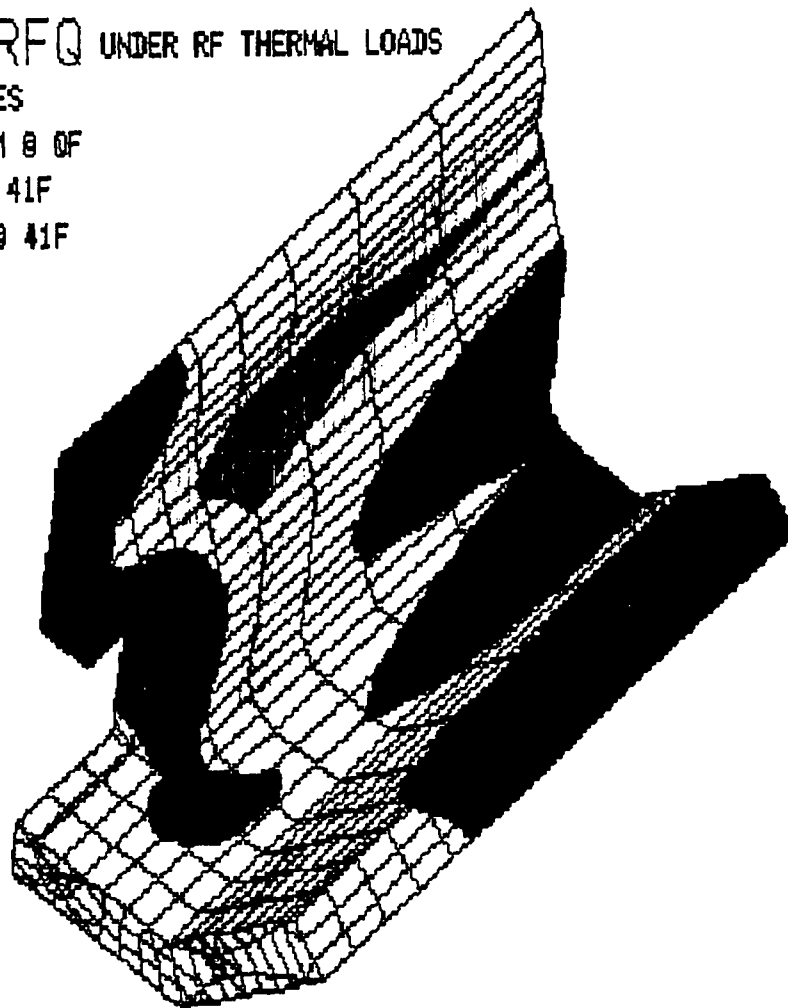End Region Coolant Path
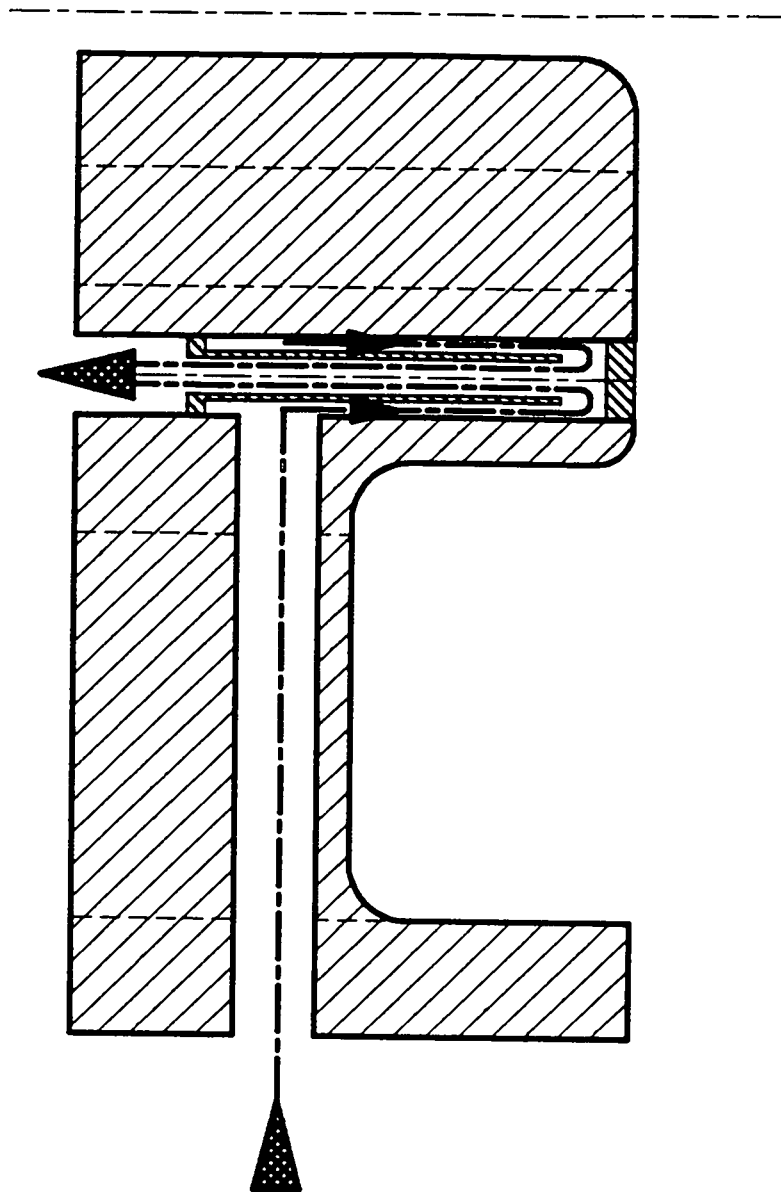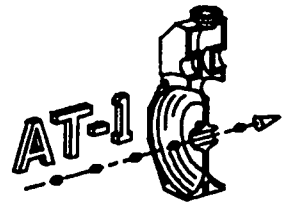
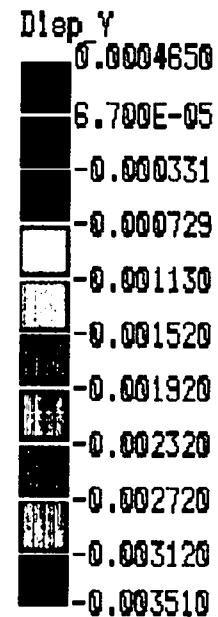THERMAL Step=1 APT RFQ UNDER RF THERMAL LOADS

15 FT/SEC IN ALL PASSAGES
CENTRAL PASSAGE: 4.2 GPM @ 0F
BASE PASSAGE: 3.6 GPM @ 41F
WALL PASSASGE: 3.6 GPM @ 41F
MAX TEMP RISE = 100.6 F

Temp
100
90.
80.
70.
60.
50.
40.
30.
20.
10.
0.0

MODEL: APTEND.GEO
INPUT: APTEND.CN4

GEO >AXIS
     Draw Axis [1] >0
GEO >AXIS
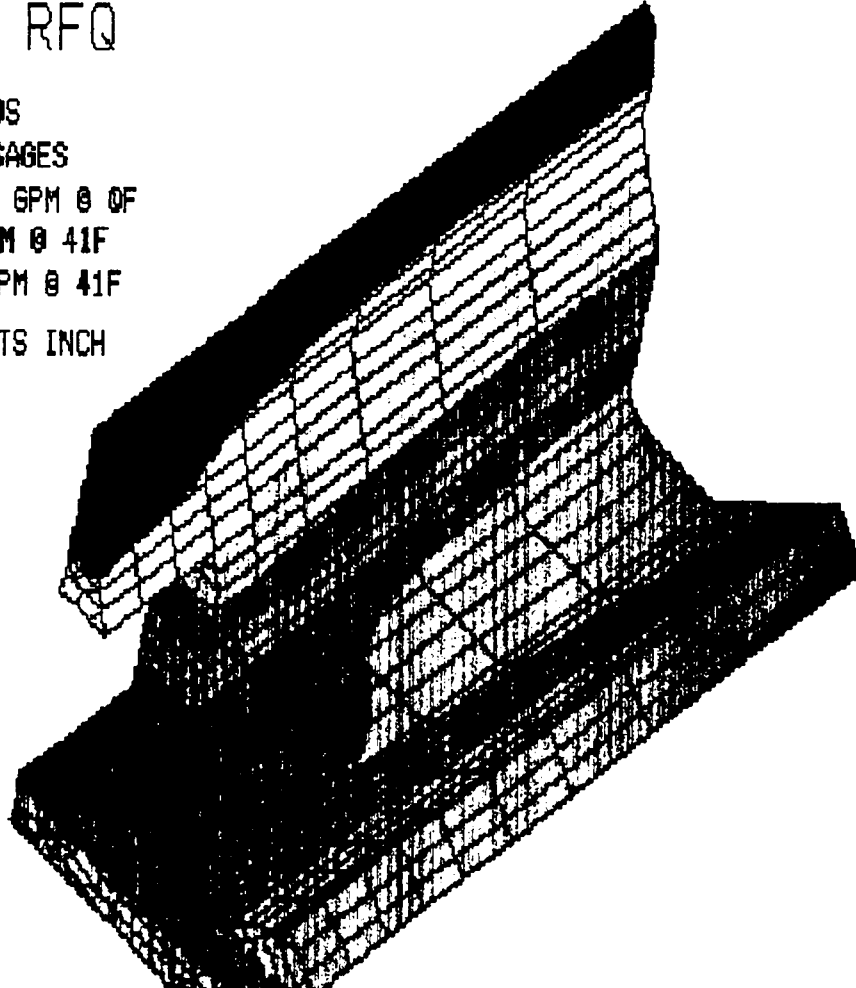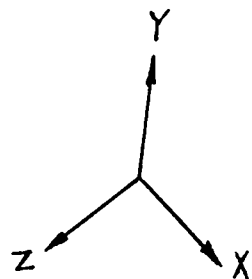GEO >repaint

FIGURE V-11
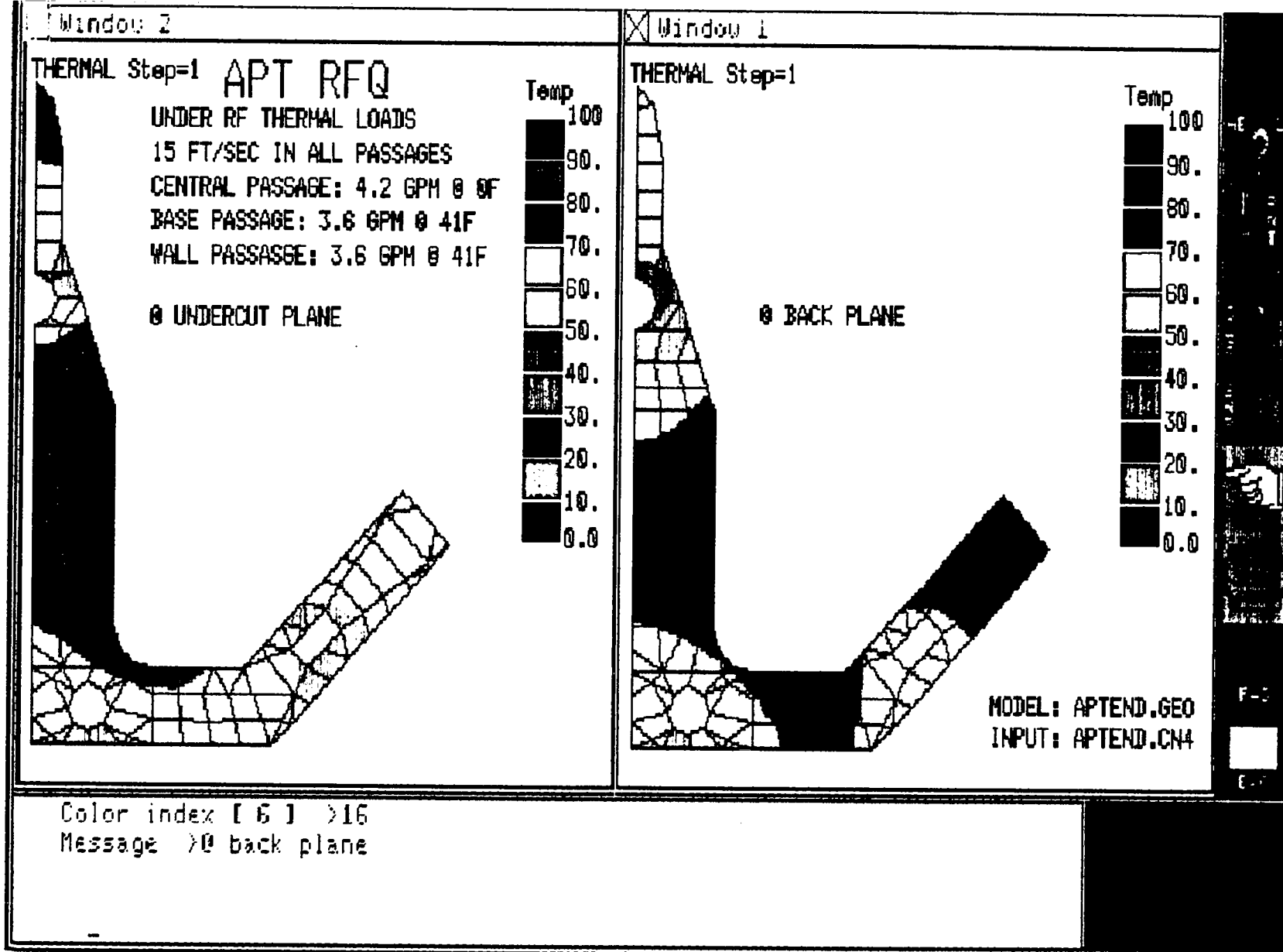
FIGURE V-12

FIGURE V-13

Window 2

APT RFQ

UNDER RF THERMAL LOADS

15 FT/SEC IN ALL PASSAGES

CENTRAL PASSAGE: 4.2 GPM @ 0F
BASE PASSAGE: 3.6 GPM @ 41F
WALL PASSASGE: 3.6 GPM @ 41F

VERTICAL DISPLACEMENTS INCH

@ UNDERCUT PLANE

Y

X

Window 1

Lin DISP Lc=1

VERTICAL DISPLACEMENTS INCH
@ BACK PLANE

Disp_Y

0.0004650
6.700E-05
-0.000331
-0.000729
-0.001130
-0.001520
-0.001920
-0.002320
-0.002720
-0.003120
-0.003510

MODEL: APTEND.GEO
INPUT: APTEND.CN4
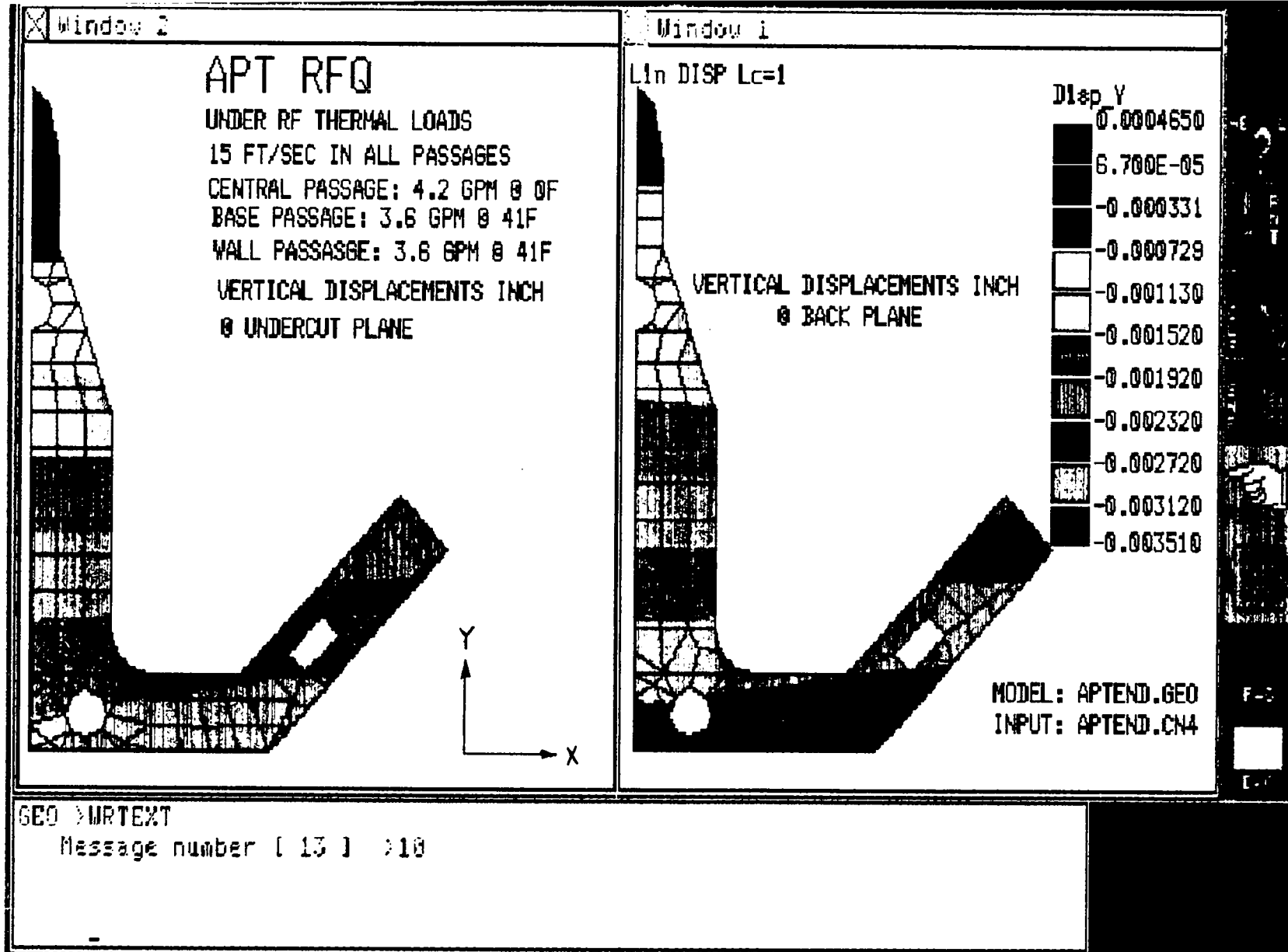
GEO >WRTEXT
    Message number [13] >10

FIGURE V-14

COOLANT PASSAGE ARRANGEMENT:

With a maximum bulk velocity of 15 feet per second, a total of 69 GPM of coolant can flow through the cross-section. Since it is desirable to minimize the longitundial variations of temperature and local frequency, it is planned that the maximum coolant flow be utilized. Furthermore, in order for the coolant passages in the wall to clear the vacuum pumping ports and rf drive loop (or waveguide iris) ports located at the mid-sections, the coolant passage arrangement will be as shown on Figure V-15. The coolant passages in each section will terminate at mid-length. The arrangement shown on the figure should serve to minimize the temperature rise in the end regions as well as minimizing the longitudinal variation of the temperature and frequency.

With an average longitudinal heat load of 150 kilowatts per meter, the average coolant temperature rise will be 0.375° Fahrenheit per inch. Over the 20 inch-long coolant path, there will be a frequency change of 3750 Hz. Since there will be two coolant loops per section, a total of sixteen, the total coolant flow will be 1104 GPM for each 8 section RFQ. The total pumping power will be approximately 500 hp per RFQ.

Los Alamos National Laboratory
Accelerator Technology Division
Group At-1
350 MHz RFQ Linac for the
Accelerator Production of Tritium

Figure V-15:
Coolant Passage Arrangement

Undercut
Region

Section
Match
Region
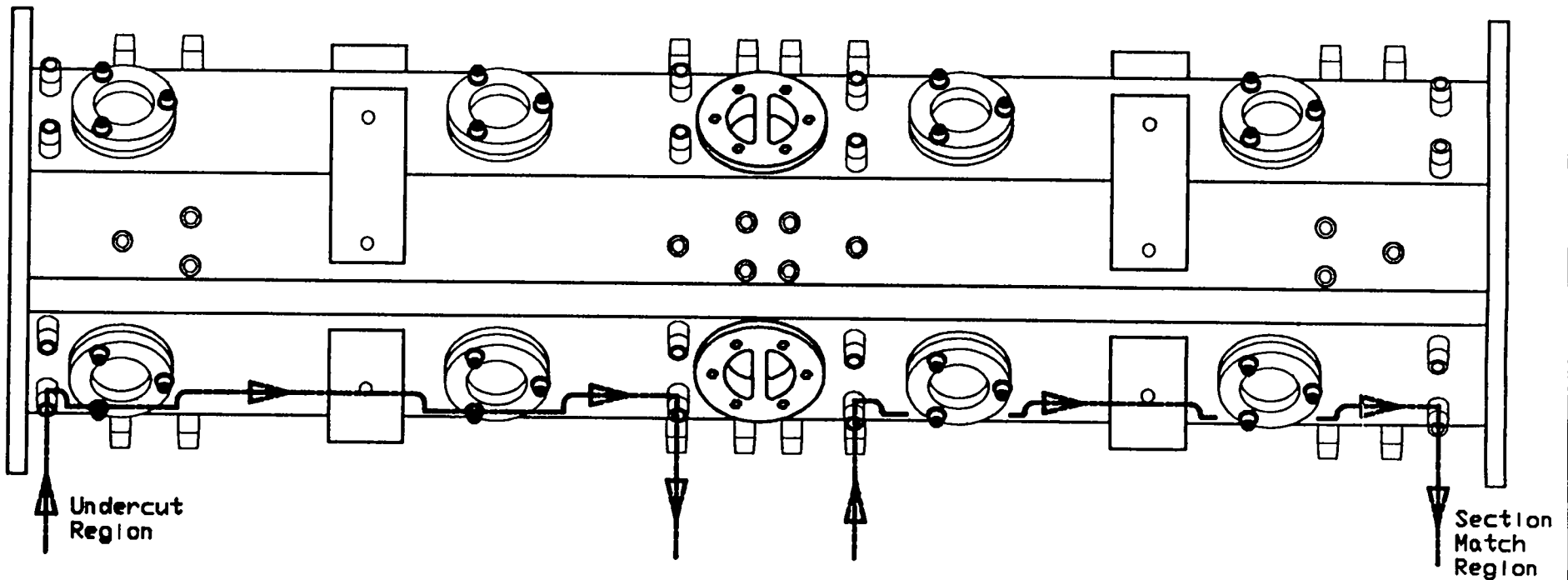
VI. FABRICATION

The fabrication sequence for the APT RFQ's is for the most part a direct up-scaling of that used for the CWDD RFQ[3]. The APT machines each comprise eight one-meter electroformed assemblies (Figure I-1) whereas the CWDD RFQ consists of four one-meter electroformed assemblies. The most noticeable difference in the APT design is the fabrication of the cooling channels. The CWDD RFQ employed a single deep drilled hole for vane tip cooling. All other cooling channels were machined slots that were covered with electroformed copper. For the APT RFQ the original concept was to use three drilled holes for vane tip and vane base cooling. The cavity walls were to be cooled via machined slots covered with an electron-beam (E-beam) welded cover. The thermal analysis has shown however, that the wall cooling is non-critical. Therefore, the method chosen for fabrication is to use two additional deep drilled holes in each quadrant wall rather than the more complex slot with cover.

As stated in Section IV, the material of choice for the vanes/cavity is OFE copper C10100. Although it is more difficult to machine than the tellurium copper alloy used for the CWDD and SSC[1] RFQ's, the ability to easily and reliably weld the material is seen as a distinct advantage for the APT application both for primary fabrication and for repairs that may be necessary either during fabrication or service. Electron beam welding will be used to close the ends of the drilled cooling passages and to install the coolant fittings. This is deemed necessary because of the high reliability required over the long machine life cycle.

The RFQ design employs eight one meter electroformed assemblies. Each of these assemblies consists of four vane/cavity quadrants which are machined from OFE copper extruded bars. The concept approach is to fabricate these by the same method as used for the BEAR[7], CWDD, and SSC RFQ's which is to machine the complete vane/cavity quadrants from solid stock. Because of the integral flange at the ends of each assembly, the bars must have a 7 inch × 8.34 inch cross section (Figure VI-1). The extrusion must also leave approximately 0.5 inch excess per side to comfortably allow for warpage and twist. It should be noted that if GLIDCOP is chosen for use that a larger section will be necessary due to the poor near surface characteristics of the alloy.

The 7 × 8.34 inch section results in an ultimate material usage of approximately 10%. More important than the material usage is the effect that the integral flange has on the electroforming process. The need to grow the electroformed joint around the inside corner at the flange is the most time consuming aspect of the process. During preliminary/final design other methods of achieving the flanged ends by welding or brazing will be explored as well as consideration of revised flange designs. Material usage alone is not adequate incentive to modify the flange, the alternative must show significant benefit in the electroforming.

The fabrication process begins with the rough machining of the rectangular bars to remove the bulk of the excess material from the vane region and to finish the external features of the quadrant including the raised tuner bosses and the back sides of the end flanges. The deep hole drilling of the cooling channels is now done by drilling from each end. The

cooling concept calls for passages that have an input at each end of a one meter length and output near the center. As such, the length for drilling is approximately 18 inches which results in maximum L/D's of between 75 and 85 depending upon the minimum passage size chosen. Although the pure copper material will be more difficult to drill than the TeCu used in CWDD and SSC, the conservative edge distances employed in the design should alleviate any problems of drift. The Figure VI-1 cross-section shows the approximate locations of the coolant passages. In addition to the deep longitudinal holes, the cross holes for coolant feed and return are also drilled and finished at this time.

With the cooling holes complete the E-beam welding of the hole plugs and the coolant fittings can be done. Although this is a straight forward application of E-beam welding it is deemed less risky to perform the operation at this point in the fabrication sequence on the single, low value added, vanes rather than after the electroformed assembly process. This approach can be changed if the presence of the coolant fittings poses any difficulties in machining or electroforming. Once the welding is complete the vane/quadrant assemblies will be pressure and leak tested.

Final machining of the quadrants brings all internal cavity and vane surfaces excluding the modulated vane tip to final dimension. This includes the vane undercut at one end of each quadrant. The process at this point will be influenced by whether or not a cold model cavity is built. If a cold model is made then the vane undercut dimensions can be final machined at this time to the dimensions determined from the cold model. If there is no cold model these dimensions will have to be determined from testing of the assembled segments so the undercuts can only be conservatively roughed in at this time. A cold model could also be used to determine the axial gaps between vane tips at the segment joints. This machining step also finishes the details of the electroformed joint area along the length of each side of the quadrant (Figure VI-2).

At this point in the process the four, one meter vane/quadrant details that make up each section are identical. The next step is to machine the modulated vane tip thereby designating X and Y vanes. Because of the flexibility of the electroformed assembly process, the vane tip modulation is machined to 0.002 inch total indicated runout (TIR) relative only to itself. This is because the vanes do not have mating surfaces that dictate the assembly. The electroform joint spans a .030 inch nominal gap between the vanes and therefore allows for variation in the vane tip position relative to the joint. The machining is done in a climate controlled room using a three axis NC milling machine and an auxiliary direct drive spindle. The machining technique is the 45 degree ball end mill process developed by LANL for the BEAR project[7] (Figure VI-3) The auxiliary spindle eliminates effects associated with spindle growth due to heat generated by cutting load during the 12 to 16 hour tip machining process. The 45 degree angle keeps the cutting speed of the tool relatively constant as the ball passes the peak of the vane. It also maintains the same character of cut (i.e. climb or conventional) over the full tip profile. This will be especially important for achieving a good finish in a material like OFE copper.

VANE PROFILE

EXTRUSION CROSS-SECTION

.50

6.00 R
FLANGE

7.00

.50

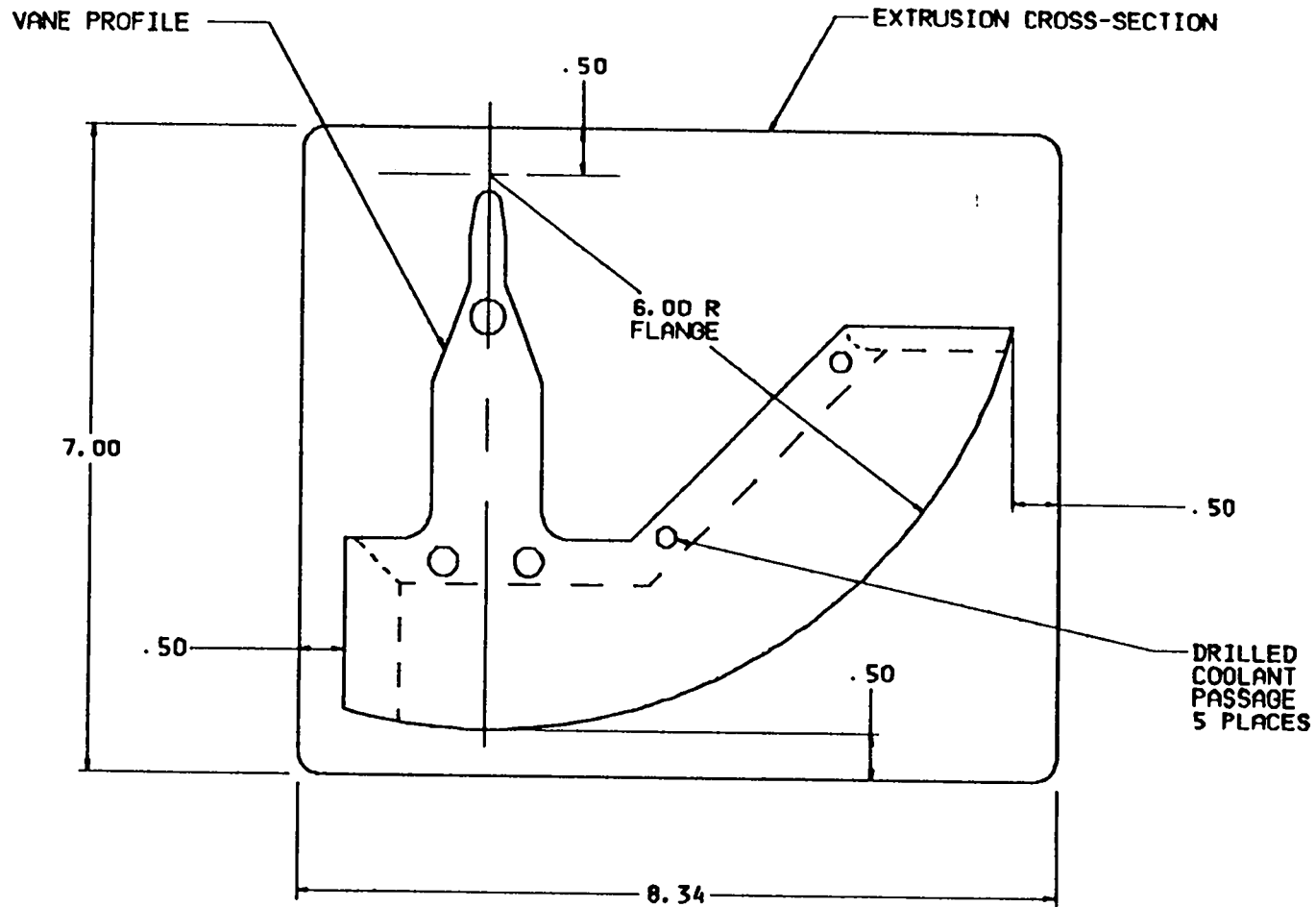.50

DRILLED
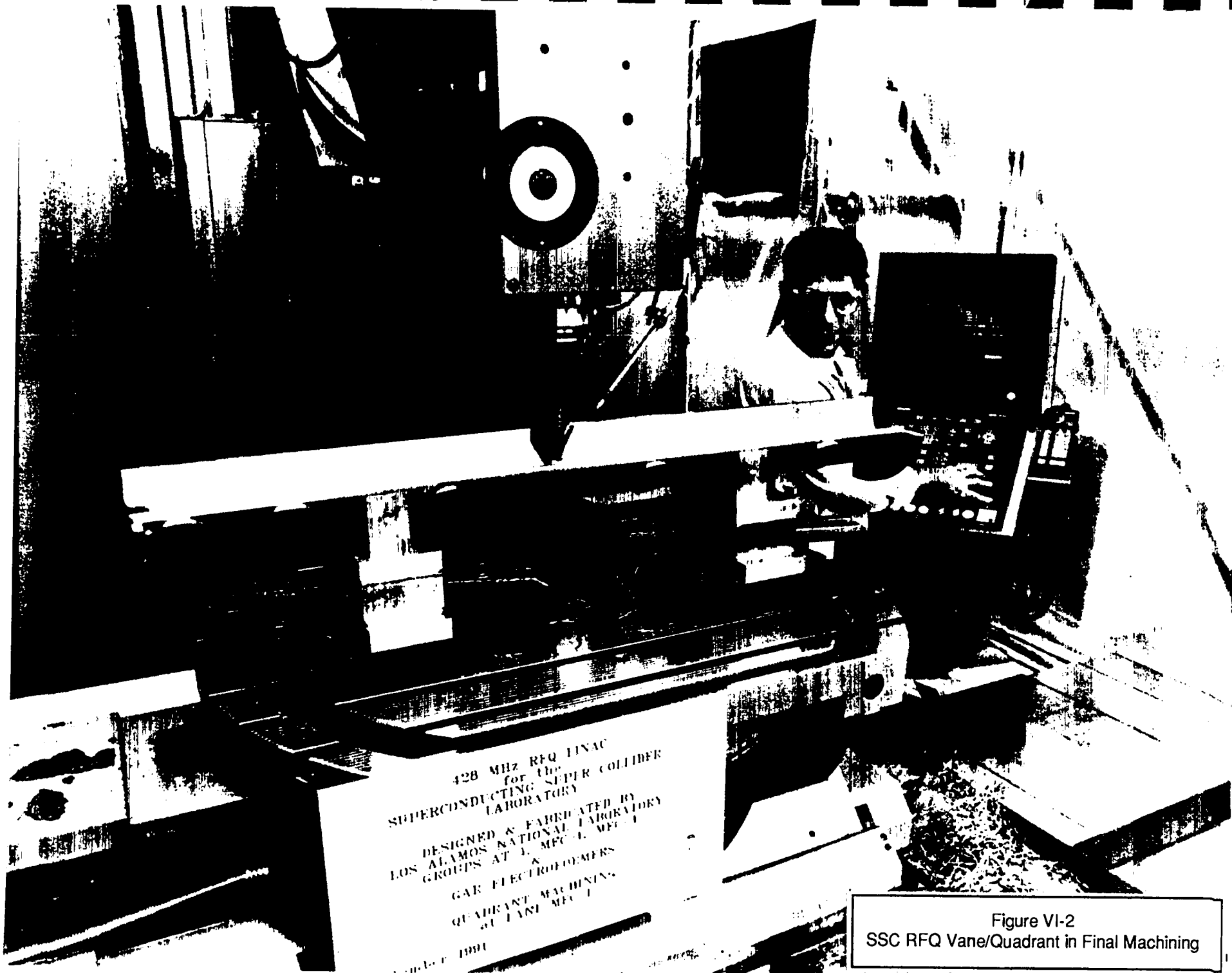COOLANT
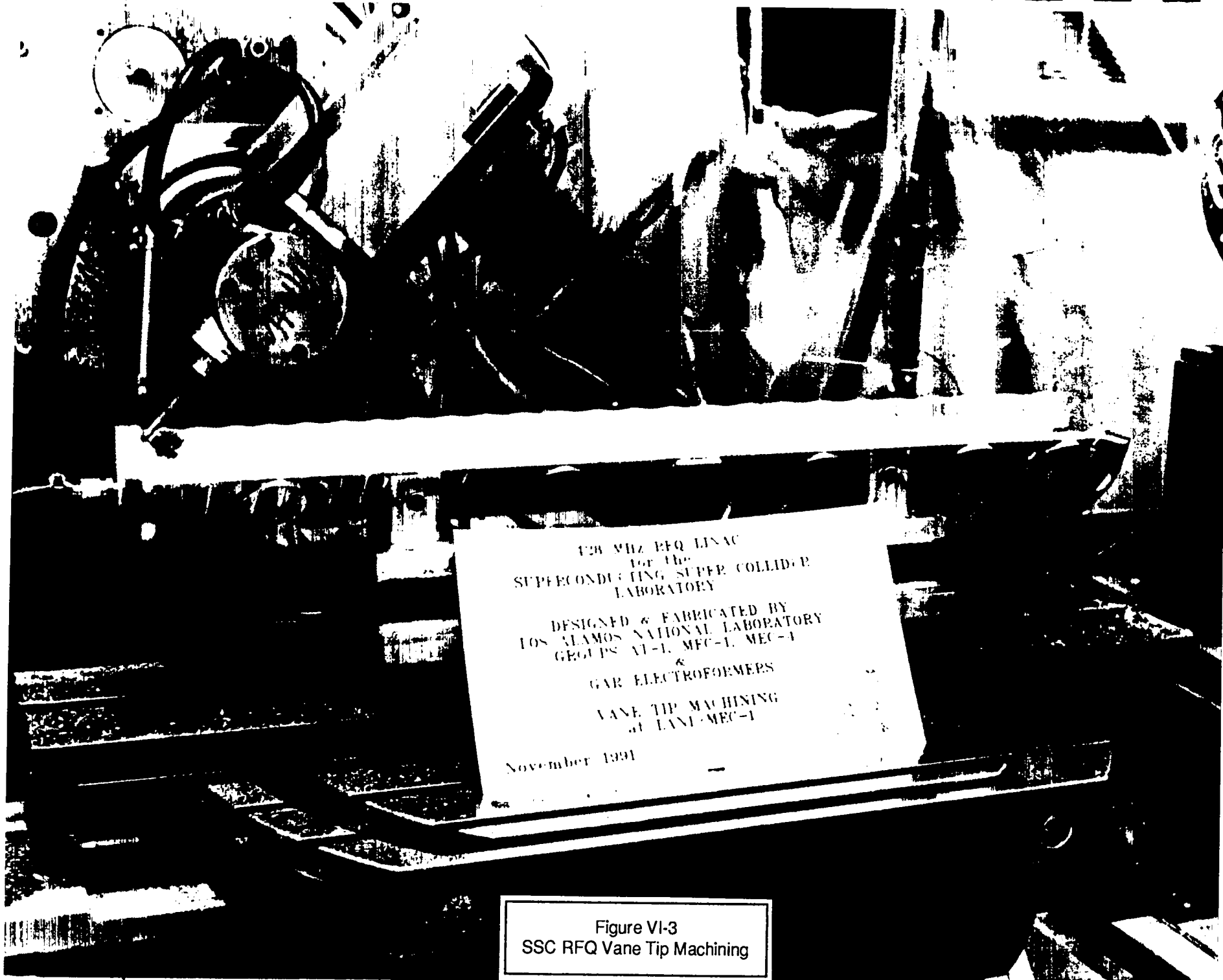PASSAGE
5 PLACES

.50

8.34

Figure VI-1
Vane Quadrant Extrusion Requirements
(Dim's in Inches)

428 MHz RFQ LINAC
for the
SUPERCONDUCTING SUPER COLLIDER
LABORATORY

DESIGNED & FABRICATED BY
LOS ALAMOS NATIONAL LABORATORY
GROUPS AT 1. MEC-1. MEC-4

GAR ELECTROFORMERS

QUADRANT MACHINING
AT TANE MEC-4

October 1990

Figure VI-2
SSC RFQ Vane/Quadrant in Final Machining

Figure VI-3
SSC RFQ Vane Tip Machining
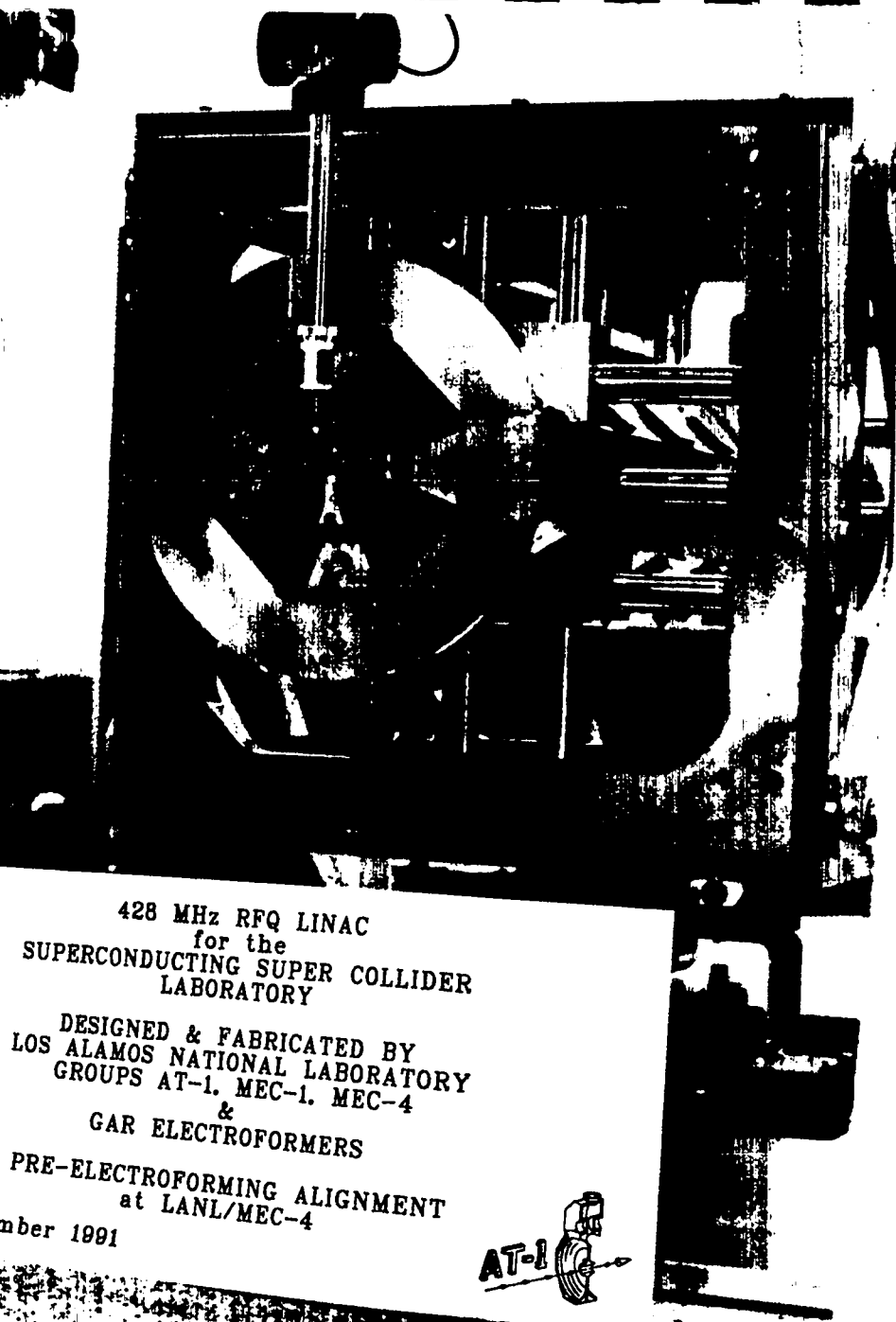
428 MHz RFQ LINAC
for the
SUPERCONDUCTING SUPER COLLIDER
LABORATORY

DESIGNED & FABRICATED BY
LOS ALAMOS NATIONAL LABORATORY
GROUPS AT-1, MEC-1, MEC-4
&
GAR ELECTROFORMERS

PRE-ELECTROFORMING ALIGNMENT
at LANL/MEC-4

December 1991
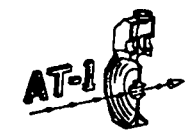
Figure VI-4
SSC RFQ Vane Alignment in E-Form Fixture

Figure VI-5
Vane Tip-to-Tip Measurements

Figure VI-6
Two SSC RFQ Sections During RF Testing

Figure VI-7
Installation of Internal Tooling - CWDD

Figure VI-8
View of Joint Area at Flange Interface
Tooling Bar Spans Joint Inside

Figure VI-9
CWDD RFQ Section in Electroforming

Figure VI-10
CWDD RFQ Section - Post E-Form Machining

Figure VI-11
Complete CWDD RFQ Section Prior to Alignment Pin Installation

Figure VI-12
CWDD RFQ Full Assembly in Vertical Assy Fixture

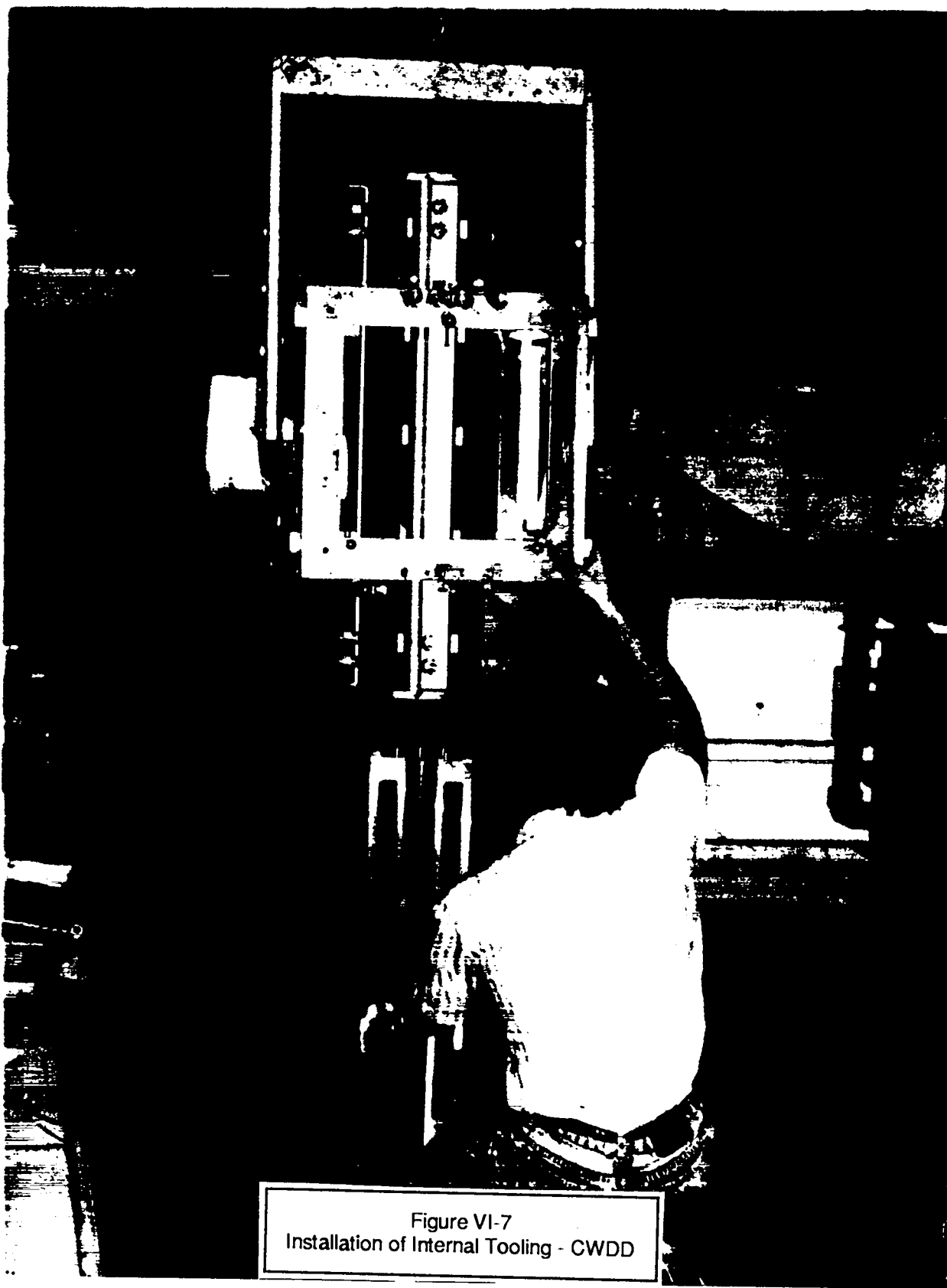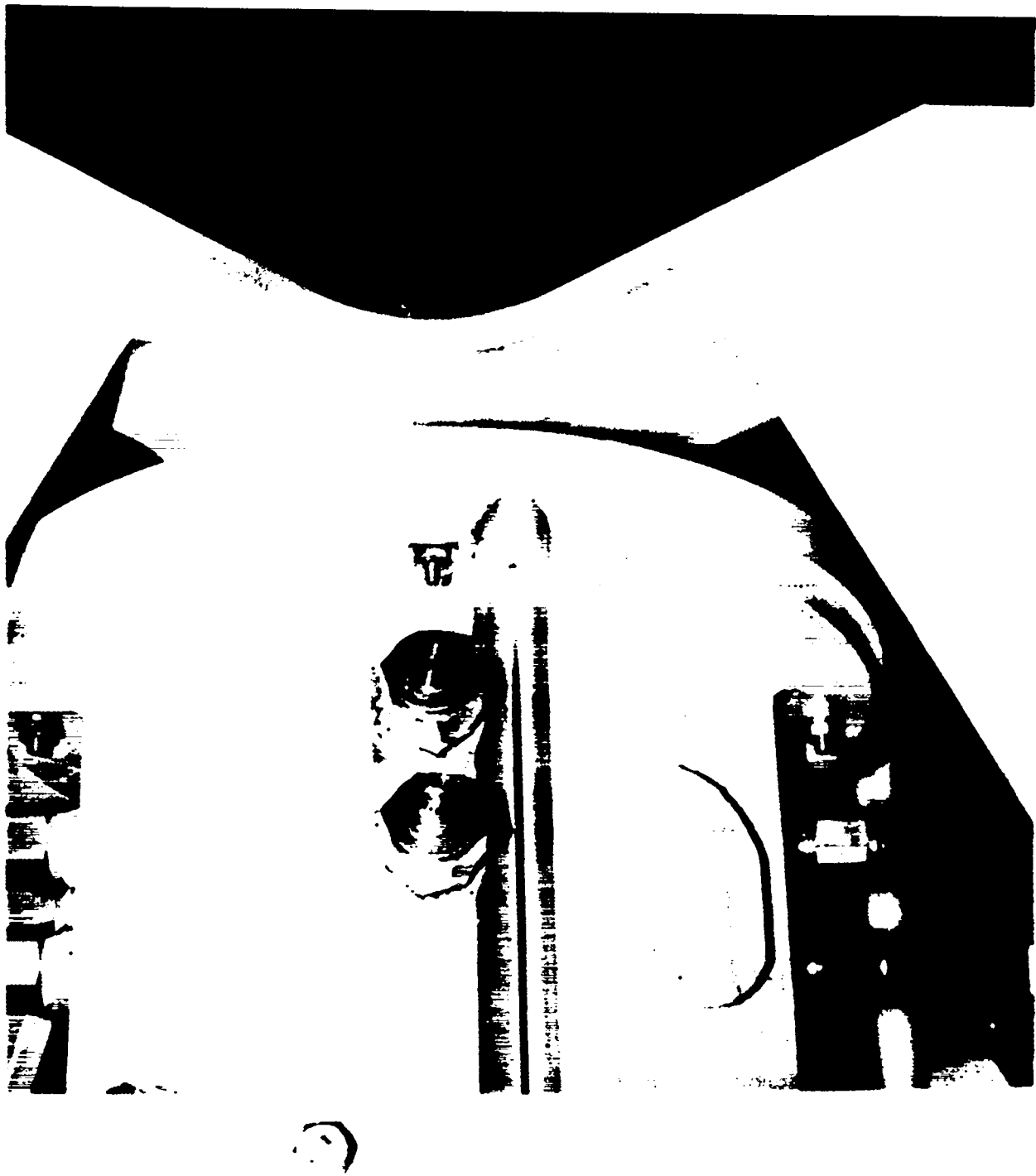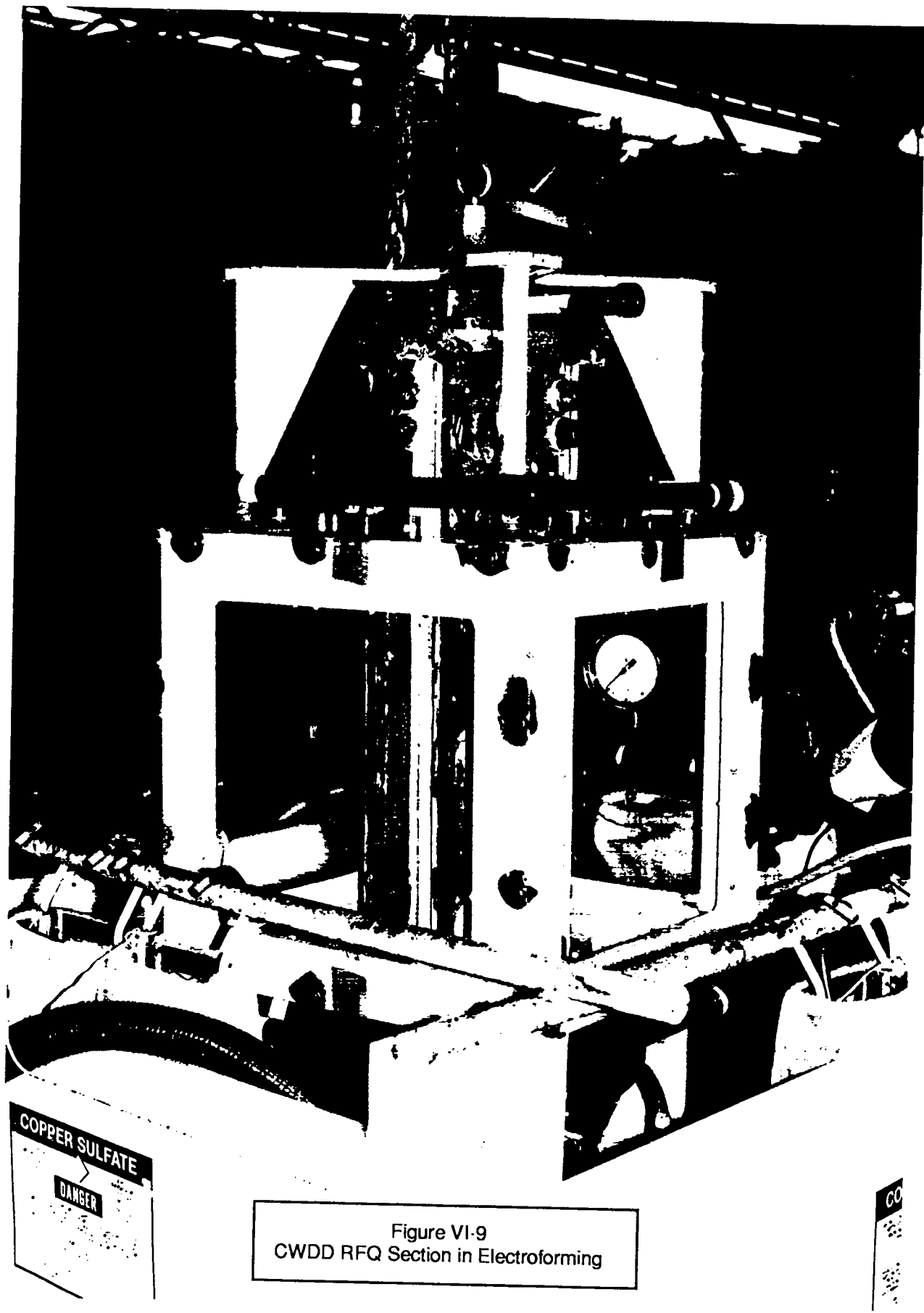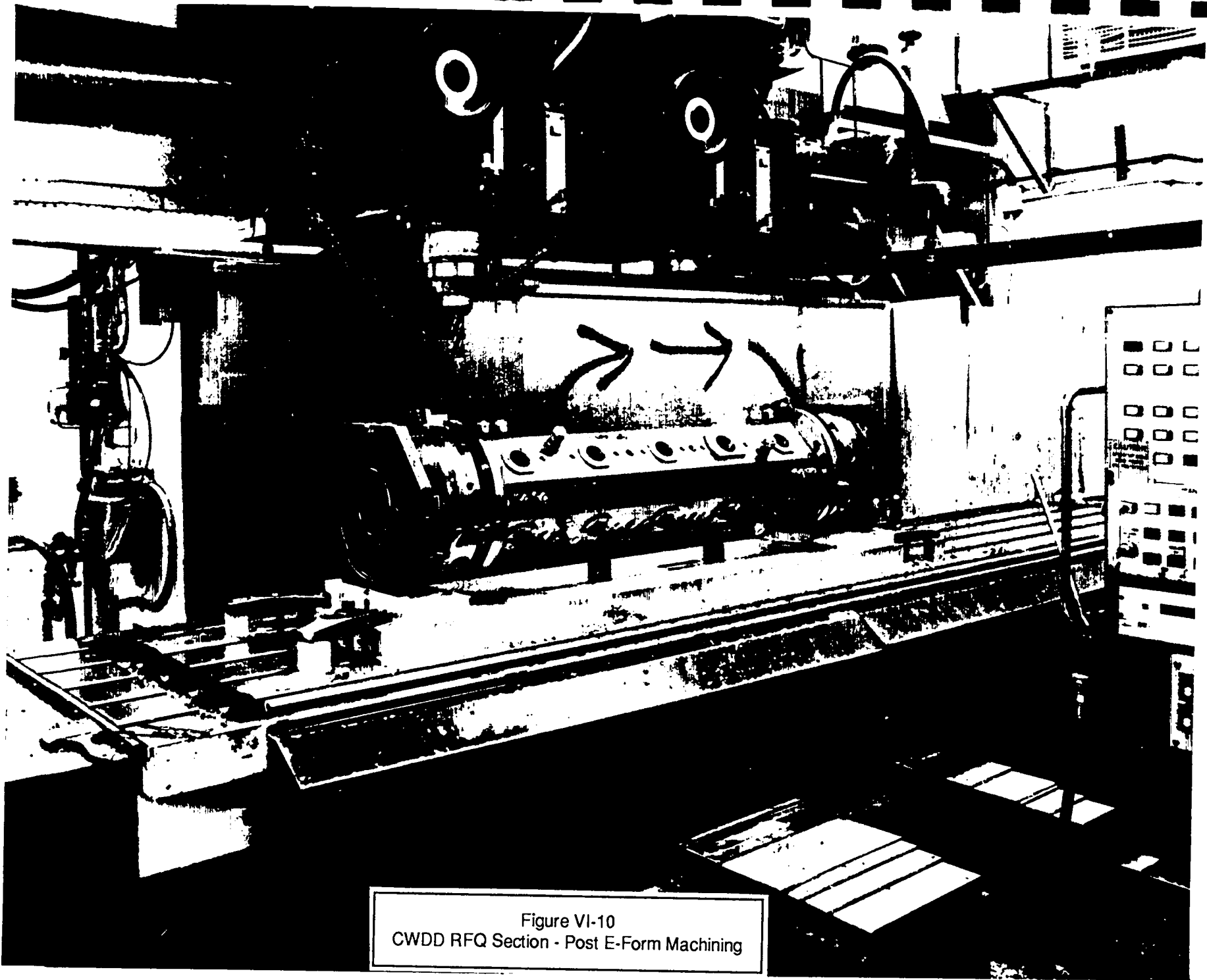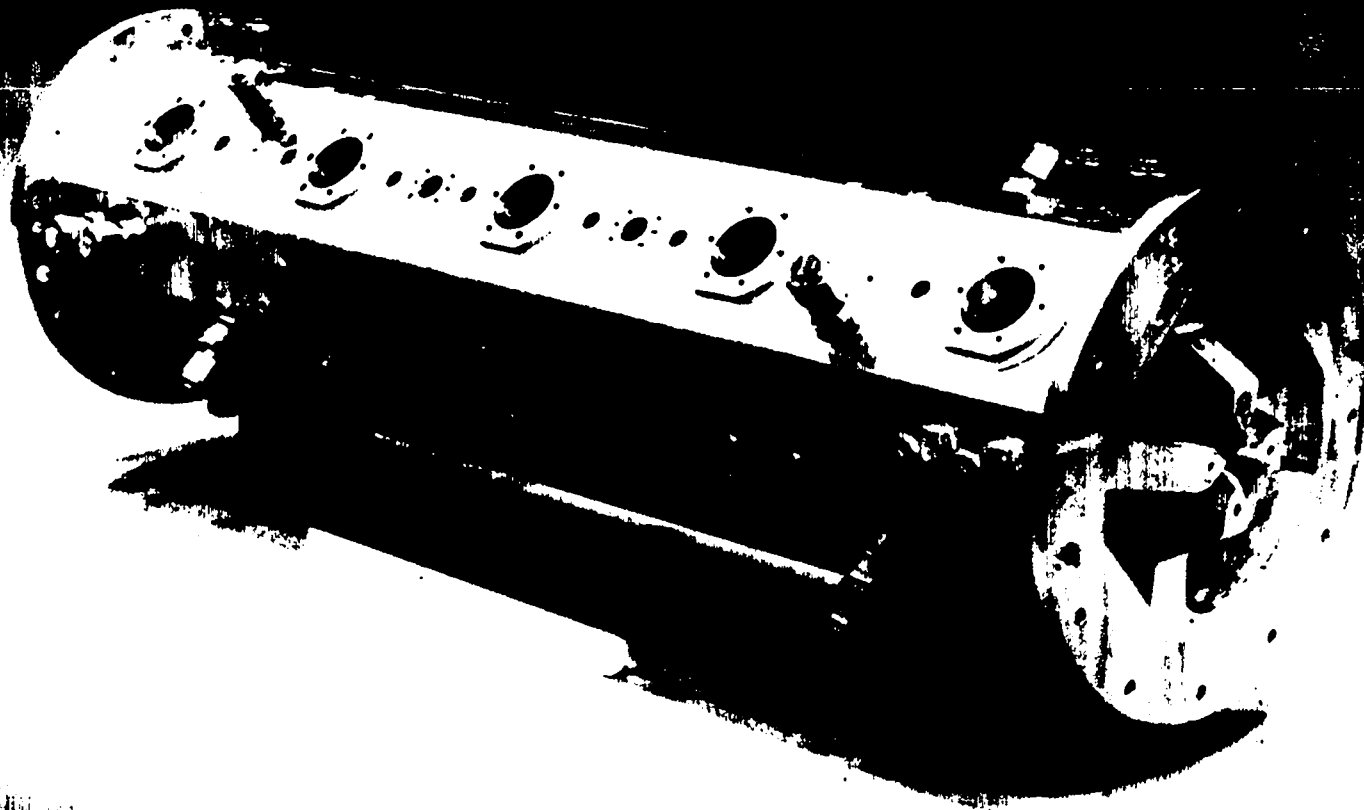After the modulations are complete, the vanes ends are cut to final length. The flange area of the vane/quadrant detail is left about .010 inch full to allow for a post-electroform clean up cut.

The completed vanes are assembled into the electroforming fixture which holds them rigidly with respect to each other. Each vane is supported in a pseudo-kinematic fashion allowing the adjustment of five of the six degrees of freedom (axial alignment is done via a banking surface at the end) by shimming of the support points. The assembly is set up on a coordinate measuring machine (CMM) which measures the relative positions of the vanes (Figure VI-4). Adjustments are determined using the LANL developed code RFQALIGN[26]. This code uses the measured vane positions and calculates the necessary shim adjustments to achieve alignment. With the vanes within about ± .002 inch, the final fine adjustments are made "by eye" using precision gauge pins graduated in increments of 0.0001 inch These pins are used to measure the vane tip to vane tip spacing of adjacent vanes (Figure VI-5). Alignment accuracies of ± 0.0005 inch have been achieved using this method. The plan for APT is to perform the alignment of the two one meter sections of a two meter resonant segment at the same time and then join them together to run a low power RF test prior to electroforming (Figure VI-6). This RF testing is discussed in Section VII.

The electroforming process is planned to be done in the same way as for the BEAR, CWDD and SSC RFQ's. The process is tedious and time consuming but it is well developed and offers distinct and unique advantages with respect to structural, vacuum, and thermal integrity. After a final RF test of the sections at the electroforming facility, internal tooling bars are installed inside the cavity (Figure VI-7) and fitted tightly behind the joint area effectively spanning the 0.030 inch gap (Figure VI-8). The electroformed copper grows across the surface of the stainless steel tooling bar without bonding to the stainless and rigidly joins the vanes together. The joint is a two layer deposit with a non-structural lead filler. Each copper layer is 0.100 inch thick and results in a cavity whose structural and thermal behavior is nearly that of a monolithic block of copper. A view of a section being lowered into the electroforming tank is shown in Figure VI-9.

A large fraction of the effort in electroforming involves removal, grinding the deposit, and replacement in the tank to grow the joint around the corner at the end flanges (shown in Figure VI-8). Significant time is dedicated to depositing copper in the corner only, while the remainder of the joint masked off. As discussed earlier, the flange design will be a focus of effort during preliminary design.

In order to produce the APT RFQ's to a reasonable schedule, a minimum of four should be undergoing electroforming at the same time. This is a significant increase in effort over the previous maximum of three in process at the same time which was done for the CWDD program. This may require an investment in facility upgrades to allow the handling of the greater number of units without a significant increase in the calendar time required per section.

Post-electroform operations will begin with an RF tuning check followed by final machining. This machining will bore and finish all of the ports for slug tuners, drive loops, vacuum attachments, etc. including all threaded fastener holes and inserts (Figure VI-10). As discussed earlier, if no cold model is used the final undercut dimensions will be determined and cut at this time. In addition the mating flanges of the segments will be skim cut to final length. Once the flanges have been finished the *segments will be*

inspected and the final thickness of the inter-section vacuum sealing plate which goes between the sections of a segment can be cut to fit. This plate carries an O-ring groove on both sides and is sized to guarantee exact fit-up of the sections such that the vane/cavity ends touch at the same time as the flanges contact the inter-section plate. A similar process will be done to size the thickness of the inter-segment plates which separate the resonant segments. These plates are somewhat more complex than the inter-section plates in that they incorporate dipole stabilizer posts[27] and therefore require integral cooling passages. They also have double O-ring grooves like the inter-section plates but additionally have an indium wire RF seal because the field direction at the resonant ends are parallel to the end wall. The inter-section plates do not require RF seals because the fields are perpendicular to the flange.

The final step prior to segment assembly will be to bore the flanges and install precision alignment pins in each end. This is done using a single precision drill fixture for all sections. The fixture is aligned to the beam axis of each individual section both translationally and rotationally on the CMM to an accuracy of ± 0.0005 inch and the holes are transfer drilled through the flange (Figure VI-11). Precision beryllium copper pins, one round in shape and the other a diamond, are then cryo-fitted in the holes. The inter-section and inter-segment plates are drilled using the same drill fixture and receive precision stainless steel bushings which are also cryo-fitted in place. Also at this time the optical targets will be installed on each section such that their position relative to the beam axis can be adjusted and documented using the CMM.

Segment assembly will be done on the bench. Each two meter resonant segment will be assembled with the inter-section vacuum plate and preliminary beadpull testing and cavity tuning will be done. This will save time and effort when the full RFQ is tested in the vertical fixture.

Final assembly of the RFQ will be done vertically similar to the CWDD RFQ (Figure VI-12). This serves to eliminate sag as a source of problems in assembly and more importantly, will allow the beadpulls and tuning to be done vertically. The CWDD RFQ showed the effects of bead sag and wall contact during the beadpull operations. The APT RFQ's, in addition to being twice as long as CWDD, have inter-segment plates in three locations internally through which the bead must travel. Current techniques for bead testing are not adequate to test an eight meter cavity horizontally so the vertical assembly has been baselined. If better techniques arise in the future this approach can be changed.

Unlike the CWDD RFQ which was assembled vertically and then layed down and removed from the fixture, it is proposed that the APT RFQ's be built up in vertical fixtures which then become the permanent support structure of the RFQ in the beamline. This approach is discussed fully in Section VIII.

The vertical assembly process is simply a sequence of stacking the four segments with the inter-segment plates to complete the assembly. Each subsequent piece is guided down onto the alignment pins and the connecting hardware is installed. With the precision machined end faces, alignment pins and the absence of gravity effects in the vertical fixture, the assembly is fully self aligning.

Since the fixture is also the final support structure, the transverse supports will also be installed and the entire assembly will be evaluated optically to ensure proper alignment. Loads to simulate gravity loads such as that from the cantilevered solenoid magnet at the low energy end can be applied during the tuning process. With the RFQ in the vertical orientation the tuning will be completed and the 128 fixed slug tuners will be installed and verified. The tuning process will include the installation of the RF feed network consisting of a minimum of 12 and a maximum of 16 drive loops. The drives will be fed from WR2300 waveguide in groups of four at a give axial location (one in each quadrant). The full feed network will be installed during the tuning process and used to drive the cavity during testing. Refer to Figure VIII-5 for a view of the RF feed installation concept. The drive loop coupling coefficients will be set for optimum high power performance as discussed in section VII. RF pick-up loops will be used for field sampling at many locations throughout the RFQ. They will be incorporated as brazed assemblies integral with slug tuners. It will be desirable to set the coupling of the pick-up loops at this time when the design field profile is known to exist. The pick-ups may then be used later to diagnose field errors.

Although the APT RFQ's are novel in the use of coupled resonant cavities, and they will be the electrically longest RFQ's ever built, they require no unproven techniques in fabrication. With the minor exception of the drilled cooling channel design, these cavities employ a combination of exactly the same techniques for fabrication as those used for the BEAR, CWDD and SSC RFQ's.

VII. RF TUNING AND ALIGNMENT

This RFQ has been designed with a constant ρ/r_0 ratio of 0.85. This is a compromise between minimizing peak electric fields and rf power and minimizing the effects of the higher order multipoles in the rf fields on the beam transmission. The average radial aperture of the RFQ is r_0 and the radius of the vane tip is ρ. Because r_0 varies along the length of the RFQ while ρ/r_0 remains constant the capacitance will change and that will change the cut off frequency of RFQ along the length. Previous RFQ's with a variable r_0 used a variable ratio of ρ/r_0 to maintain a constant capacitance and frequency. The APT RFQ will maintain a constant frequency cross section by varying the width of the vane base. This will result in a nearly flat, dipole-free field distribution before and after the vanes are joined by electroforming. The slug tuner adjustments produce the desired longitudinal field distribution and remove small residual dipole-field components.

The field strength in an RFQ is measured with the bead pull technique.[28] In this technique a metal bead is suspended on nylon line and is drawn through the four quadrants of the RFQ near the outer wall. The bead perturbs the structure and changes the resonant frequency depending on the electric and magnetic field strength. In this case the technique actually measures the magnetic field strength because the electric field is weak near the outer wall where the magnetic field is strong. In RFQ's with constant capacitance the electric field strength is directly proportional to the magnetic field strength. In the APT RFQ the capacitance between the vane tips is not constant and therefore the relation between the electric field strength and the magnetic field is not constant. The magnetic field at several points along the RFQ will be calculated with SUPERFISH. The magnetic field profile will then be interpolated from the required electric field and the SUPERFISH data. The magnetic field profile will be input to the program RFQTUNE along with the bead pull data. RFQTUNE will calculate the position of the tuners that adjust the fields in the RFQ to the desired profile. The program has tuned the following RFQ's: CWDD, GTA, SSC, and the 4 m long segmented cold model at 348 MHz. The CWDD RFQ and the 4 m long cold model each had 80 tuners. The APT RFQ will have 128 tuners.

The alignment of vanes in the APT RFQ will be performed the same way as the vanes were aligned on the CWDD RFQ and the SSC RFQ.[1] The vanes are mounted in a frame. They are kinematically supported with 5 supports, three in one plane and two in another plane. A pair of tooling holes is provided in each end of the vane-and-cavity quadrants and the positions of these holes relative to the centerline of the vane tip are measured with an accuracy of better than 0.008 mm with a coordinate measuring machine (CMM). The CMM is used to measure the relative position of the eight holes on each end. The measurements are input to a program, RFQALIGN,[26] that calculates shim thicknesses corresponding to displacements and rotations of the vane-and-cavity quadrants. The vanes are aligned to provide the correct spacing between the vane tips and equalize the volume of the four quadrants. One of the vanes is used as the reference and the position of the other three vanes are adjusted with shims in the supports. The accuracy of this alignment method is on the order of ±0.001 inch that has proved to be sufficient with the CWDD and SSC RFQ's. With the vanes mounted in the frame and electrical contact made across the joints between the vanes preliminary rf measurements can be made. These measurements assure that the RFQ will be tunable after the vanes are joined permanently.

Final rf tuning includes:

1. Machine the vane end undercuts to achieve the desired shape of the fields at the end of the vanes.

2. Machine the end of the vanes at the segment joints to adjust the resonant coupling. This is to adjust the frequency of the nearby quadrupole modes to equalize the spacing of the modes.

3. Machine the end stabilizers to the proper lengths to establish the optimum frequencies of the dipole modes.

4. Machine the slug tuner lengths to achieve the required frequency, the required quadrupole field profile, and minimum dipole field.

VIII. STRUCTURAL SUPPORT

The requirements for the RFQ structural support system are shown in Table VIII-1.

TABLE VIII-1

SUPPORT STRUCTURE REQUIREMENTS

RFQ MATERIAL

OFE Copper (CDA101)

ρ = 0.323 lbs/in^3

σ_y = 7000 psi

E = 17$\times$10^6 psi

υ = 0.36

α = 9.5$\times$10^{-6} °F

SPECIFICATIONS

Operating Load

Max. Deflection:	± 0.010inch
Max. Slope:	0.25 mrad
Max. Stress:	3000 psi (von Mises)

Live Load

Max. Deflection:	± 0.0005 inch
Max. Slope:	0.25 mrad

Operating + Live Load

Max. Deflection:	± 0.010inch
Max. Slope:	0.25 mrad
Max. Stress:	3000 psi (von Mises)

LOADS

Operating Load

Weight of RFQ:	8.8 lbs/inch
Misc. Items:	@ 1.0 lbs/in
Total	10.0 lbs/in

LEBT Magnet: 600 lbs at 3.75 inch in front of Low Energy End

Live Load

CASE 1:	100 lbs transverse force at any point along length
CASE 2:	1000 in-lb moment at any point along length
CASE 3:	500 in-lb torque at any point along length
CASE 4:	Case 1 + Case 2 (Force + Moment)
CASE 5:	Case 1 + Case 3 (Force + Torque)

DESIGN CONCEPT

The concept design for the RFQ support structure is shown in Figures VIII-1, VIII-2 and VIII-3. The concept employs a box structure that serves as both the in-service support system and the vertical assembly/tuning fixture. Once the RFQ has been assembled and aligned in the box there will be no further need to adjust the redundant RFQ to box connections. The box structure in turn will be kinematically supported in the beamline and all alignment will be done by adjusting these supports. As discussed later in this section, the box structure is designed to operate with a variety of live loads in addition to the load of the RFQ. In this way it can function as the structure for other equipment such as the vacuum system and the RF feed system without undergoing excessive deflection. This will be most beneficial in the case of the coolant distribution lines and headers. The structure can support the headers and allow complete installation, leak testing, and flow balancing of the distribution system prior to installation in the beamline. The complete RFQ subsystem is then installed as a pre-tested unit.

The RFQ is supported vertically and horizontally at five locations within the box. These locations are the low energy end, high energy end, and each of the three segment to segment joints. The low energy end also incorporates a double vertical support which restrains the rotational degree of freedom about the beamline axis. The supports are pin ended struts with rod end bearings at each end. These allow movement in all degrees of freedom other than translation along the strut axis. These type of supports were employed on the CWDD RFQ.

The rod assemblies incorporate a differential thread adjustment system that allows fine adjustment of the RFQ position. In the center of each rod is a threaded shaft attaching the two rod halves together. One thread is 20 thread per inch (TPI) while the other is 18 TPI. Rotation of this shaft changes the length of the rod by the difference of the thread pitches which in this case is 0.0055 inch per rotation. This method was successfully employed on the CWDD and SSC RFQ's. Because of the redundancy of the support system, each rod assembly will incorporate a load cell to allow monitoring during the adjustment process and prevent accidental overloading of the RFQ.

The rod assemblies will be installed with the RFQ in the vertical orientation and preliminary alignment will be done using optical alignment techniques and the load cell readings. Once the RFQ is layed down final alignment in the box structure will be done if necessary to compensate for small deflections of the box itself. Once this is complete the RFQ to box alignment will remain fixed. All subsequent alignment of the RFQ will be done by moving the box structure.

Axial restraint of the RFQ is not currently shown in the structure. It is anticipated that the RFQ will be restrained axially at either the injector or the DTL interface and the design will depend upon the details of that equipment. This support could be built into the box structure or be provided by structures associated with the other equipment. In either case the box structure will provide temporary or permanent axial restraint to the RFQ for use in the vertical orientation. The restraint itself can be similar in nature to the gimbal ring axial mount used on the CWDD RFQ which provides single degree of freedom restraint (Figure VIII-4).

324.61

RF FEED ASSEMBLIES (4)

RFQ SUPPORT STRUTS

W14 X 53 (TYP)

8×8 TUBE

COOLANT HEADER

4×4 TUBE

LEBT SOLENOID 600 LBS

58.00

14.00 CLEAR

SUPPORT POINT

VAC PUMP(4)

SUPPORT POINT

FACILITY FLOOR

PIVOT POINT FOR ROTATION TO VERTICAL
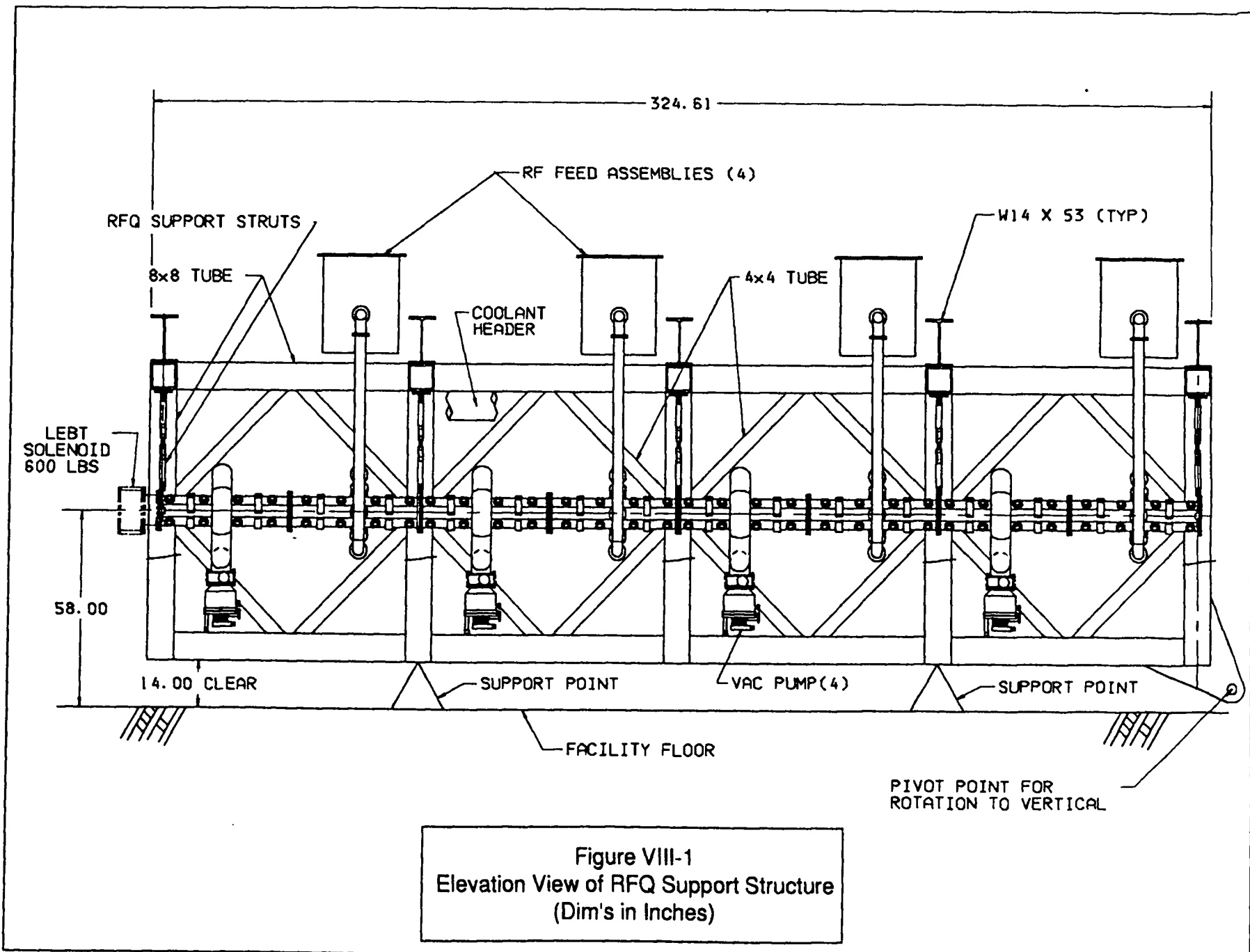
Figure VIII-1
Elevation View of RFQ Support Structure
(Dim's in Inches)

W14 X 53
(I OF COMPOSITE
SECTION = 1570 in**4)

COOLANT HEADER

DUAL VERTICAL
(CONTROLS ROLL)

LATERAL
RESTRAINT

58.00

4X4 TUBE

8X8 TUBE

FACILITY FLOOR
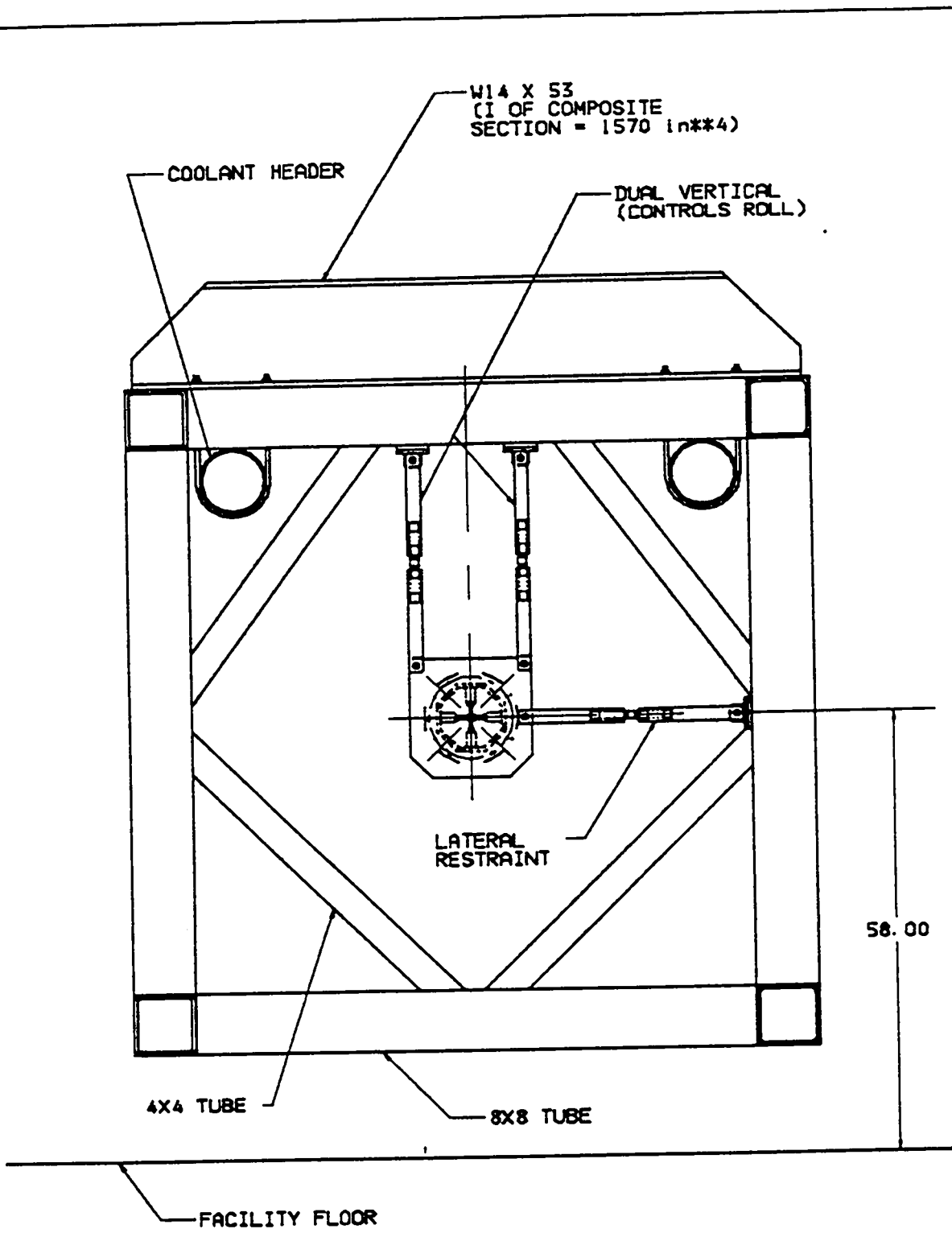
Figure VIII-2
Section at Low Energy End Support
(Dim's in Inches)

ROD END
BEARINGS

DIFFERENTIAL
THREAD SHAFT

72. 00

14. 00

72. 00

FACILITY FLOOR

Figure VIII-3
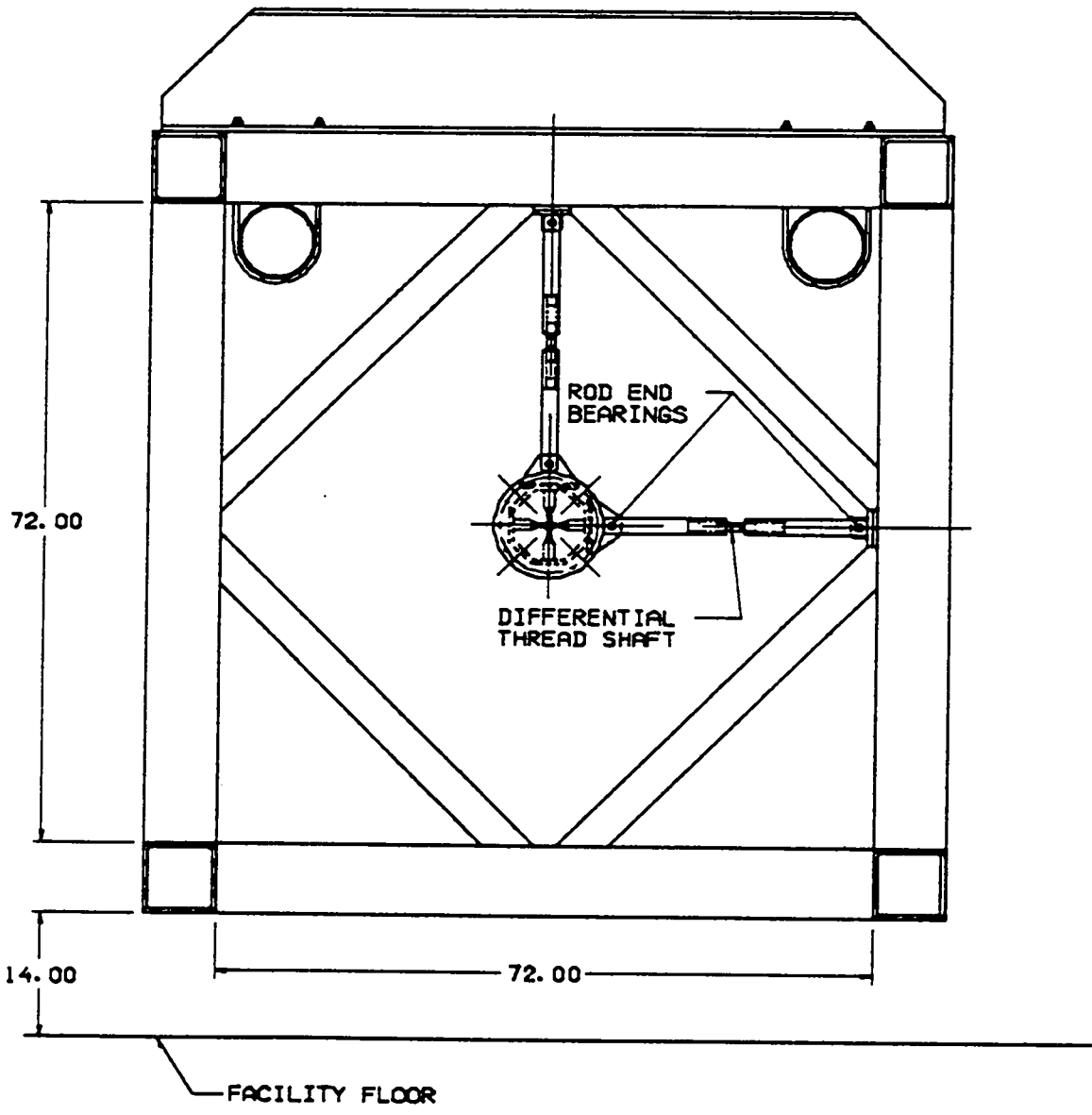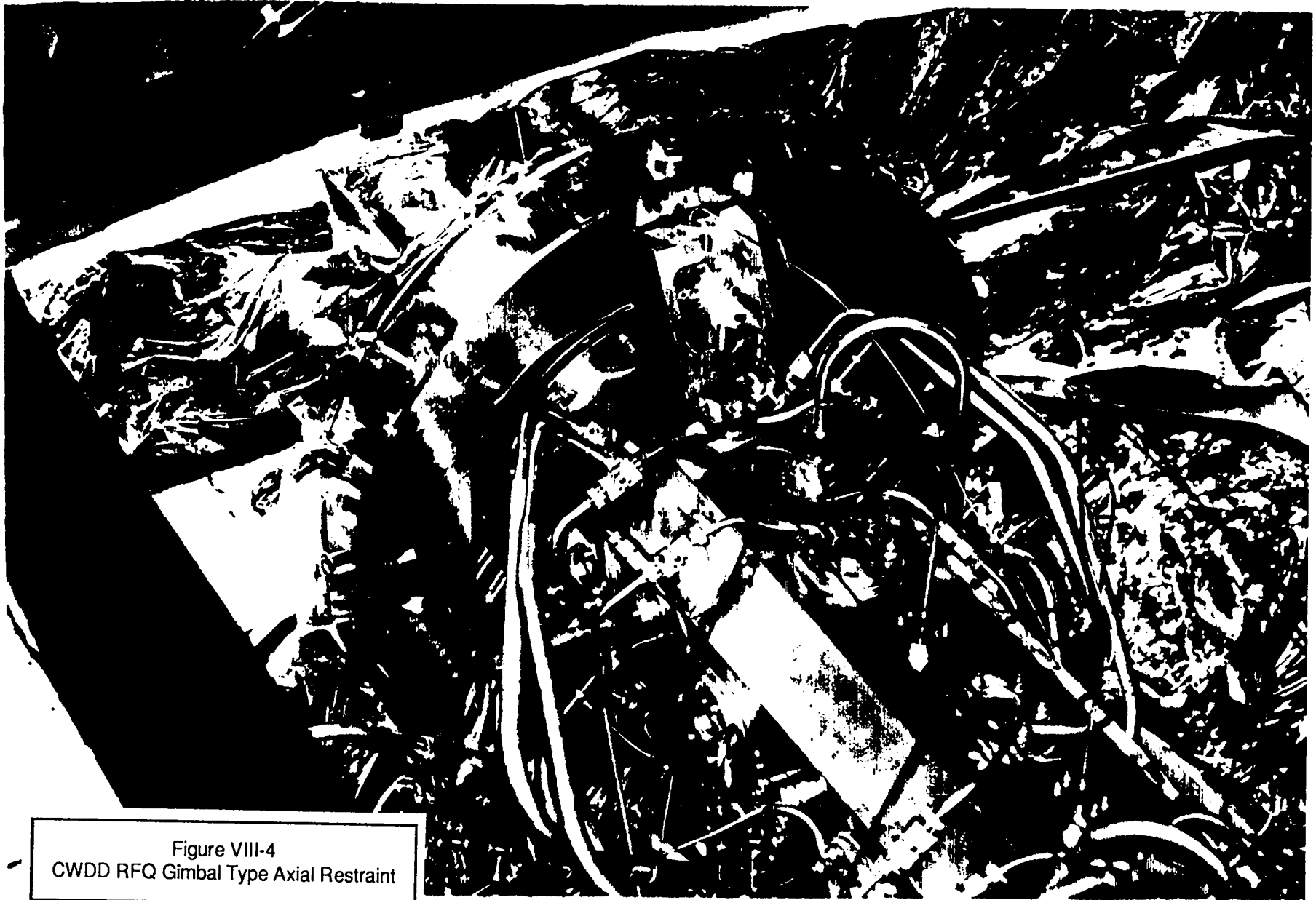Section at Downstream Support Points
(Dim's in Inches)

Figure VIII-4
CWDD RFQ Gimbal Type Axial Restraint

The box structure is built up from 8×8×0.5 inch wall structural tubing. The 8×8's form the four longitudinal members as well as the square frames at each RFQ support point. To stiffen the square panels but still provide maximum access to the core of the structure, 4×4×0.5 inch wall tubes are used as knee braces at all corner locations. To locally stiffen the top members that are carrying the weight of the RFQ at center span, W14×53 wide flange beams are provided. This added stiffness in the top members will also aid in supporting the RF waveguides and feed systems when they are installed. The box structure will also directly support the vacuum equipment and the coolant header piping. Concepts for the installation of the RF, vacuum and coolant headers are shown in Figures VIII-5 and VIII-6.

The overall crossection of the box was selected to provide a large clear area around the RFQ for equipment and for access during tuning and maintenance while staying within the limitations of the 58 inch beamline height above floor. The box has a 72 inch clear inside dimension which leaves 14 inches clear below to the floor. This area will house the kinematic adjusters for the box. The support of the box will be at the second and fourth frame location (25% and 75% points) to minimize overall deflections.

RFQ STRUCTURAL PERFORMANCE

The five point RFQ support system was selected based upon performance under live load conditions. A summary of the performance of the RFQ with a variety of supports is shown in Table VIII-2. The RFQ cross-sectional properties are shown in Figure VIII-7.

TABLE VIII-2

RFQ Support Scheme Performance

# Supports	Load Case	δ Max (in)	σ Max (psi)
2 (Kinematic)	Operating	.045	1490
2	Live	.045	312
3	Operating	.0127	872
3	Live	.0025	95
4	Operating	.0060	344
4	Live	.00096	68
5	Operating	.00095	187
5	Live[a]	.00045	61

a. For the case of 5 supports only the live load case was expanded to include alternating positive and negative 100 lb forces at the center of each segment.

As shown in the table the five support system is the only one that meets all of the requirements. The four support system is close and would be a candidate if the live load deflection limits were relaxed. Because the live load case dominates the selection it is clear that the lateral support must also have five support points. Another argument for the five support case is that the RFQ becomes more robust against unanticipated local loading

STUB SUPPORTED 3.125 COAX BEND
WATER COOLANT INJECTION

COAX SUPPORTED
FROM STRUCTURE

WR2300 WAVEGUIDE
DUAL COAX TRANSITION

COOLANT
HEADER

STRAIN ISOLATION
IN THIS SECTION

DRIVE LOOP (4)

WATER INJECTION

FACILITY FLOOR
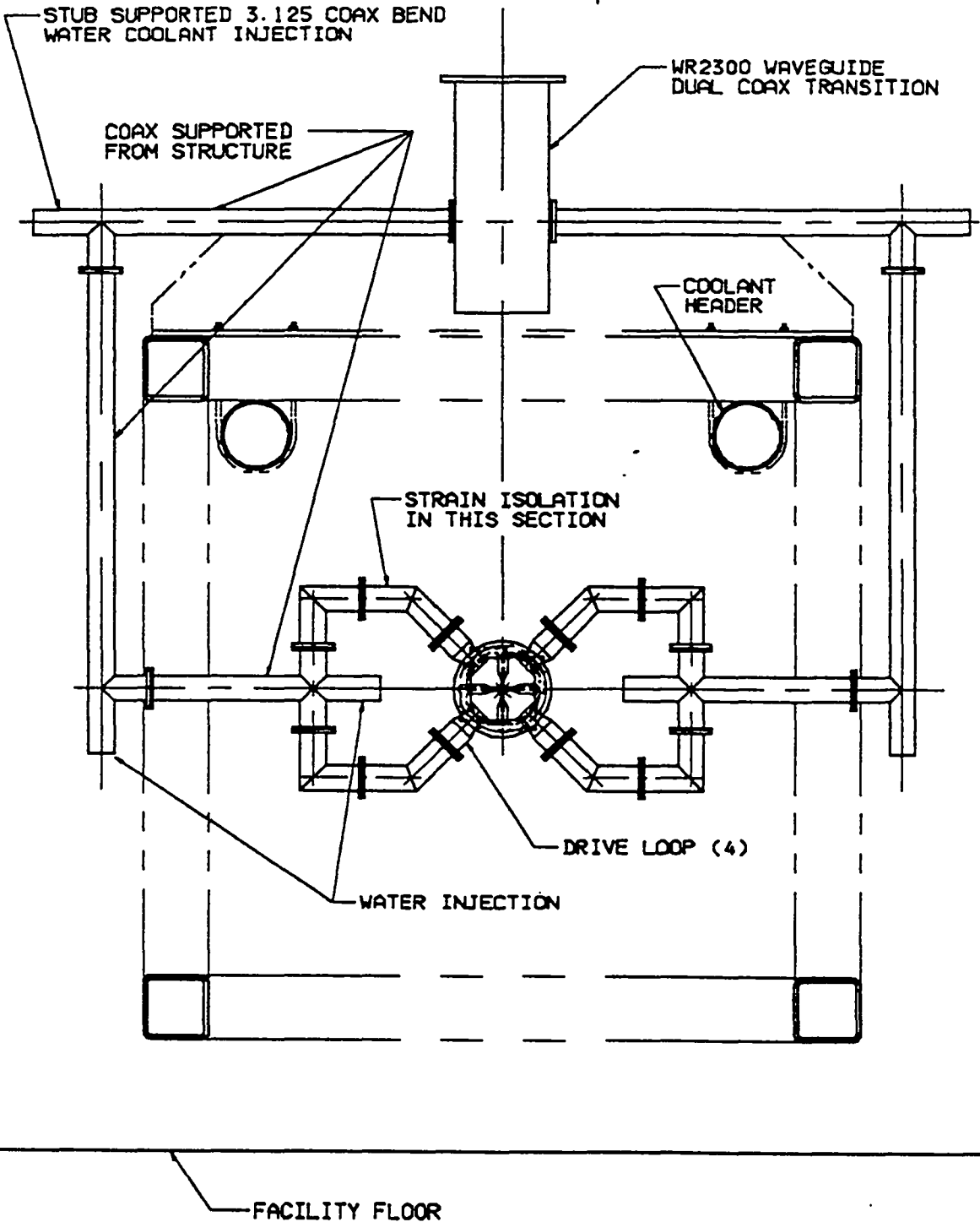
Figure VIII-5
RF Feed System Installation Concept

COOLANT HEADER

ISO CLAW CLAMP
FLANGE

Ø4" DUCT
WITH BELLOWS

VACUUM SYSTEM
HANGERS

Ø6" MANIFOLD

TURBOMOLECULAR PUMP
LEYBOLD MODEL TMP1000
(TMP600 MEETS SPEC)

VAT SERIES 10
Ø6" GATE VALVE
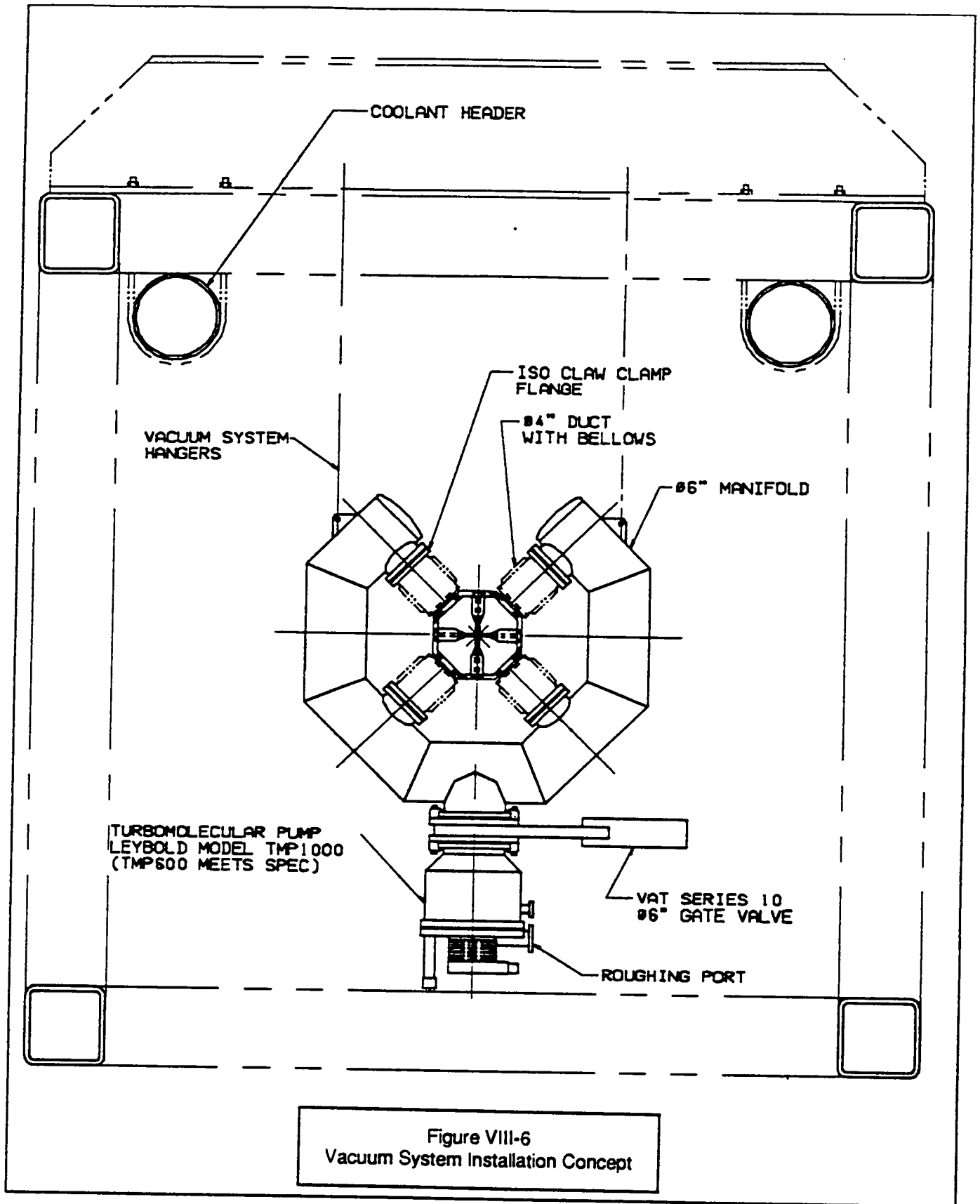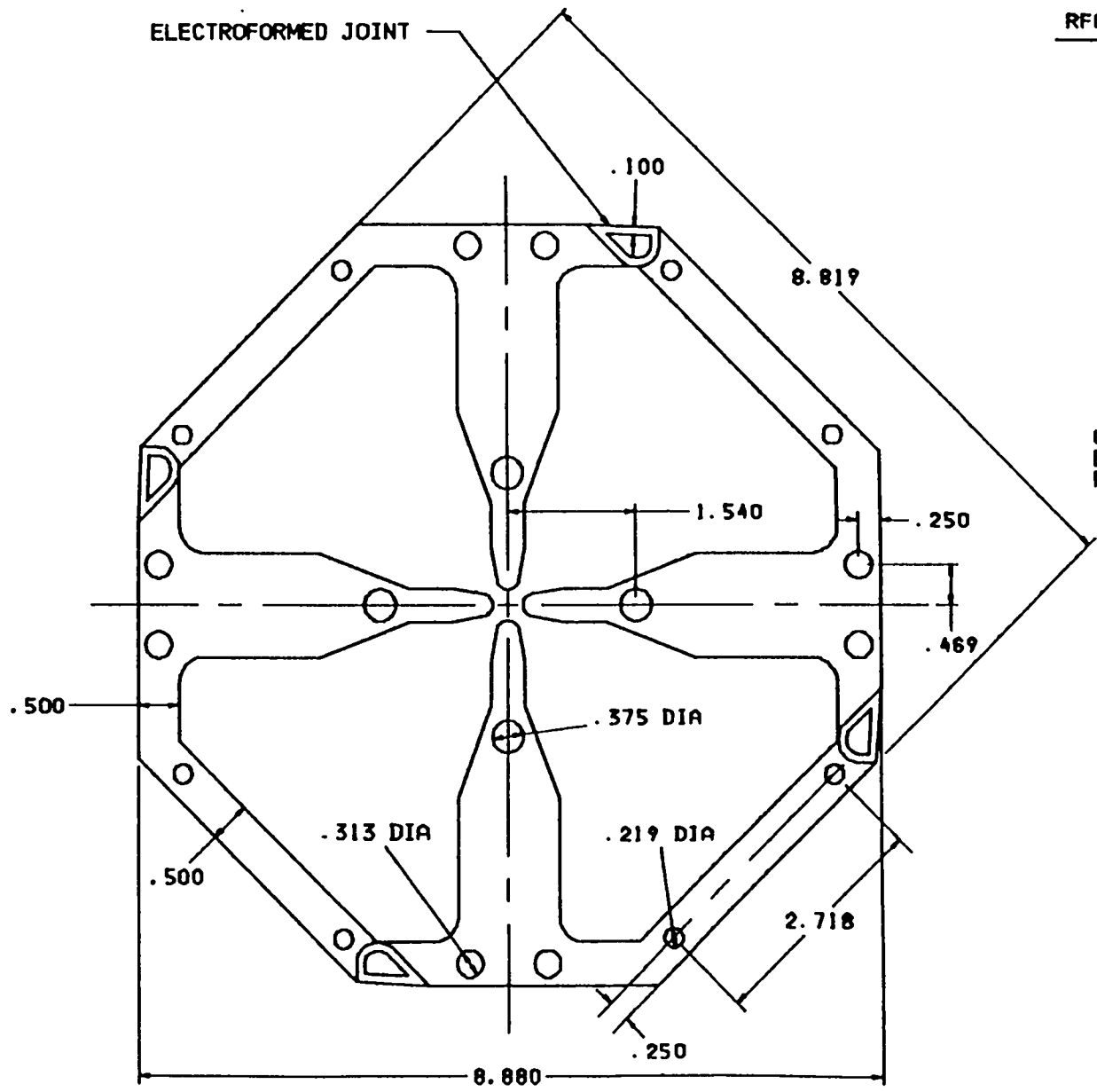
ROUGHING PORT

Figure VIII-6
Vacuum System Installation Concept

RFO SECTION PROPERTIES

AREA = 25.280899
XBAR = 0.0000000
YBAR = 0.0000000
IY-Y = 162.97200
IX-Y = 0.0000000
IX-X = 162.97181
RY-Y = 2.5389857
RX-X = 2.5389843
ZETA = 45.000003
IPY-Y = 162.97191
IPX-X = 162.97191
RPY-Y = 2.5389850
RPX-X = 2.5389850
IZ-Z = 325.94400

COOLING PASSAGES AND
ELECTROFORMED JOINT
FILLERS REMOVED

ELECTROFORMED JOINT

.100

8.819

1.540

.250

.469

.500

.375 DIA

.313 DIA

.219 DIA

.500

2.718

.250

8.880

Figure VIII-7
RFO Section Properties
(Units - Inches)

while still being forgiving of misadjustment of a given support. A forced deflection of .010 inch at the center support point only results in a stress of 490 psi in the RFQ body while having an indicated load on a load cell at that point of approximately 800 pounds.

The strut type support system is subject to alignment variations due to thermal transients. With the high heat loads in the RFQ the possibility of cosine errors induced by axial expansion of the cavity must be considered. With a pin to pin dimension on the struts of 24 inches the RFQ can translate ± 0.155 inch from nominal and remain within the ± 0.0005 inch deflection limit for live loads. This corresponds to a bulk temperature rise in the RFQ of 100° F assuming axial restraint at one end.

BOX STRUCTURE PERFORMANCE

The box structure must be rigid under live load conditions. Deflections under dead loads should be reasonable so as not to compromise the integrity of the RFQ (i.e. , <0.010inch), but because the RFQ can be final aligned in the box after it is layed down the important feature is the subsequent stability under live loads. A second important aspect of the box structure is that it provide access to the RFQ for the initial assembly and tuning and to the vacuum, RF and diagnostic equipment for maintenance throughout its service life. The design described above using the 8x8 primary members and 4×4 secondary knees meets these requirements but is not the most efficient truss structure possible. Progressively stiffer designs have to be evaluated for access to the RFQ and ancillary equipment and not simply on structural performance alone.

TableVIII-3 lists some alternate concepts and their relative performance. The dead loads are those derived from gravity plus the applied loads of the RFQ. The RFQ loads are increased by 50% for this analysis and are shown in Figure VIII-8. For the live load case it was considered that loads of 500 lbs are applied at the top corner nodes of each of the five transverse frames (Figure VIII-9). This amounts to a total of 5000 lbs of live load.

The four design cases considered are:

Design 1. The concept design presented above

Design 2. The concept design except that the 4×4 knees are replaced by 8×8 knees

Design 3. The concept design except that the knees are replaced in total by 8×8 full diagonals in the top, bottom and side bays (transverse bays have 8×8 knees)

Design 4. A theoretically ideal beam. A solid cross-section selected to have the same area and moment of inertia about the horizontal transverse axis as the truss structures. This section is also assumed to be 100% effective in shear.

Cases 2 and 3 are reasonable structures that simply trade off stiffness for access. This trade can be fully considered during preliminary design. Case 4 is provided simply for comparison.

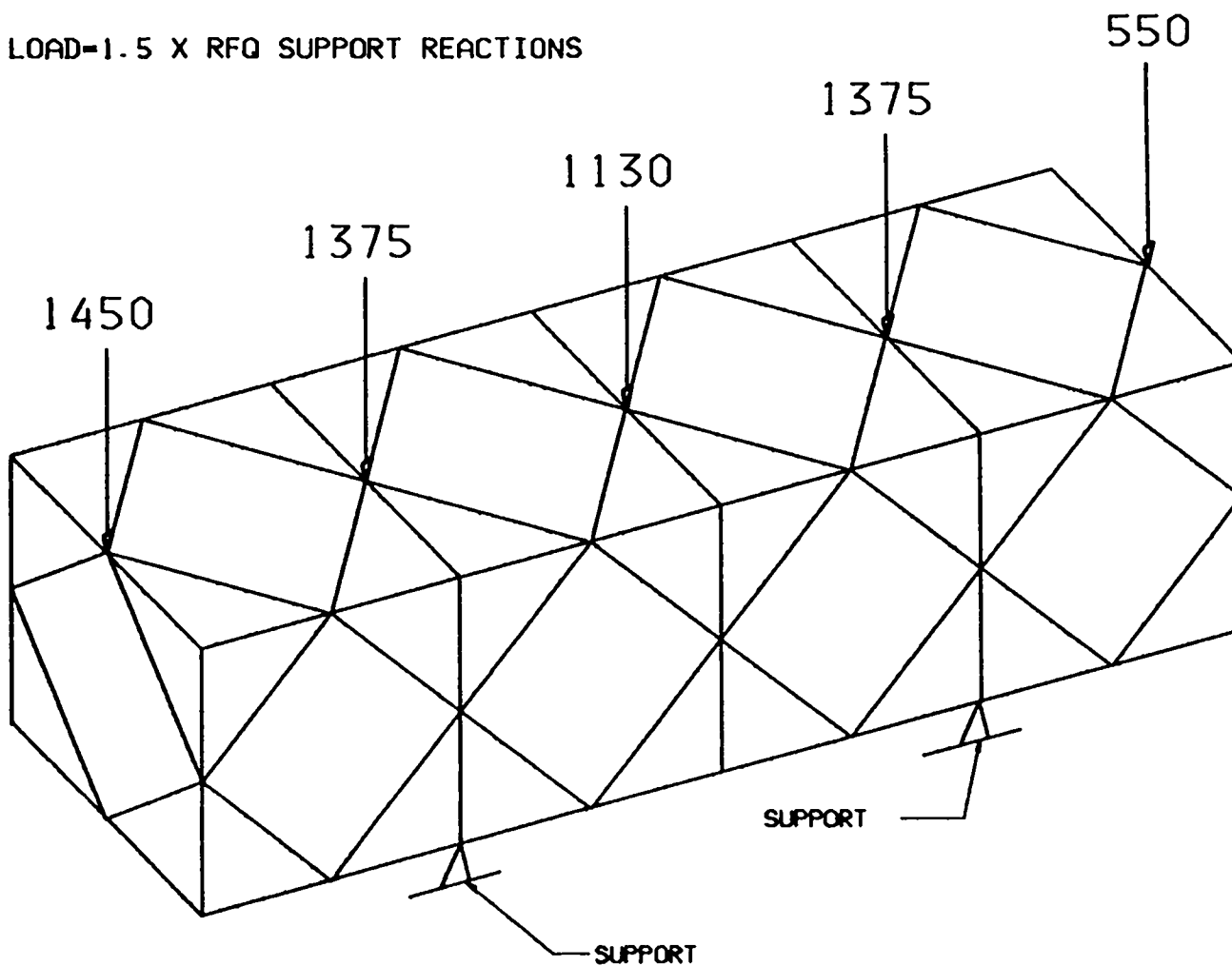LOAD=1.5 X RFQ SUPPORT REACTIONS

550

1375

1130

1375

1450

SUPPORT

SUPPORT

Figure VIII-8
Dead Loads for Truss Structure Analysis
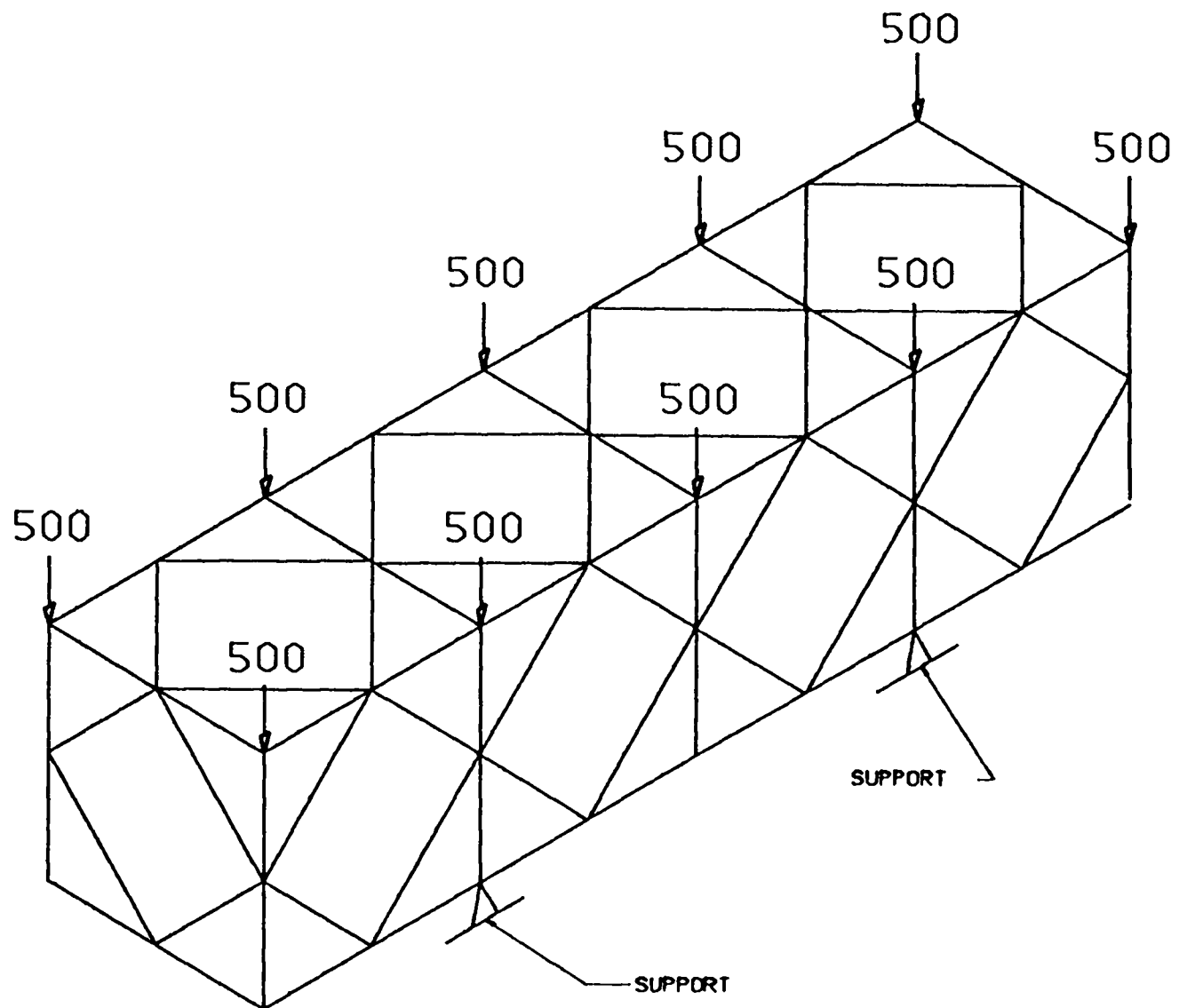(Gravity Included But Not Shown)
(Loads in Pounds)

Figure VIII-9
Live Loads for Truss Structure Analysis
(Loads in Pounds)

Table VIII-3

Relative Performance of Candidate Structures
Deflection in Inches - Dead Load Includes Gravity

Design Case

Load	Design 1	Design 2	Design 3	Design 4
Dead Load	.0035	.0032	.0029	.00067
Live Load	.00063	.00046	.00046	.00023

It can be seen from the table that adding larger section knees or going to a full diagonal in each bay is at the point of diminishing returns as far as performance under live load. All designs shown are considered to be well within limits for dead load deflection since the applied loads from the RFQ to the structure were increased by 50% for the analysis. The live load deflection value for the concept design is slightly above the RFQ cavity criteria but this could be brought down easily by taking minimal care to not apply large loads the extreme ends of the cantilever ends. Indeed, the concept structure was further analyzed for a case where 1000 lb loads were applied at the six internal top frame nodes while the original 500 lb loads were left at the four cantilevered top nodes (Figure VIII-10). This increases the total live load applied to 8000 lbs. For this case the maximum deflection only increased to .00064 inch.

It is clear that the structure performance can be more significantly improved if larger section tubes are used for the longitudinal members. This was not considered because it would result in a reduction in either the clear space available around the RFQ or in the clear space between the structure and the floor, neither of which was considered desirable. This can be re-evaluated in preliminary design.

DYNAMIC CONSIDERATIONS

A large support structure of this type is always scrutinized for dynamic response when supporting a precision device such as the RFQ. No guidelines have as yet been set for the APT structures but it is generally desirable to keep the fundamental frequency of the structure as high as possible while avoiding any specific problem frequencies associated with a given facility. When supported in the kinematic fashion the fundamental frequency of the concept structure is approximately 34 Hz. This frequency can be brought up to 54 Hz by simply adding some additional vertical and lateral restraints to the system. It is proposed that, if necessary, this can be done without impacting the alignment and kinematic adjustment of the system and that the accelerator tunnel environment will be stable enough so as to prevent any unexpected deformation due to thermal transients. After final alignment in the beamline, screw down support pads can be extended to provide the additional dynamic restraint without being pre-loaded to the point of causing noticeable deflection.
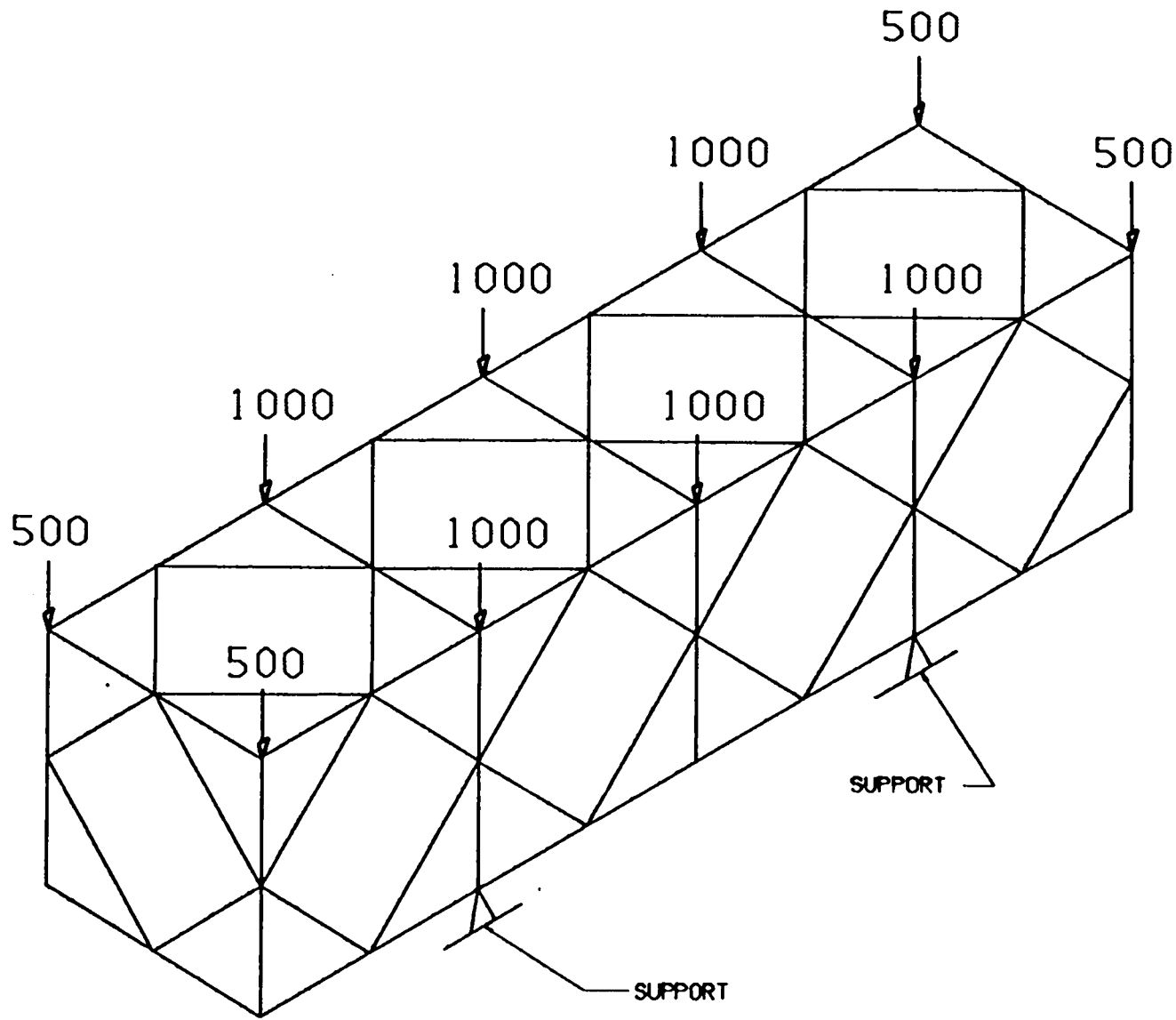
Figure VIII·10
Increased Live Loads Applied to Concept Design
(Loads in Pounds)

IX. VACUUM SYSTEM

The APT RFQ vacuum pumping system is described in this section. The pumping system is based on the use of turbomolecular high vacuum pumps. All hardware items used in the APT RFQ vacuum pumping system are standard catalog items requiring no development. A schematic of the pumping system is shown in Figure IX-1 while the concept for the installation is shown in Figure IX-2.

The vacuum pumping system for the APT RFQ must provide "accelerator-grade" vacuum levels in the RFQ interior corresponding to an internal pressure in the RFQ of less than 5×10^{-6} Torr during normal operation and a pressure of less than 5×10^{-5} Torr with a 100% beam spill. During normal operation the gas load is equivalent to the loss of 10% of the entering beam, or 11.7 mA, plus the gas streaming from the LEBT operating at a pressure of 1×10^{-5} Torr and is assumed to be uniformly distributed among the pumping ports. The gas to be pumped is hydrogen and the pumping system must be capable of pumping hydrogen continuously.

Sputter-ion pumps, cryopumps, and turbomolecular pumps are all capable of providing the required APT RFQ pumping. Sputter-ion pumps have a simple pumping mechanism and good radiation resistance but are inordinately large and heavy for the pumping speed provided. They also suffer a loss of pumping speed in the 10^{-5} Torr range. Cryopumps pump hydrogen effectively at all expected APT RFQ pressures and provide a higher pumping speed for a given flange size than turbomolecular pumps but have a limited hydrogen capacity and would require periodic regeneration when pumping hydrogen. Turbomolecular pumps are light weight, compact devices that provide continuous pumping of hydrogen and are not expected to be effected by the low level radiation environment at the low energy end of the APT linac.

The pumping system design is based on the RFQ pumping ports shown in Figure IX-3. The conductance of this segmented port was estimated by calculating the conductance of the circular portion of the port and subtracting a conductance equal to that of the rectangular divider. A molecular flow conductance for hydrogen of 733 l/s is obtained for each port including the exit correction. Initial concepts for the RFQ pumping system called for a pumping station on each of the eight one meter sections. At each station 4 ports (one in each quadrant) are connected to a pumping manifold by a 4 inch OD by 6 inch long tube. These ducts are in turn manifolded to a single pump with a 6 inch O.D. manifold (Figure IX-2). In this configuration with the eight pumping manifolds a turbomolecular pump having a hydrogen pumping speed of only 210 l/s results in an RFQ internal pressure of $1.2 \times \times 10^{-6}$ Torr during operation and 1.2×10^{-5} Torr during 100% beam spill. Each pump is also equipped with an isolation gate valve which will be closed automatically in the event of pump shutdown during accelerator operations. This will allow continued accelerator operation

ION ION ION ION

PUMPING MANIFOLD

RFQ

CONV.

GATE VALVE - NW160

FREQ.
CONV.
TYP-4

TURBOMOLECULAR
PUMP

CONV.
TYP - 4

CONV.

FT

ROTARY VANE
MECH. PUMP
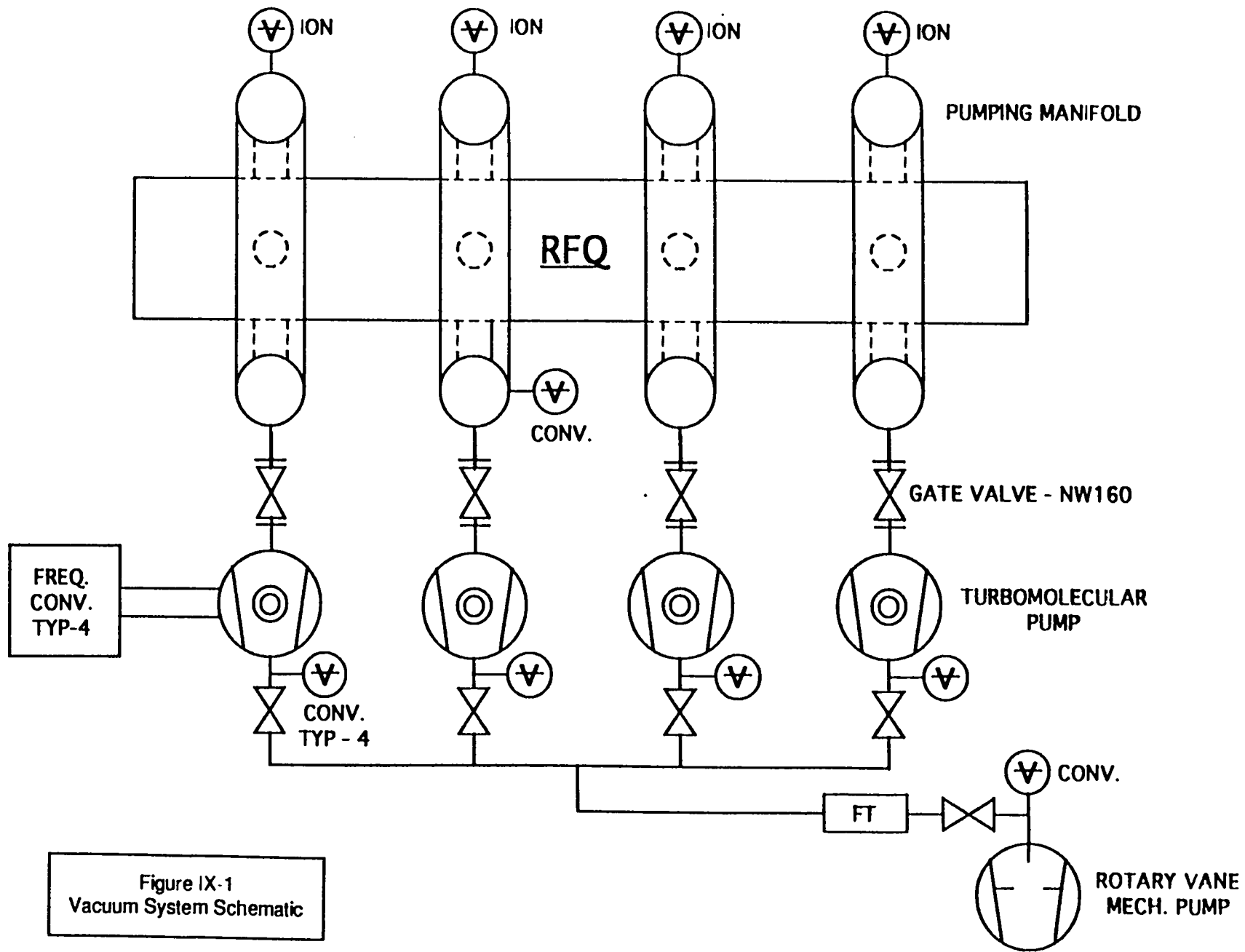
Figure IX-1
Vacuum System Schematic

COOLANT HEADER

ISO CLAW CLAMP
FLANGE

#4" DUCT
WITH BELLOWS

VACUUM SYSTEM
HANGERS

#6" MANIFOLD

TURBOMOLECULAR PUMP
LEYBOLD MODEL TMP1000
(TMP600 MEETS SPEC)

VAT SERIES 10
#6" GATE VALVE

ROUGHING PORT

Figure IX-2
Vacuum Pumping Station

.522
OFFSET

.375
SEPTUM

2.25 DIA
DUCT

3.80 DIA
BOSS

.750
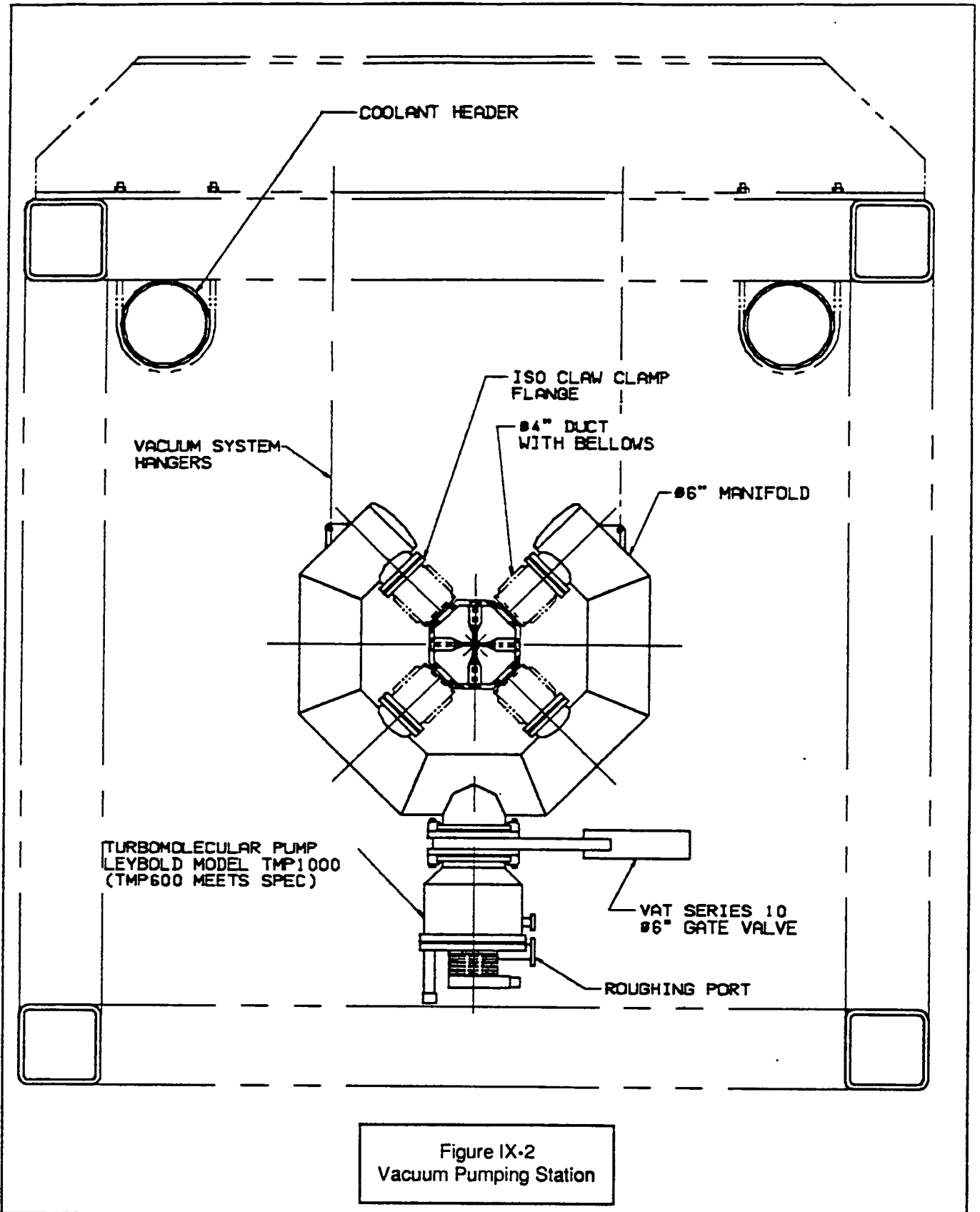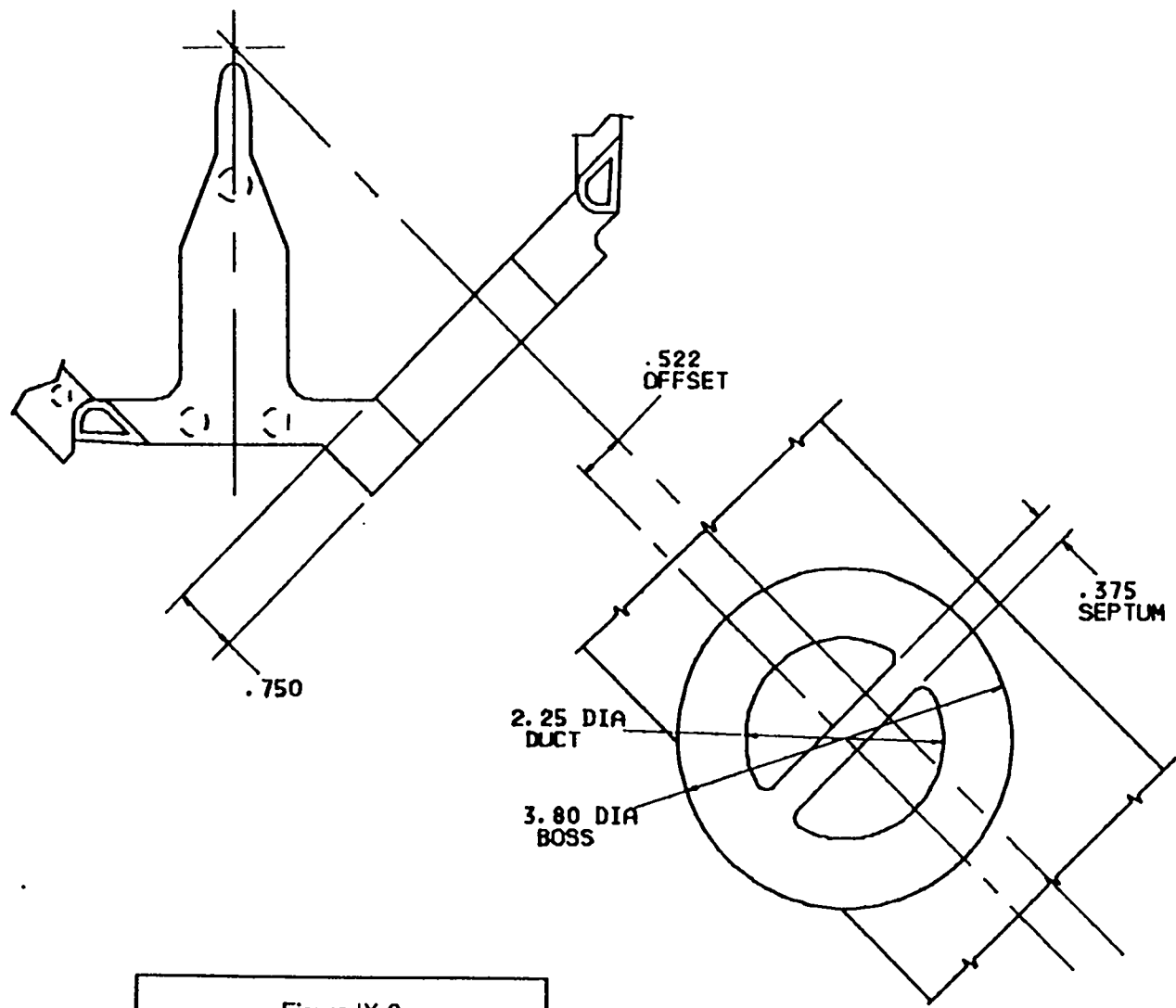
Figure IX-3
RFQ Pumping Port Configuration
(Dim's in Inches)

Because of the premium that will be placed on space around the RFQ it was decided to reduce the number of pumping stations on each RFQ to four. This quite conveniently leads to the configuration shown in Figure VIII-1 where each two meter resonant segment incorporates one vacuum pumping station and one RF feed location. Using the same RFQ vacuum manifolds described above and turbomolecular pumps with a hydrogen pumping speed of 570 l/s, the four pump configuration yields pressures of 8.9×10^{-7} Torr during beam operation and 8.9×10^{-6} Torr during 100% beam spill. Should additional margin on the pressures be desired, turbomolecular pumps with a hydrogen pumping speed of 900 l/s can be installed on the same size port as the 570 l/s units and will result in a pressure of 6.7×10^{-7} Torr during operation and 6.9×10^{-6} Torr during 100% beam spill. The baseline vacuum system design and costing analysis uses the smaller pumps since they meet the APT RFQ vacuum requirements. However, for the layout of the RFQ shown in Figure IX-2 and allocation of space, the larger pumps are shown.

Of particular concern with use of only 4 pumping manifolds is the effect of loss of one pump on the RFQ pressures. Two cases were analyzed which were considered to be "worst case" scenarios:

- During operation, the segment #4 pump is lost and all beam loss gas is generated at the high energy end of the RFQ.

- During 100% beam loss, the segment #1 pump is lost and all beam loss gas is generated in segment #1 (low energy end).

In both cases an aperture between segments of 3.25 inches diameter by 0.5 inch long is assumed. In both cases a further "worst case" was analyzed by assuming that the pumping station adjacent to the failed station pumps all of the additional gas load with no aid from the other two remaining pumps. For these scenarios a maximum RFQ pressure of 3.7×10^{-6} Torr would be obtained in segment #4 during beam operation and 3.7×10^{-5} Torr in segment #1 during 100% beam spill. Both values are within the required operating pressure envelope.

X. CONCLUSIONS & RECOMMENDATIONS

The general conclusion from the results of the work presented herein is that the APT RFQ as specified can be designed and fabricated with reasonably predictable cost, schedule, and performance. While there are a few issues of concern, there are none which cannot be resolved by careful design work and prototype testing. There are, however, a few areas where cost and schedule can possibly be reduced and/or robustness enhanced at the expense of prototype development activities. Some of the these are identified and described in following paragraphs. The conceptual design presented herein has had little optimization and it is assumed that a significant amount of additional physics and engineering analysis as well as testing will be carried out prior to establishing final design parameters.

COLD MODELING:

There is currently no operating experience with an RFQ constructed of resonantly-coupled segments. Although low power rf measurements have been made on a 350 MHz, two-segment cold model RFQ which is four meters long, it is not possible to complete the full exploration of rf field distribution perturbations on a half-length structure. Given the importance of the resonantly-coupled cavity concept to the success of the RFQ design it is prudent that a full-scale cold model be constructed and tested. One very important technique that does need to be developed for both the cold model and the final units is a method for performing a bead pull on this structure while in a horizontal orientation. The sag of the required large bead(s) will be quite large.

The rf drive loop design selected for the conceptual design exercise is a duplicate of that which was utilized for the SSC RFQ. This was a very low duty factor (0.05%) implementation. Although similar to that which has been in CW service at CRNL, it is not clear whether this drive loop design will hold up through long term CW operation. A more robust alternative would be an iris- coupled wave guide. This should be tested on a full-scale cold model.

THERMAL STABILITY:

A major concern is the thermal behavior of the cavity. The item at issue is that with the large average thermal load (114 Kw/m^2) which has significant longitudinal variation there is a concern that the longitudinal variation of the cavity local frequency may be such as to cause the field tilt to exceed the 2.5 percent per meter value beyond which the transmission is reduced. The thermal loads predicted by MAFIA have been verified in that these predictions are in good agreement with rf field distribution measurements made on the four meter long cold model RFQ. While this has provided some confidence in the calculated performance, no such long, high duty factor RFQ has ever been operated. At the present time there is no clear choice of a technical demonstration of the thermal stability of this design. However, some such demonstration should be completed as part of the final design process.

Thus far there has been no optimization of the engineering design with regard to location of coolant passages to minimize thermally-induced frequency shift. Nor has there been any transient analysis of the startup or shutdown conditions. The finite element models utilized for the preliminary conceptual design were either two-dimensional or truncated-length three dimensional models. Prior to final design there must be extensive analysis for optimization followed by transient analysis of full-length models.

MATERIAL SELECTION:

For the purpose of this conceptual design study, oxygen-free copper (OFE, C10100) was selected as the material for the RFQ. The low yield stress of OFE copper places significant constraints on the design of the structural support and limits the design margins for the thermal loads. Clearly, a material with higher yield stress, such as GLIPCOP™ (30000 #/in^2 verses 9000#/in^2 for OFE), would be more desirable. Experimentation with GLIDCOP or some other higher strength copper with respect to electroforming, welding, and machinability might lead to a reduction in machining costs (and time) for the RFQ quadrants as well as design and fabrication costs for the support structure while at the same time adding to the design margins.

ALTERNATE JOINT FILLER:

The joint filler used on the BEAR, CWDD, and SSC RFQ's was a lead tape. This has been proven to work quite satisfactorily in the temperature range of -390° F to 190° F. The concern is that the thermal expansion coefficient of the lead (1.61×10^{-5} /° F) is fifty percent higher than that of the copper (0.96×10^{-5} /° F). Since the lead is surrounded by the copper, the result of excessive thermal expansion would lead to yielding of the copper. Although the thermal analysis predicts that temperatures in the joint area will not exceed 170° F under normal operating conditions, there is always the possibility of reaching higher temperatures under abnormal circumstances.

There were searches for other fillers on the BEAR project and experiments with copper tape on the CWDD project. Neither resulted in a satisfactory alternative to the lead tape. One possibility would be use of a plasma-sprayed copper or copper alloy. Study of this would require some testing regarding compatibility of the plasma-sprayed material with the electroforming process and methods of application.

ALTERNATE STRUCTURAL DESIGN CONCEPTS:

The electroformed joint process utilized in the BEAR, CWDD, and SSC RFQ's and proposed for the APT RFQ has the perceived disadvantage of being rather time consuming. The electroforming of a single one-meter long section requires approximately fourteen weeks. It is of course possible to electroform multiple units in parallel. However, this will entail

some investment in facilities and training of personnel. Electroforming of the total sixteen one-meter sections would require over a year if they were processed in groups of four.

Investigations of alternative joining methods, such as welding, as well as revisions to the electroforming process to reduce the time required might be warranted. The payoff for a shorter fabrication time span for the RFQ's would be earlier commissioning and operational experience. However, any alternative joining processes would of course have to demonstrate structural, vacuum, and thermal performance comparable to the electroforming process.

XI. REFERENCES

1   D. Schrage, et al, "Radio Frequency Quadrupole Linac for the Superconducting Super Collider," 12th Conference on the Application of Accelerators in Research & Industry, Denton, TX, 1992.

2   T. Bhatia, et al, "Beam Dynamics Design of an RFQ for the SSC Laboratory," 1991 IEEE Particle Accelerator Conference.

3   J. Rathke, et al, "Engineering Design of the Radio Frequency Quadrupole (RFQ) for the Continuous Wave Deuterium Demonstrator (CWDD)," Technical Symposium and Scientific Interchange on Neutral Particle Beam Technology, Monterey, CA, 1989.

4   L. Young, "Segmented Resonant Coupled Radio Frequency Quadrupole (RFQ)," Proceedings of the 1993 Particle Accelerator Conference, Washington, D.C.

5   G. Arbique, et al, "Beam Parameter Measurements on the CW RFQ1-1250 Accelerator," Proceedings of the 1992 Linear Accelerator Conference, Ottawa, ON.

6   W. Cornelius, "CW Operation of the FMIT RFQ Accelerator," Proceedings of the 1985 Particle Accelerator Conference, Vancouver, BC.

7   D. Schrage, et al, "A Fight-Qualified RFQ for the BEAR Project," Proceedings of the 1988 Linear Accelerator Conference, Williamsburg, VA.

8   L. Young, "Tuning and Stabilization of RFQ's," Proceedings of the 1990 Linear Accelerator Conference, Albuquerque, NM.

9   N. Ueda, et al, "Construction of the RFQ 'TALL,'" Proceedings of the 1984 Linear Accelerator Conference, Vancouver, BC.

10   G. E. McMichael "High-Current CW RFQ's" Conference Record of the 1991 IEEE Particle Accelerator Conference, San Francisco, CA.

11   T.P Wangler, "Space-Charge Limits In Linear Accelerators," LA-8388, Dec. 1980.

12   K. R. Crandall, R. H. Stokes, and T. P. Wangler, "RF Quadrupole Beam Dynamics Design Studies," Proceedings of the 1979 Linear Accelerator Conference, Mantauk, New York.

13   W. D. Kilpatrick, "Criterion for Vacuum Sparking Designed to Include Both rf and dc", The Review of Scientific Instruments, Vol 28, No. 10, 824-826, October, 1957.

14   J. Y. Sheikh and R. J. Burton, "Tuning and Conditioning of RFQ101250 Cavity", Proceedings of the 1992 Linear Accelerator Conference, Ottawa, ON.

15   A. Cucchetti, "Error Study for the APT RFQ," Accelerator Technology Division Technical Note No AT-1:92-281, August 19, 1992.

16   R. H. Stokes, K. R. Crandall, J. E. Stovall, and D. A. Swenson, "RF Quadrupole Beam Dynamics" IEEE Transaction on Nuclear Science, Vol. NS-26, No. 3, June 1979.

17   F. W. Guy "Three-Dimensional Space Charge and Image Charge Effects in Radio-Frequency-Quadrupole Accelerators" Conference Record of the 1991 IEEE Particle Accelerator Conference, San Francisco, CA.

18   K. F. Johnson, et al, "commissioning of the Ground Test Accelerator RFQ", 1992 Linear Accelerator Conference Proceedings, Ottawa, ON.

19   L. Young, "Segmented Resonant Coupled Radio Frequency Quadrupole (RFQ)," To be presented at the 1993 IEEE Particle Accelerator Conference, Washington, DC.

20   R. Ryne, et al, "Recent Advances in the POISSON/SUPERFISH Codes," Proceedings of the 1992 Linear Accelerator Conference, Ottawa, ON.

21   D. Schrage, et al, "BEAR RFQ - Beam Experiment Aboard Rocket," 10th Conference on the Application of Accelerators in Research & Industry, Denton, TX, 1988.

22   N. Bultman et al, "Preliminary Design of a CW RFQ for Culham Laboratory," LANL Design Review, July 1987.

23   M. Van de Voorde, "Effects of Radiation on Materials and Components," CERN Technical Report #70-5, 1970.

24   K. Christensen, et al, "Design and Fabrication of an RFQ Cold Model for the CWDD Accelerator," Second Neutral Particle Beam Technical Symposium, San Diego, CA, 1990.

25   J. Merson, "Power-Loss Densities for Three Versions of the APT RFQ," memo, AT-7:STN-93-10, March 1993.

26   J. Billen, "Documentation for RFQALIGN," Los Alamos National Laboratory, 1992.

27   M. Vretenar, Proceedings of the First Workshop on the INFN Eliosatron Project, Erice, Scicily (Plenum, NY) 1986, p.271.

28   E. Gintzon, Microwave Measurements, McGraw-Hill, 1957, Chapter 10.